INFORMATION TO USERS

This manuscript has been reproduced from the microfilm master. UMI films the text directly from the original or copy submitted. Thus, some thesis and dissertation copies are in typewriter face, while others may be from any type of computer printer.

The quality of this reproduction is dependent upon the quality of the copy submitted. Broken or indistinct print, colored or poor quality illustrations and photographs, print bleedthrough, substandard margins, and improper alignment can adversely affect reproduction.

In the unlikely event that the author did not send UMI a complete manuscript and there are missing pages, these will be noted. Also, if unauthorized copyright material had to be removed, a note will indicate the deletion.

Oversize materials (e.g., maps, drawings, charts) are reproduced by sectioning the original, beginning at the upper left-hand corner and continuing from left to right in equal sections with small overlaps.

Photographs included in the original manuscript have been reproduced xerographically in this copy. Higher quality 6" x 9" black and white photographic prints are available for any photographs or illustrations appearing in this copy for an additional charge. Contact UMI directly to order.

UMI®

UNIVERSITY OF ALBERTA

BLOCK COPOLYMER MICELLES FOR THE ENCAPSULATION AND

DELIVERY OF AMPHOTERICIN B

BY

AFSANEH LAVASANIFAR ©

A THESIS

SUBMITTED TO THE FACULTY OF GRADUATE STUDIES AND RESEARCH

IN PARTIAL FULFILLMENT OF THE REQUIREMENTS FOR THE DEGREE OF

DOCTOR OF PHILOSOPHY

IN

PHARMACEUTICAL SCIENCES

Faculty of Pharmacy and Pharmaceutical Sciences

Edmonton, Alberta

Fall, 2001

The author has granted a non-exclusive licence allowing the National Library of Canada to reproduce, loan, distribute or sell copies of this thesis in microform, paper or electronic formats.

The author retains ownership of the copyright in this thesis. Neither the thesis nor substantial extracts from it may be printed or otherwise reproduced without the author's permission.

L'auteur a accordé une licence non exclusive permettant à la Bibliothèque nationale du Canada de reproduire, prêter, distribuer ou vendre des copies de cette thèse sous la forme de microfiche/film, de reproduction sur papier ou sur format électronique.

L'auteur conserve la propriété du droit d'auteur qui protège cette thèse. Ni la thèse ni des extraits substantiels de celle-ci ne doivent être imprimés ou autrement reproduits sans son autorisation.

0-612-68961-1

Canadä

UNIVERSITY OF ALBERTA

LIBRARY RELEASE FORM

NAME OF AUTHOR: **AFSANEH LAVASANIFAR**

TITLE OF THESIS: **BLOCK COPOLYMER MICELLES FOR THE**

ENCAPSULATION AND DELIVERY OF AMPHOTERICIN B

DEGREE: **DOCTOR OF PHILOSOPHY**

YEAR THIS DEGREE GRANTED: **2001**

PERMISSION IS HEREBY GRANTED TO THE UNIVERSITY OF ALBERTA LIBRARY TO REPRODUCE SINGLE COPIES OF THIS THESIS AND TO LEND OR SELL SUCH COPIES FOR PRIVATE SCHOLARLY, OR SCIENTIFIC RESEARCH PURPOSES ONLY.

THE AUTHOR RESERVES ALL OTHER PUBLICATION AND OTHER RIGHTS IN ASSOCIATION WITH THE COPYRIGHT IN THE THESIS, AND EXCEPT AS HEREIN BEFORE PROVIDED, NEITHER THE THESIS NOR ANY SUBSTANTIAL PORTION THEREOF MAY BE PRINTED OR OTHERWISE REPRODUCED IN ANY MATERIAL FORM WHATEVER WITHOUT THE AUTHOR'S WRITTEN PERMISSION.

A. Lavasanifar

ADDRESS

805 11111 82 Ave,

Edmonton, Alberta, Canada

T6G 0T3

Date: Oct and , 2001

UNIVERSITY OF ALBERTA

FACULTY OF GRADUATE STUDIES AND RESEARCH

THE UNDERSIGNED CERTIFY THAT THEY HAVE READ, AND RECOMMEND TO THE FACULTY OF GRADUATE STUDIES AND RESEARCH FOR ACCEPTANCE, A THESIS ENTITLED **BLOCK COPOLYMER MICELLES FOR THE ENCAPSULATION AND DELIVERY OF AMPHOTERICIN B** SUBMITTED BY **AFSANEH LAVASANIFAR** IN PARTIAL FULFILLMENT OF THE REQUIREMENTS FOR THE DEGREE OF **DOCTOR OF PHILOSOPHY IN PHARMACEUTICAL SCIENCES.**

Dr. J. Samuel (Supervisor)

Dr. G.S. Kwon (Co-supervisor)
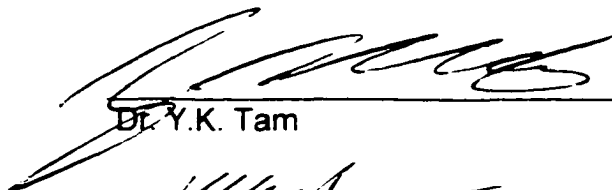
Dr. Y.K. Tam

Dr. H. Uludag

Dr. L.I. Wiebe (Chairman)

Dr. X. Li (External Examiner)

Date: Oct 1st , 2001

Dedications

This manuscript is dedicated to

My dear husband, Mohamed, whose support and encouragement has been an invaluable resource

for me.

My lovely daughters, Maryam and Leyla, whose kindness, patience and compromise with a busy

mom let me to finish this work.

And my beloved parents whose belief has given me the motivation, confidence and determination

to start.

Abstract

The attachment of drug compatible moieties in the core can be used as a tailoring strategy to modify the encapsulation and release of drugs loaded by physical means into polymeric micelles. In this context micelles self-assembled from poly(ethylene oxide)-*b*-poly(L-amino acid) (PEO-*b*-PLAA)s are of interest since a systematic alteration in the chemical structure of the core through PLAA side chains is attainable. In this thesis, this concept has been explored for the encapsulation and delivery of a model membrane active drug, amphotericin B (AmB), by a polymeric micellar nanocarrier. The incorporation of saturated fatty acid esters in the micellar core was proposed to mimic structural aspects of natural carriers of AmB, i.e., lipoproteins. PEO-*b*-poly(L-aspartic acid) (PEO-*b*-P(Asp)) derivatives conjugated to fatty acids on the core-forming block were synthesized and self-assembled into nanoscopic micelles at low critical micelle concentrations. A high viscosity and a low polarity were evidenced for the core in micelles self-assembled from fatty acid conjugates of PEO-*b*-P(Asp) derivatives. Increasing the level of fatty acid esters was found to be an efficient approach that modified micellar stability, core polarity and AmB encapsulation, reduced AmB release and haemolytic properties, but retained its antifungal activity *in vitro*. A solvent evaporation method of drug loading was used for the encapsulation of AmB into polymeric micelles, which was beneficial to a dialysis method in terms of better control over the rate of drug release and reduced toxicity without a loss of antifungal activity (haemolysis and minimal inhibitory concentration). The use of polymeric micelles for solubilization and delivery of AmB may open a new horizon in treatment of life-threatening systemic fungal diseases.

Acknowledgements

The present research has been fulfilled by the collaboration of a group of people and organizations. In this section I would like to thank some of them in particular:

Table of contents

6. THE EFFECT OF FATTY ACID SUBSTITUTION ON THE *IN VITRO* RELEASE OF AMPHOTERICIN B FROM MICELLES COMPOSED OF POLY(ETHYLENE OXIDE)-*b*-POLY(*N*-HEXYL STEARATE-L-ASPARTAMIDE) ....

7. GENERAL DISCUSSION AND CONCLUSIONS 145

List of Tables

List of Figures

List of abbreviations:

AFM	atomic force microscopy
AmB	amphotericin B
AUC	area under the curve
BLA	(β-benzyl-L-aspartate)
CD	circular dichroism
CMC	critical micelle concentration
DCC	dicyclocarbodiimide
DLS	dynamic light scattering
DMAP	dimethylaminopyridine
DMF	N,N- dimethyl formamide
DMSO	N,N- dimethyl sulfoxide
DSC	differential scanning calorimetery
G	gravitational force
h	hour
HDL	high-density lipoprotein
2-HP	2-hydroxypyridine
I_1/I_3	relative intensity of the first to the third band in the fluorescence emission spectrum of pyrene
I_e/I_m	relative intensity of the eximer to monomer band in the fluorescence emission spectrum of 1,3-(1,1'-dipyrenyl) propane
LDL	low-density lipoprotein

M_n	number average molecular weight
M_w	weight average molecular weight
MIC	minimum inhibitory concentration
μL	microlitre
μg	microgram
mL	millilitre
MTX	methotrexate
nm	nanometer
PASA	poly[*N*-(alkyl stearate)-L-aspartamide]
PASP	poly(L-aspartic acid)
P(Asp)-DOX	doxorubicin conjugate of poly(L-aspartic acid)
PBLA	poly(β-benzyl-L-aspartate)
P(BLA,C16)	poly(β-benzyl-L-aspartate-*co*-cetylaspartate)
PBLG	poly(β-benzyl-L-glutamate)
PCL	poly(caprolactone)
PDLLA	poly(D,L-lactide)
PDLLACL	poly(D,L-lactide-*co*-caprolactone)
PEMA	poly[*N*-(2-ethyl myristate)-L-aspartamide]
PESA	poly(*N*-(2-ethyl stearate)-L-aspartamide]
PEO	poly(ethylene oxide)
PGACL	poly(glycolide-*co*-caprolactone)
P(Glu)	poly(α-glutamic acid)
PHAA	poly(hydroxyalkyl-L-aspartamide)

PHCA	poly[*N*-(6-hexyl caprate)-L-aspartamide]
PHEA	poly(hydroxyethyl-L-aspartamide)
PHHA	poly(hydroxyhexyl-L-aspartamide)
PHMA	poly[*N*-(6-hexyl myristate)-L-aspartamide]
PHSA	poly[*N*-(6-hexyl stearate)-L-aspartamide)]
PLAA	poly(L-amino acid)
PLA	poly(lactic acid)
PLGA	poly(lactic-*co*-glycolic acid)
PPO	polypropylene oxide
RBC	red blood cell
RES	reticuloendothelial system
SAS	statistical analysis software
SAX	small angle X-ray scattering
SDS	sodium dodecyl sulfate
sec	seconds
SEC	size exclusion chromatography
TEM	transmission electron microscopy
Tg	glass transition temperature

Chapter 1

Introduction

A version of this chapter has been submitted to *Advanced Drug Delivery Reviews* for publication.

1

1.1. Introduction

The concept of selective delivery of drugs to their site of action was first introduced by Paul Erhlich early in the 20th century. He proposed a "Magic Bullet", i.e., carriers with specific affinity for certain organs, tissues or cells for drug targeting (1). Since then delivery systems such as liposomes, microspheres and nanoparticles have been developed for this purpose. In many cases they have been able to widen the gap between the "efficacy" and "toxicity", i.e., therapeutic index of drugs. However, there is still a long way towards a real "Magic Bullet".

Among different drug carriers used for controlled drug delivery, there has been a rising interest in self-assembled block copolymers over the past decade (2-14). This is owed to the similarity of polymeric micelles to natural carriers, e.g., viruses and serum lipoproteins. Polymeric micelles mimic aspects of biological transport systems in terms of structure and function. A hydrophilic shell helps them to stay unrecognized during blood circulation (15;16). A viral-like size (< 100 nm) prevents their uptake by the reticuloendothelial system (17) and facilitates their extravasation at leaky sites of capillaries, leading to passive accumulation in certain tissues (18-20). The small size will also ease further penetration of the micellar carrier to cells. The incorporation of recognizable moieties on micellar surface (21-24) or the development of thermo- or pH-sensitive block copolymers (25;26) has been pursued to enhance cellular interaction in specific sites for active targeting. Finally, polymeric micelles have been used for gene delivery and have shown a great potency in directing therapeutics to sub-cellular targets (11; 27).

2

The multifunctional nature of polymeric micelles appears to fulfil several tasks required for an ideal carrier capable of selective drug delivery at different levels. Emphasis has been placed on micelles made of poly(ethylene oxide)-*b*-poly(L-amino acid)s (PEO-*b*-PLAA) as synthetic analogs of natural carriers with a unique ability for chemical modification. Free functional groups on a PLAA block provides sites for the attachment of drugs (28-30), drug compatible moieties (31;32) or charged therapeutics such as DNA (27). In either case, it may be possible to fine tune the structure of the core-forming block and enhance properties of PEO-*b*-PLAA micelles for drug delivery (33;34). This concept has been explored for the selective delivery of a model membrane-acting drug, amphotericin B (AmB) to fungal cells in this thesis. The following background sets the stage for the development of such a drug delivery system.

1.2. Block copolymers: definition and classification

Copolymers are composed of different types of monomers in a polymeric chain. Based on the arrangement of monomers, copolymers are classified into three groups: random, alternating and block copolymers (Figure 1.1). Block copolymers themselves can be classified to subgroups depending on the arrangement of the polymeric blocks in the structure of the copolymer. To date, di- and tri-block copolymers have been the most commonly used copolymers for drug delivery since characteristic functions of a certain block can be expressed in a separate domain in those structures without influence from the other blocks (3; 4; 10).

3

- **Random copolymer**	AABAAABBABABBAAABA
- **Alternating copolymer**	ABABABABABABABABAB
- **Block copolymer:**	
i) Di-block type	AAAAAAAAAAABBBBBBBBBB
ii) Tri-block type	AAAAAAAAAAABBBBBBBBBAAAAAAAAAA
iii) Multi-segment type	(AAAAAAAAAABBBBBBBBBB)$_n$
iv) Graft copolymer	AAAAAAAAAAAAAAAAAAAAAA

```
                    AAAAAAAAAAAAAAAAAAAAAA
                    B         B         B
                    B         B         B
                    B         B         B
                    B         B         B
                    B                   B
                    B                   B
                                        B
```

Figure 1.1. A schematic representation of different types of copolymers (**A** and **B** are hydrophilic and hydrophobic monomer units, respectively).

1.3. Self-assembly: the hydrophobic effect

Amphiphilic di- or tri-block copolymers, as well as graft copolymers with sufficiently long grafts and flexible backbones, tend to self-assemble into core/shell architectures in a selective solvent above their critical micelle concentration (CMC) (2;12). A selective solvent is a good solvent for one block and a non-solvent for the other. In an aqueous environment the hydrophobic blocks of the copolymer form the core while the hydrophilic blocks form the outer shell. The hydrophobic core acts as a nanoreservoir for drug solubilization while the hydrophilic shell interfaces the biological media (Figure 1.2) (8;10).

Self-association of block copolymers was first verified by small angle X-ray scattering (SAXS) of an ABA block copolymer, poly(styrene)-*b*-poly(butadiene)-*b*-poly(styrene), in ethyl methyl ketone, which is a selective solvent for the poly(styrene)

4

block (35). Formation of micelle like structures in aqueous media was confirmed later for different block copolymers by atomic force microscopy (AFM), dynamic light scattering (DLS) and transmission electron microscopy (TEM) techniques (36-39).
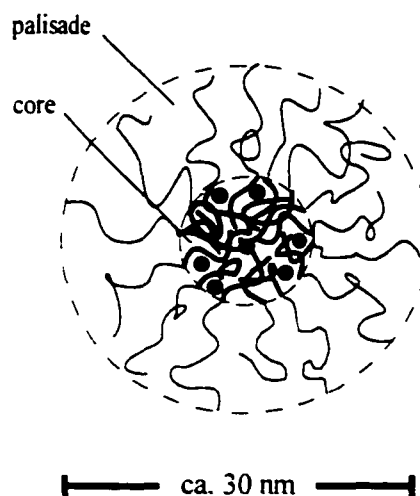
Figure 1.2. Sketch of a polymeric micelle loaded with drug in core.

Micellization is a spontaneous process leading to a net decrease in the total free energy of the system. The amount of change in the free energy, ΔG, is dependent on changes in the enthalpy, ΔH, and the entropy, ΔS, of the system (Eq 1.1):

$$\Delta G = \Delta H - T\Delta S \qquad (Eq\ 1.1)$$

In organic solvents, micellization is exothermic (enthalpy-driven). In aqueous solvents, micelle formation is often endothermic (entropy-driven). Therefore, elevated temperatures would stimulate micelle formation in an aqueous environment while causing the solubilization of micelles in an organic solvent (12).

The key to understanding the entropy driven micellization in an aqueous environment is the hydrogen bonding of water. Hydrogen bonds between water

5

molecules are broken at the edge of the hydrocarbon chain of an amphiphile, leading to a positive enthalpy contribution. Because of surface tension, water molecules become more ordered around the hydrocarbon chain with an attendant decrease in entropy. Formation of micelles from individual amphiphiles allows the cavity to revert to the structure of pure liquid water and an increase in entropy (hydrophobic effect) (40). The entropy driven micellization process may proceed further by a combination of hydrophobic interaction, electrostatic interaction, metal complexation and hydrogen binding of block copolymers (27).

Evidence points to a closed association for micellization of block copolymers, where sufficient cohesive forces in the micellar core exist (41). An estimate for the changes in standard free energy of micellization, $\Delta G°$, by closed association is given by equation 1.2:

$$\Delta G° = RT \ln [CMC] \qquad Eq\ (1.2)$$

where R is the gas constant and T is the absolute temperature (40). The thermodynamic tendency of micellization, is represented by a negative value of $\Delta G°$ and a low CMC.

1.4. Functional properties of polymeric micelles for passive drug targeting

Carriers should meet several conditions for effective drug delivery, including water solubility, non-toxicity, non-immunogenicity, lack of long-term accumulation in host, *in vivo* stability and selective delivery to the target site. Besides a capacity for the encapsulation of poorly water-soluble drugs, the carrier is required to prevent drug release before reaching the site of action to achieve targeted drug delivery. The multiple

6

properties of the core/shell structure in polymeric micelles allow the simultaneous fulfilment of these somewhat opposing requirements.

1.4.1. Water solubility – Polymeric carriers often tend to precipitate in water due to a localized hydrophobicity caused by the drug and the hydrophobic portion of the polymeric chain. The problem is more significant for drug-polymer conjugates where water-soluble functional groups of the drug, (e.g., amino and carboxyl groups) are converted to more hydrophobic groups (e.g., amide) by the conjugation process. With a core/shell structure, the polymeric carrier may stay water-soluble if $N_A \gg N_B^{2/3}$. N_A and N_B are the number of monomers in the shell and core-forming block, respectively (42).

1.4.2. Biocompatibility – Toxicity studies have been mostly carried out on Pluronics[®], block copolymers composed of PEO and poly(propylene oxide) (PPO) (PEO-*b*-PPO-*b*-PEO). They are fairly safe, particularly those with a high content of PEO (43; 44). PEO is widely used in the design of non-immunogenic carriers. Block copolymers with biodegradable core-forming blocks such as poly(D,L-lactic acid) (PDLLA) and poly(L-amino acid) (PLAA) are of increasing interest, because they may undergo hydrolysis and/or enzymatic degradation, producing biocompatible monomers of lactic or amino acids. Polyesters such as PDLLA have been used safely in human for a long time. Studies on degradability of PLLAs are few. Nevertheless, results indicate a dependence of enzymatic degradability on the chemical structure and physicochemical properties of the PLAA chains (45-48).

7

Lastly, block copolymers having molecular weights less than 50,000 $gmol^{-1}$ can be excreted by the kidneys (49).

1.4.3. Micellar stability – The stability of micellar structures should be assessed in two different aspects: thermodynamic stability and kinetic stability.

Large molecular dimensions of the core-forming segment in block copolymers induce a strong tendency for aggregation, in other words high thermodynamic stability. This pushes the CMC to very low levels (4;50) (Equation 1.2) (42). A reverse relationship between the hydrophobicity of the core-forming block and CMC has been shown in many studies (50-52).

The entropy driven self-assembly of block copolymers may be followed by a hydrophobic or electrostatic interaction in the core depending on the structure of the core-forming blocks. Strong cohesive forces resulting from these interactions make the micellar system kinetically stable. As a result, a slow dissociation rate may exist for polymeric micelles below the CMC, and polymeric micelles may not necessarily exist in equilibrium with polymeric unimers. Kinetic stability may be high for polymeric micelles with stiff or bulky core-forming blocks due to hindrance of rotation. The strength of cohesive forces may be characterized by glass transition temperatures (T_g) (53), degree of crystallinity and cross-linkage in the micellar cores.

Micelles are subject to extreme dilution upon intravenous injection into humans. If kinetically stable, slow dissociation allows polymeric micelles to retain their integrity and perhaps drug content in blood circulation above or even below CMC for some time. This may give them a chance to reach the target site before decaying to single chain

8

unimers. In this situation, interactions of polymeric micelles with components of blood (serum proteins) and cells must be weighed in terms of micellar stability and drug release.

1.4.4. Biological half-life: lessons from nature – Long circulation times are

prerequisite to achieve depot properties. Carriers with insufficient stabilities tend to break up and be removed rapidly from blood by kidneys. The molecular weight of polymeric micelles ($\geq 10^6$ gmol^{-1}) prevents renal elimination unless the micelle dissociates to unimers (37;49). Supramolecular structures with sufficient stability often end up accumulating in the liver and spleen due to a large size or protein adsorption, both triggering a rapid uptake by the reticuloendothelial system (RES). For this reason, drug delivery to organs other than liver and spleen is limited for such carriers.

Delivery systems that are smaller than 200 nm have low uptake by RES and may circulate in blood for prolonged periods (9;16;17; 20;54-56). Polymeric micelles usually range in size between 10 to 50 nm (5;9). This range is much smaller than the size of other self-assembled delivery systems and similar to the size of serum lipoproteins and viral particles. The nanoscopic size facilitates the extravasation of polymeric micelles at leaky sites of capillaries e.g., tumours and sites of inflammation (20;54;55). They may even enter cells by different mechanisms (57-60). Other advantages associated with nanoscopic dimensions of polymeric micelles include the ease of sterilization via filtration and safety of administration (5;7).

The presence of a hydrophilic polymeric brush on the surface of polymeric micelles (e.g., PEO shell) induces steric repulsive forces and stabilizes the micellar interface. This prevents adsorption of biological components to the delivery system (16).

9

As a result, polymeric micelles may escape the uptake of RES efficiently. The extent of steric stabilization is dependent on length of the hydrophilic block and its density on colloidal particles (15). In fact, block copolymers were originally used as stabilizers for colloidal dispersions such as emulsions, liposomes or nanoparticles. The adsorption of block copolymers on the surface of those carriers was found to affect the pharmacokinetics and biological fate of the delivery system, leading to a long circulation and accumulation in sites with leaky capillaries (16; 61).

1.4.5. Morphology – Most of the polymeric micelles designed and used for drug delivery are reported to be spherical, evidenced by atomic force microscopy (AFM), dynamic light scattering (DLS), regular and cryo-TEM (30;34;39;51;52;62-65). A transfer to ellipsoid, rod and lamellar micelles may occur as the proportion of core to shell-forming block, copolymer concentration, type and concentration of electrolytes in the medium, temperature, organic solvent, and the method of micellar preparation are altered. The effect of such factors on the shape of polymeric micelles has been reviewed (9;66). The effect of micellar morphology on loading, release and efficacy of drugs remains to be explored.

1.4.6. Drug loading – Micellar cores serve as a nanoresorvoir for loading and release of hydrophobic molecules that are conjugated or complexed with the polymeric backbone or physically encapsulated in the core (8;9;27). The extent of drug incorporation in polymeric micelles by physical means is dependent on several factors including the molecular volume of the solubilizate, its interfacial tension against water,

10

length of the core and shell-forming blocks in the copolymer, and the polymer and solubilizate concentration (67-69). The partition coefficient of the hydrophobic molecule between the micellar core and surrounding aqueous medium describes the extent of drug entrapment in polymeric micelles (67). The greatest degree of solubilization occurs when high compatibility exists between the micellar core and the solubilizate, assessed by the Flory-Huggins interaction parameter (χ_{sp}):

$$\chi_{sp} = (\delta_s-\delta_p)^2 V_s/RT \qquad \text{(Eq 1.3)}$$

where δ_s is the Scatchard-Hildebrand solubility parameter of the solubilizate, δ_p the Scatchard-Hildebrand solubility parameter of the core-forming polymer, V_s is the molar volume of the solubilizate, R is the gas constant and T the Kelvin temperature. The highest compatibility is achieved when $\delta_s = \delta_p$.

The chemical conjugation of drugs or complex formation between block copolymers and charged therapeutics has been used as an alternative approach in drug delivery by polymeric micelles (27). In either case, existence and accessibility of functional groups on the polymeric backbone is a requirement.

1.4.7. Release characteristics – Evidence points to sustained release characteristics for many solubilizates encapsulated in polymeric micelles by chemical or physical means (30;34;62;70-74). The stability of the micellar structure is a prerequisite for control over the rate of drug release. For drugs physically encapsulated in stable structures of polymeric micelles, release is controlled by the rate of drug diffusion in the micellar core or break up of the micelles (Figure 1.3). The diffusion rate may be quite low if a favourable interaction exists between the solubilizate and the core-forming block

11

in a rigid core (32;75;76). An inordinate slow release rate of indomethacin in an unionized form compatible with a nonpolar core of a micellar carrier has been shown (70).
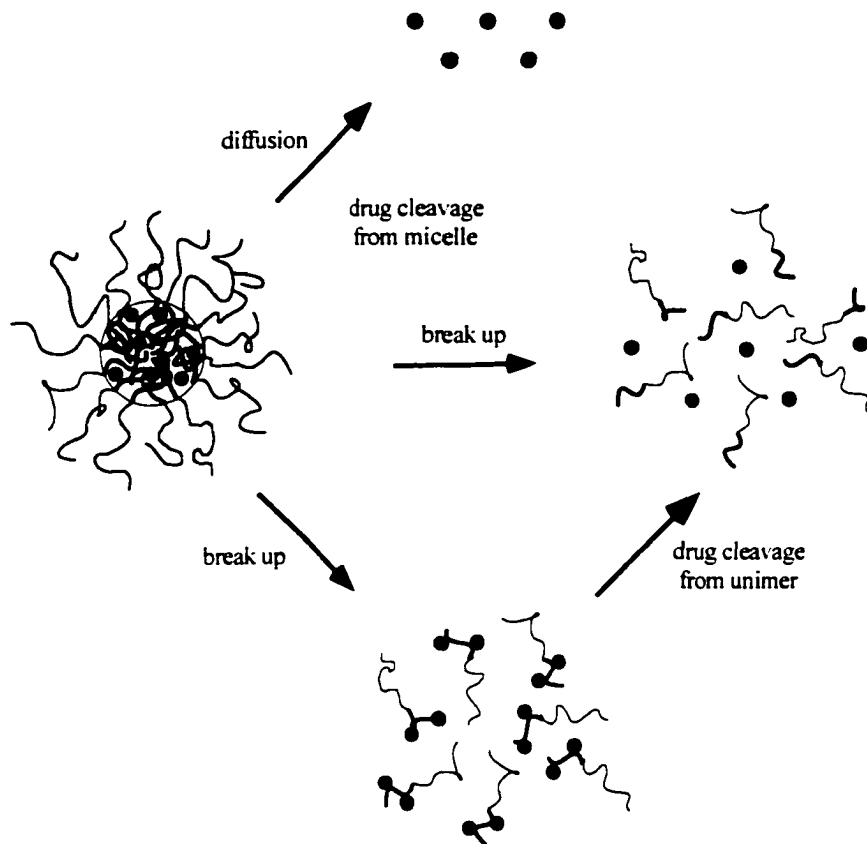
Figure 1.3. Mechanisms of drug release for polymeric micelles.

The physical state of the micelle core and encapsulated drug plays an important role. The same factors may contribute to enhanced kinetic stability for the micelle structure as described earlier. The design of block copolymer micelles with glassy cores under the physiological condition (37°C) would favour the release in a sustained manner. Glassy cores of poly(styrene) and poly(tert-butyl acrylate) have been proposed to slowly release pyrene from a micellar carrier (diffusion constant of 10^{-18} to 10^{-16} cm^2/sec). In

12

contrast, pyrene was released too rapidly to be assessed from swollen cores of poly(2-vinylpyridine), which are liquid like under the experimental conditions (77). Drug release may be sustained following an increase in the loading content, owing to the crystallization of solubilizate in the polymeric carrier, evidenced by differential scanning calorimetery (DSC) in a few cases (51;52;62). The localization of the solute in the core/shell structure, micellar size and molecular volume of the drug are among other factors influencing the rate of drug diffusion in the polymeric carrier.

In case of drug conjugates, the covalent bond between the therapeutic molecule and the polymer has to be cleaved for drug release. Water penetration and hydrolysis of the liable bonds in the micellar core (bulk erosion), followed by drug diffusion may occur in relatively hydrophilic liquid-like core structures (Figure 1.3). Water diffusion into hydrophobic and rigid cores may be restricted. Therefore, in this case release may be dependent on the rate of micellar dissociation. The slow dissociation of the micellar structure to single polymeric chains and further hydrolysis of the liable bonds may result in a sustained drug release (34). If the micellar structure is sufficiently stable, drug release might even be delayed until carrier reaches target cells. It might be possible to tailor the chemical structure of polymeric micelles and adopt either of these mechanisms to fulfil specific requirements of drug release.

1.5. Polymeric micelles versus surfactant micelles for drug delivery

Similar to block copolymers, low molecular weight amphiphiles are well known to form micelles that solubilize hydrophobic drugs for parenteral administration. For the

13

purpose of drug delivery clear advantages may exist for polymeric micelles, mainly due to the polymeric nature of these systems.

The tendency for micellization is overall much higher in block copolymers in comparison to surfactants since the exposure of a long hydrophobic block to water is unfavourable to a greater extent. Thermodynamic stability is characterized by low CMC values, which are usually in the μmolar range for polymeric micelles. This contrasts with typical millimolar CMC levels of low molecular weight surfactants (39;50). Following self-association, the concentration of free amphiphile remains at the CMC level. As a result, one can assume a higher number of micelles to be formed in a given concentration for block copolymers in comparison to surfactants.

Hurter and Hatton have shown a greater capacity of solubilization for polymeric micelles in comparison to low molecular weight surfactants for toluene (78). This was attributed to higher number of micelles formed from self-assembly of block copolymers and larger cores.

Upon dilution in blood, the polymeric micelles may remain kinetically stable, while the surfactant micelles are diluted to values below CMC and rapidly dissociate (Figure 1.4). The concentration of the low molecular weight surfactant cannot be raised to compensate for the situation, since high concentrations of low molecular weight surfactants are usually toxic and not suitable for administration (79). The slow dissociation rates (in hours and days) have been reported for polymeric micelles under sink conditions even below their CMC (2). The kinetic stability of polymeric micelles with rigid cores is in sharp contrast to surfactant micelles, which tend to break up in milliseconds upon dilution and are in continuous exchange with their unimers in solution

14

(2). ^{1}H NMR and fluorescent probe studies (30;50) evidence the existence of rigid cores in polymeric micelles.

Unlike low molecular weight surfactant micelles that typically have mobile cores, sustained and controlled drug release may be achieved with polymeric micelles. As a result, the rapid loss of drug from micelles with attendant risk of intravascular precipitation of water-insoluble drug poses less risk. Further, polymeric micelles may potentially act as a nanoscopic drug depot and influence the pharmacokinetics of drugs in a favourable manner. In this sense, polymeric micelles mimic serum lipoproteins for drug

slow break up

(sec, min to hrs)

block copolymer micelle

fast break up

(milliseconds)

low molecular weight
surfactant micelle
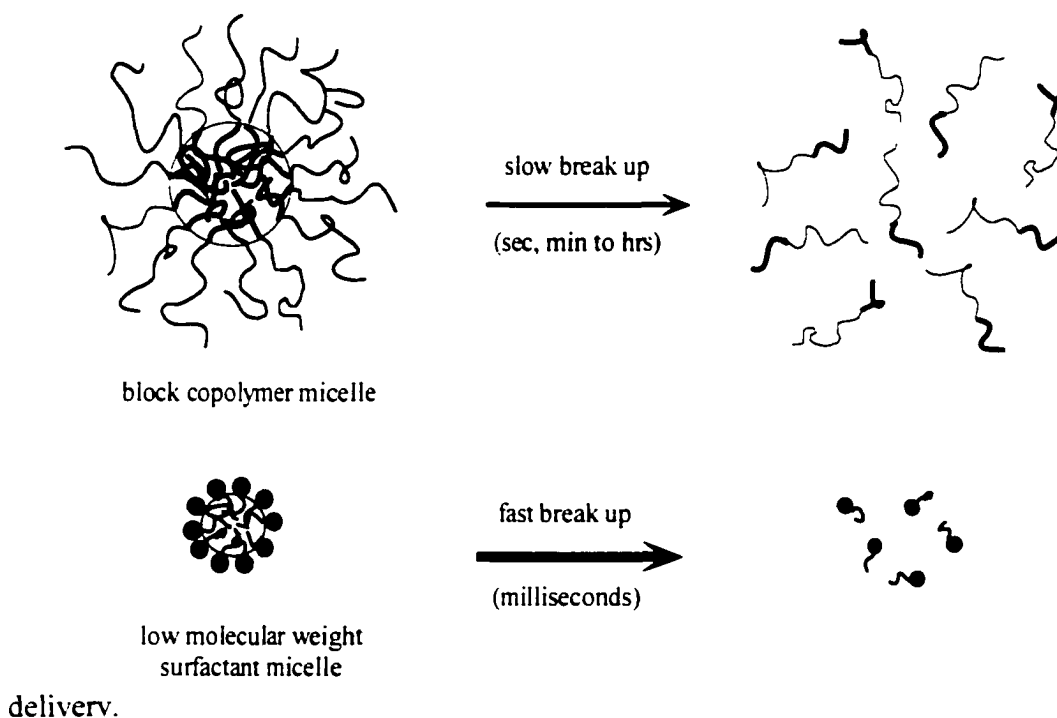
delivery.

Figure 1.4. Break up of polymeric micelles versus low molecular weight surfactant micelles.

1.6. Block copolymer micelles used for drug delivery

Micelle-forming block copolymers have been the focus of several studies over the past few years (3;4;9;36;57;69;80-84). Efforts have led to the preparation of micellar

15

carriers that can be safely administered to humans and adequately solubilize drugs. The hydrophilic block in these systems is usually PEO with a molecular weight ranging from 1,000 to 20,000 $gmol^{-1}$. PEO has been used safely in humans. The use of other hydrophilic polymers as shell-forming blocks has been reported for bioadhesive (85) or thermoresponsive (36;63;86) properties. Unlike the shell-forming block, the choice for a core-forming block is relatively diverse. The length of the core-forming block is usually equal or shorter than the PEO block to maintain water solubility and form spherical core/shell micelle structures.

Most of the studies on block copolymers have been conducted on Pluronics®. Like low molecular weight surfactants, Pluronics® demonstrate solubilizing effects for parenteral drug administration (43;44;87). Pluronics® have been used to solubilize haloperidol (21;88), indomethacin (89), doxorubicin (DOX) (83), epirubicin (83) and amphotericin B (AmB) (90). Overall, many Pluronics® used for drug solubilization have high ratios of PEO to PPO and are non-toxic relative to many low molecular weight surfactants, e.g., Tween 80, especially in terms of cell membrane lysis, e.g., haemolysis.

Relatively hydrophobic Pluronics®, on the other hand, have been used to induce immune responses, i.e., act as an adjuvant (91;92). Pluronics® have shown other important biological effects, inhibiting P-glycoprotein, which is believed to be at least partly responsible for multi-drug resistance in cancer cells (57;83). Lastly, Pluronics© have been used to increase the transport of drugs across membrane barriers (21;58).

To avoid long-term toxicities, biodegradable block copolymers with polyester core-forming structures such as poly(lactic acid), poly(glycolic acid), poly(caprolactone) and their copolymers have been developed and used for drug delivery. Polyesters have a

16

history of safe use in humans as biodegradable surgical sutures, bone fracture fixture devices and controlled drug delivery systems. The synthesis of PEO-*b*-polyesters was reported back in 1950s (93). In 1994, Gref *et al.* prepared block copolymers of PEO-*b*-poly(lactic-*co*-glycolic acid) (PEO-*b*-PLGA) and PEO-*b*-poly(caprolactone) (PEO-*b*-PCL). Following self-assembly by an O/W emulsion process, nanospheres with an average diameter of 140 nm were formed from PEO-*b*-PLGA, showing an enhanced blood circulation particularly at a high PEO content. The carrier was used successfully to encapsulate lidocaine and prednisolone (45 % w/w drug to polymer) (62).

In a separate study long circulating nanospheres of PEO-*b*-PDLLA were developed (94). The same block copolymer was shown to form a micellar fraction (< 50 nm in size), which was able to solubilize model hydrophobic drugs, such as sudan black B and testosterone in 63.9 and 0.74 % w/w drug to polymer, respectively (39). The greater extent of solubilization for sudan black B was attributed to its higher hydrophobicity. A family of PEO-*b*-poly(lactic acid) (PEO-*b*-PLA) block copolymers with different lengths of the PLA block were prepared recently, and used to encapsulate a water soluble drug (95). An increase in the length of the PLA block caused an increase in the size of nanoparticles but did not affect their encapsulation properties.

Micelles of PEO and PDLLA block copolymers, poly(D,L-lactic acid-*co*-caprolactone) (PDLLACL) or poly(glycolic acid-*co*-caprolactone) (PGACL) have been used to encapsulate taxol (96). The greatest physical stability was observed for the taxol formulation of PEO-*b*-PDLLA micelles with no sign of precipitation in 24 h . This was attributed to higher hydrophobicity and T_g of the PDLLA block. The loading weight proportion of taxol in PEO-*b*-PDLLA micelles with higher PDLLA contents reached 25

17

%, and its solubility increased 5000 fold (97), which contrasts with the loading of 0.5 % for the same drug in Pluronic® micelles.

Taxol in PEO-*b*-PDLLA micelles shows a similar *in vitro* cytotoxicity, a five-fold increase in maximum tolerable dose and an increased efficacy after interperitoneal injection in murine P388 leukemia model in comparison to its standard formulation in Cremophor (98). Slow drug release from the micellar carrier was anticipated based on a high core viscosity and an interaction between taxol and PDLLA segment, evidenced by ^{1}H NMR and solubility data, respectively (97). A similar distribution in protein components of the human plasma for free and PEO-*b*-PDLLA incorporated taxol (99), rapid dissociation of tritium labelled taxol after IV injection to rat models and the elimination of micellar carrier within 15 h. however, did not support a sustained drug release behaviour for taxol in PEO-*b*-PDLLA micelles (96;100).

PEO-*b*-PCL self assembles into micelles that can encapsulate indomethacin (76;101), dihydrotestostrone (75), taxol (102) and a number of neurotrophic agents with hydrophobic properties (82;103). There are reports on the use of poly(glycolic acid) (104), PLGA (105) and PLA (106) as blocks for the encapsulation of indomethacin and DOX. The size of resulting particles was found to be above 100 nm, however.

Kataoka *et al.* have reported on the preparation of functional PEO-*b*-PDLLA micelles with aldehyde groups on their surface by a method illustrated in Figure 1.5 (22;65). More than 80 percent of the acetal group on the micelle surface was converted to aldehyde within 4 h of reaction under acidic conditions (65). No change in micellar size and shape was evidenced after this conversion. The reaction of aldehyde group with benzoic hydrazide as a model compound was evidenced by an increase in the UV

18

absorption of the micellar peak in SEC chromatograms. Recently, the authors have reported the conjugation of peptidyl ligands to the aldehyde group of the micellar surface through Schiff base formation and further reduction (23). Chemical engineering of the core-forming blocks in such carriers in underway (107).

In a separate approach, PEO blocks having site-specific sugar groups at their chain ends have been achieved through ring opening polymerization using D,L-lactide. The block copolymer form micelles with glucose or galactose moieties on their surfaces. The galactose residues bind sugar binding sites of RCA1-lecetine molecule (108). Such strategies may be used to achieve intelligent polymeric micelles for active targeting by receptor-mediated endocytosis.

EtO
   \
    >CHCH₂CH₂O(CH₂CH₂O)-(COCHO)-H
   /   x | y
EtO   CH₃
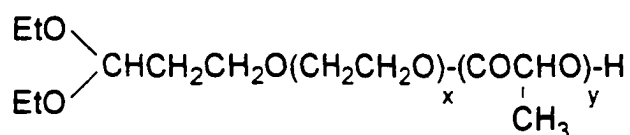
Poly(ethylene oxide)-*block*-poly(lactic acid)

water
⟶
sonication

H⁺
⟶

OHC
OHC
CHO
CHO
OHC
OHC
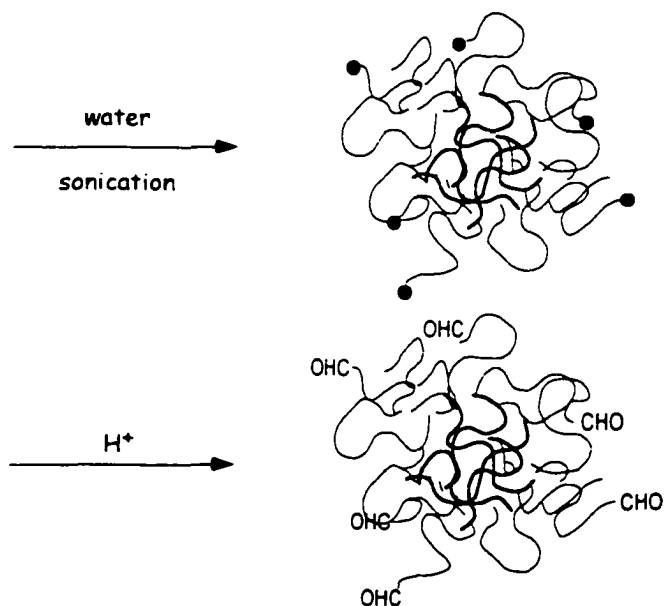
Figure 1.5. Preparation of PEO-*b*-PDLLA micelles with functional groups on their surface.

19

1.7. Micelle-forming PEO-*b*-PLAAs for drug delivery

Micelles based on PEO-*b*-PLAA block copolymers are unique among drug carriers owing to a tailor-made non-polar core of PLAA, which can take up and protect water-insoluble drugs. A primary advantage of PEO-*b*-PLAA over other micelle-forming block copolymers is a potential for attachment of drugs, drug compatible moieties, genes or intelligent vectors in the micellar core through free functional groups (e.g., amine or carboxylic acid) of the amino acid chain. A systemic alternation in the structure of the core-forming block may lead to a better control over the extent of drug loading, release or activation. Preparation of PEO-*b*-PLAA micelles with functional groups on the surface for the attachment of recognizable moieties has recently been reported (109). Lastly, there is evidence that PEO-*b*-PLAA micelles may easily be sterilized by filtration, freeze-dried, reconstituted and administered safely (5).

To date, three different types of drug delivery systems based on PEO-*b*-PLAA block copolymers have been investigated (Table 1.1):

1. Micelle-forming block copolymer-drug conjugates

2. Micellar nano-containers, and

3. Polyion complex micelles.

20

Table 1.1. Micelle-forming block copolymers based on PEO-*b*-PLAA used for drug delivery.

Polymeric micelle delivery system	Core-forming block	Encapsulated molecule	Reference
Drug conjugates	Poly(L-lysine)	Cyclophosphamide	(110)
	P(Asp)	Doxorubicin	(28;111)
		Cisplatin	(29;112)
	Poly(hydroxy alkyl-L-aspartamide)	Methotrexate	(30;34)
Nano-containers	P(Asp)-(DOX)	Doxorubicin	(113)
	PBLA	Pyrene	(114)
		Doxorubicin	(72; 73;115)
		Indomethacin	(70)
		Amphotericin B	(116;117)
	P(BLA, C-16)	KLN-205	(31;118)
	PBLG	Norfloxacin	(52)
		Clonazepam	(51)
Polyion complex micelles	Poly(L-lysine)	Poly(L-aspartic acid)	(119;120)
		Plasmid DNA	(121)
	P(Asp)	Lysozyme	(122;123)
	Poly(L-lysine/L-glycine)	DNA	(124)

1.7.1. Micelle-forming block copolymer-drug conjugates – In the 1980s, Ringsdorf *et al.* were the first to prepare a micelle-forming drug-copolymer conjugate. They attached a cytotoxic agent, a cyclophosphamide-sulfido derivative, to the poly(L-lysine) of a PEO-*b*-poly(L-lysine) block copolymer and used hydrophobic moieties (palmitic acid) to induce

21

the required amphiphilicity for micelle-formation (Figure 1.6) (110). Micelle formation

was evidenced by solubilization of a hydrophobic dye (60). The liberation of the active

metabolite, 4-hydro-cyclophosphamide, could be varied within a time scale of mins to hs,

depending on the structure of the conjugate. Pendant palmitic acid residues had a marked

effect on drug release. *In vitro* studies indicated that the cyclophosphamide-containing

block copolymer acts as an intracellular depot for the active metabolite. *In vivo* studies

indicated enhanced antitumor effects of cyclophosphamide-containing block copolymer

compared to free drug (L1210 model) (110).
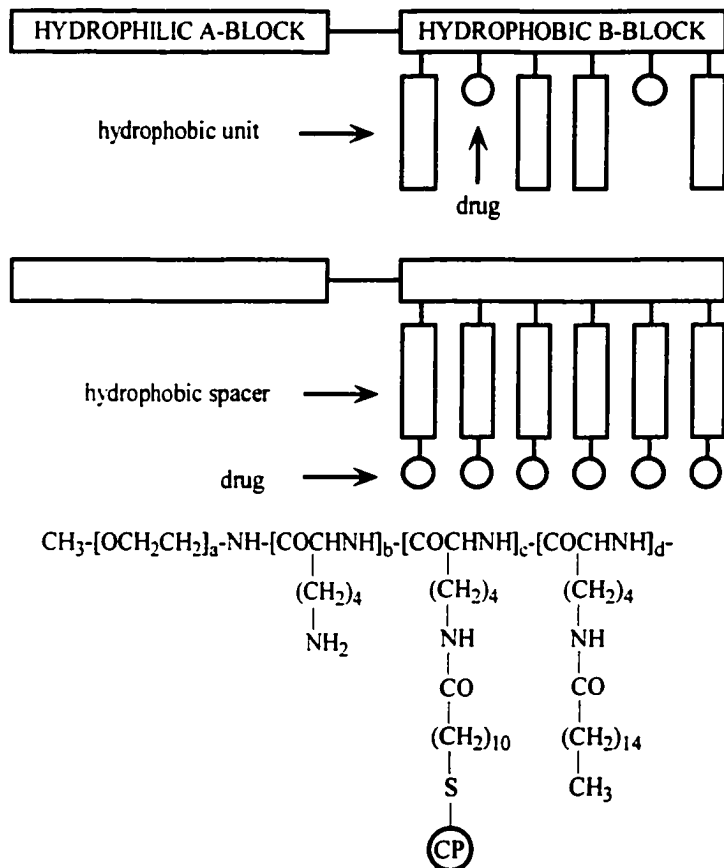
Figure 1.6. First models of micelle-forming block copolymer-drug conjugates and first example with cyclophosphamide.

22

The hydrophobicity of a therapeutic molecule itself has been utilized to achieve the amphiphilicity required for micellization of a conjugate prepared from PEO-b-poly(L-aspartic acid) and doxorubicin (PEO-b-P(Asp)-DOX) (Figure 1.7). Yokoyama *et al.* attached DOX onto the P(Asp) backbone through an amide bond between the carboxylic group of aspartic acid and the amino group of the glycosidyl residue on DOX (28;111). The level of conjugated DOX was varied by changes in reaction conditions, e.g., level of drug. Depending on the length of the PEO chain, substitution level of DOX on the polymeric backbone was kept under a certain level to avoid precipitation. DLS and SEC studies were able to reveal the presence of micelles with an average diameter of 15 to 60 nm (2;28;125;126). The quenching of DOX fluorescence and lack of ^{1}H NMR peaks for the P(Asp) block for the conjugate in water (D$_2$O) signaled the presence of micelles with rigid cores filled with self-aggregated drug. A 40-50 % of DOX substitution on P(Asp) and a decrease in proportion of P(Asp)-DOX to PEO segment was necessary to achieve stable micelles (33;127). Long PEO chains were favorable, avoiding the formation of secondary aggregates, and micelle interaction by biological components (2;28;128). The physicochemical properties of this system are reviewed elsewhere (129).

Optimized structures of PEO-b-P(Asp)-DOX formed stable micelles that could dissociate into unimers at a slow rate over a period of days in phosphate buffer (127). In the presence of 10 % rabbit serum, the dissociation rate of PEO-b-P(Asp)-DOX micelles doubled (33;127). Subsequently, radioiodinated PEO-b-P(Asp)-DOX micelles were found to circulate for prolonged periods in blood in healthy ddy mice in comparison to free DOX. The volume of distribution was 2000 mL for DOX and 3.6 mL for PEO-b-

23

P(Asp)-DOX. The accumulation of DOX in major organs was reduced, especially the heart, where DOX expresses dose-limiting cardiotoxicity (128;130).
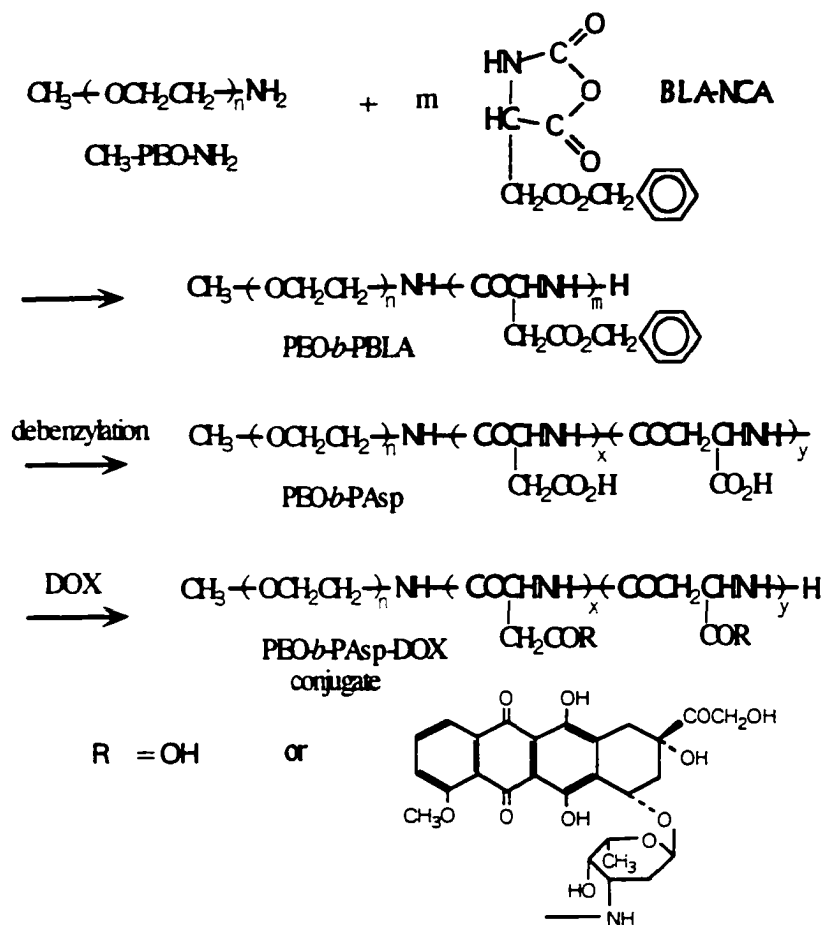
Figure 1.7. Synthesis of micelle-forming poly(ethylene oxide)-*b*-poly(aspartic acid)-doxorubicin conjugates.

The biodistribution of long-circulating PEO-*b*-P(Asp)-DOX conjugates was assessed in tumor bearing mice (female CDF1 mice, transplanted with C26 tumor cells). For PEO-*b*-P(Asp)-DOX micelles with a 12,000 and a 2100 gmol^{-1} of PEO and P(Asp) blocks, respectively, the delivery of DOX to solid tumors was enhanced in comparison to drug alone, and the tumor to heart selectivity of DOX was improved from 0.9 to 12 at 24 hs (131).

24

In a P338 murine model, DOX was active at 15 mg/kg after intraperitoneal injection (125) but caused a remarkable weight loss in animals at that dose. A similar level of activity for PEO-*b*-P(Asp)-DOX was obtained at a much higher dose (200 mg/kg of DOX), accompanied by a temporary weight loss. A similar trend was observed for several tumor models after intravenous injection of PEO-*b*-P(Asp)-DOX (130). Judging from these results, the superiority of the PEO-*b*-P(Asp)-DOX conjugates over free drug was mainly due to lowered toxicity (20 times decrease in DOX maximum tolerable dose) than improved efficacy (125;126;130). This allowed for the administration of higher doses of DOX. Adjusting the composition of the block copolymer and the dose of DOX led to improved efficacy, evidenced by complete disappearance of C26 tumors in animal subjects (132). It was later found that PEO-*b*-P(ASP)-DOX conjugates are not the active species causing tumor disappearance in C26 transplanted mice (32;113). The antitumor activity was in fact caused by non-conjugated DOX encapsulated in the micellar structure. As it turns out, the amide linkage was too stable for drug release. This finding led to use of PEO-*b*-P(Asp)-DOX conjugates as nanocontainers for physically encapsulated DOX (113).

Cisplatin has been complexed with carboxyl groups on PEO-*b*-P(Asp) to form a metal complex micelle (Figure 1.8). DLS and SEC (29) showed the existence of micelles with an average diameter of 20 nm at a critical substitution molar ratio of cisplatin to Asp units of 0.5. The cisplatin complexed micelle was stable in distilled water at room temperature. In 0.15 M NaCl, however, an exchange between the chloride ion and cisplatin lead to a sustained release of drug from its polymeric complex over 50 h (112). Accordingly, a time dependent cytotoxicity was observed for cisplatin complexes of

25

PEO-*b*-P(Asp), with an overall five fold increase in the cytotoxic concentration against B16 melanoma cells (29). Cisplatin complexes of PEO-*b*-P(Asp) demonstrated plasma AUC and tumor accumulation 5.2 and 14 times greater than cisplatin alone, respectively, and had less nephrotoxicity (133). A cisplatin complex of PEO-*b*-poly(α-glutamic acid) (PEO-*b*-P(Glu)) has shown greater stability, a prolonged circulation in blood stream and an improved accumulation in tumor site in comparison to the PEO-*b*-P(Asp) complex of cisplatin (134).

$$CH_3 \ (OCH_2CH_2)_{\overline{n}} \ NH-(COCHNH)_{\overline{x}}-(COCH_2CHNH)_{\overline{y}}H$$

PEO-*b*-P(ASP)

CH₂COOH   COOH

+

Cisplatin complex (NH₃, Pt, Cl structure)

↓ **in H₂O**

$$CH_3 \ (OCH_2CH_2)_{\overline{n}}-NH-(COCHNH)_{\overline{x}}-(COCH_2CHNH)_{\overline{y}}H$$

CH₂COOR   COOR

Cisplatin

R = Na⁺   or   (Pt complex with NH₃, Cl)   or   (Pt complex with NH₃)

Figure 1.8. Complex formation of cisplatin and PEO-*b*-P(Asp).

To overcome the excessive stability of an amide linkage between a drug and core-forming block, an ester bond has been utilized to attach another cytotoxic agent, methotrexate (MTX) and create a hydrolysable micelle-forming conjugate (Figure 1.9). The slow release of steroids attached to poly(hydroxyalkyl-L-glutamate) through an ester bond for long periods of time after a subcutaneous injection of conjugate microparticles

26

had been reported by Feijen *et al.* (135). MTX esters of PEO-*b*-poly(2-hydroxyethyl-L-aspartamide) were prepared and shown to self assemble to micellar structures with an average diameter of 14 nm as determined by TEM. MTX conjugate micelles gradually released the drug, owing to ester hydrolysis in PBS, pH = 7.4 at room temperature. Notably, MTX conjugate micelles were quite stable and could elute entirely as micelles during SEC-HPLC. Adjusting the level of attached MTX was used to control the stability of the polymeric micelles as well as influence the rate of drug release. It was concluded that MTX esters of PEO-*b*-poly(2-hydroxyethyl-L-aspartamide) could be structurally modified by varying the degree of drug substitution, which in turn changed the overall hydrophobicity of the block copolymer, thereby influencing micelle stability and controlling drug release.

$H_3O(CH_2CH_2O)mCH\ _2CH_2NH(COCHNH)x(COCHNH)n-xH$

CH$_2$ CH$_2$

CO   CONHCH$_2$CH$_2$OH

HOOC   CH$_2$CH$_2$COOCH$_2$CH$_2$ NH

H   NHCO   N   CH$_3$ NH$_2$

CH$_2$ N

NH$_2$

PEO block   Poly(L amino acid) block

alkyl spacer group ⟶

hydrophobic drug ⟶

Figure 1.9. Synthesis of MTX conjugates of PEO-*b*-poly(2-hydroxyethyl-L-aspartamide).

27

1.7.2. Micellar nanocontainers – The physical encapsulation of drugs within polymeric micelles is generally a more attractive approach than micelle-forming polymer-drug conjugates, since many polymers as well as drug molecules do not bear reactive functional groups, e.g., carboxyl, hydroxyl or amino groups, for chemical conjugation, or the free functional site may be required for the pharmacological effectiveness of the drug. In addition, conjugates of drugs may exhibit markedly dissimilar biological properties relative to parent drugs, leading to inherent difficulties in characterization and regulatory approval even for already approved drugs.

Similar to micelle-forming polymer-drug conjugates, micellar nanocontainers are expected to resist uptake by the RES and dissociation in the blood compartment, which may lead to preferential accumulation of the carrier at target sites. The carrier may then act as a depot, releasing its drug content without going through an extra step of drug cleavage. The drawbacks for micellar nanocontainers are the possibility of low encapsulation capacity or the rapid release of encapsulated drugs, i.e., dose dumping. The encapsulation and release characteristic of polymeric micelles might be modified for each particular drug or class of drugs through the attachment of drug compatible moieties to the core-forming block, which is easily attainable for PEO-*b*-PLAA micelles (5;32;39;114).

In the early 1980s, Kabanov *et al.* reported on the physical encapsulation of drugs in polymeric micelles as nanocontainers for drug delivery. They encapsulated haloperidol (21;88) and DOX (83) in Pluronic® micelles. The neuroleptic activity of solubilized haloperidol was enhanced by Pluronic® micelles, presumably owing to increased uptake into the brain. The penetration of the micellar carrier to brain was enhanced further when

28

a monoclonal antibody against specific antigen of brain glial cells, i.e., anti-α_2-GP Ab, was partially inserted on the Pluronic® micelles. As a result, mobility was drastically decreased in animals received haloperidol in anti-α_2-GP Pluronic® micelles in comparison to subjects treated with haloperidol in standard Pluronic® micelles (P85). The delivery of digoxin to brain has been revealed to be enhanced by Pluronic® P85 by the same group (136).

Physically encapsulated DOX in Pluronic® micelles (L61 and F127) significantly increased the antitumor effects of the drug *in vivo*, owing to enhanced delivery to solid tumors, increase in the influx of DOX, a decrease in the efflux of DOX (inhibition effects on P-glycoprotein), and changes in intracellular trafficking of DOX (reviewed elsewhere (137)). A parenteral formulation of DOX of Pluronic® micelles has entered Phase I clinical trials in Canada.

The primary advantage of PEO-*b*-PLAA micelles as tailor-made nanocontainers for encapsulation and release of compatible drugs is best illustrated for DOX and PEO-*b*-P(Asp)-DOX conjugate micelles (32). A strong interaction between the conjugated and physically encapsulated DOX is believed to be the basis for the improved micellar stability and sustained release properties. A careful control of the pH during the encapsulation was necessary to keep DOX in its unionized form, which favours a non-polar environment. The same factor affected drug release from polymeric micelles. DOX encapsulated in PEO-*b*-P(Asp)-DOX conjugate micelles were active against P388DI mouse leukemia cells *in vitro* and against C26 tumours *in vivo*. The presence of physically encapsulated DOX was important for antitumour activity in both cases (32;138). The maximum tolerable dose of DOX increased from 20 to 40 mg/kg/day. In a

29

C26 murine model, tumours completely disappeared at a dose of 10 mg/kg/day for all animal subjects treated with the micelle formulation. At the same dose, DOX alone caused tumour disappearance in just two out of five animals.

In pharmacokinetic studies, free DOX disappeared in 15 minutes from the blood of tumour bearing mice. For ^{14}C labelled DOX encapsulated in PEO-b-P(Asp)-DOX conjugate micelles, on the other hand, 24.6 % of the injected dose remained in blood circulation after 24 hs and 9.6 % of the dose was detected per g of the tumour at this time. The latter level was 1.3 % for free drug. The highest concentration of free drug in tumour site was observed 1 h after its administration. In case of PEO-b-P(Asp)-DOX conjugates micelles, DOX levels at tumour site increased between 15 minutes to 24 hs. Based on the findings, the superior antitumour activity of DOX in polymeric micelles was attributed to the accumulation of PEO-b-P(Asp)-DOX conjugate micelles at tumour sites (138). This system has been characterized in detail (139) and is going to move into clinical trials in Japan (27).

The intermediate polymer in the synthesis of PEO-b-P(Asp)-DOX conjugates (Figure 1.7), poly(ethylene oxide)-b-poly(β-benzyl-L-aspartate) (PEO-b-PBLA), was also used by Kataoka et al. to encapsulate hydrophobic model molecules (50;114), anticancer (72;73) and anti-inflammatory drugs (70). The existence of aromatic groups was the common feature in the chemical structures of all encapsulated molecules. A π–π interaction between the benzyl core of the micelles and aromatic ring of the drug provided means for formation of a stable system even in the presence of serum proteins (32). PEO-b-PBLA was shown to form spherical micelles around 20 nm in size with rigid cores at very low concentration (50). A spherical shape and narrow size distribution of a

30

pyrene conjugate of this block copolymer micelle has recently been illustrated by AFM (140). SEC showed prohibition of protein adsorption to PEO-*b*-PLAA micelles where micelles were incubated with serum albumin in PBS, pH 7.0 (73).

The first attempt for drug loading for PEO-*b*-PBLA micelles was carried out with DOX (72;73). Evidence for the encapsulation of DOX by PEO-*b*-PBLA micelles was provided by SEC-HPLC and fluorescence techniques. PEO-*b*-PBLA micelles protected DOX from chemical degradation in an aqueous environment. The release of DOX from PEO-*b*-PBLA micelles was slow over several days and pH dependent (72). Fifty percent of encapsulated DOX was released in 72 hs in pH 7.4 at 37°C. The release was accelerated by decreasing the pH to 5.0 probably due to ionization of the 3' NH_2 group at that pH resulting in a reduced hydrophobic interaction between drug and micellar core.

Overall, the results of biological studies with this system were not as impressive as DOX encapsulated in PEO-P(Asp)-DOX micelles. Twenty-four hs after intravenous injection into healthy BDF1 mice, only 5 % of the ^{14}C labelled DOX encapsulated in PEO-*b*-PBLA micelles was in blood. The tolerable dose of DOX increased from 10 mg/kg to 23 mg/kg for DOX loaded in PEO-*b*-PBLA micelles after administration to C26 tumour transplanted CDF$_1$ mice. In comparison to free DOX treated animals, the tumour volume after 24 days decreased significantly for DOX encapusulated in PEO-*b*-PBLA micelles administered in its maximum tolerable dose. After 60 days tumours disappeared in three out of five animal subjects. For free DOX complete recovery took place in one animal subject (115).

PEO-*b*-PBLA micelles were also used to solubilize indomethacin in a separate study (70). SEC confirmed encapsulation, and DLS provided data illustrating an increase

31

in the diameter of PEO-*b*-PBLA micelles as a result of drug loading. Similar to DOX, the rate of indomethacin release was sustained from PEO-*b*-PBLA micelles in a pH dependent manner. The maximum control was achieved in acidic pH, where indomethacin was unionized and favoured the nonpolar environment of PBLA core in polymeric micelles. A sharp raise in the rate of drug release was observed between pH 4 to 5, which is close to the pKa of indomethacin (4.5).

The synthesis of another class of PEO-*b*-PLAA based block copolymer with aromatic structure in the core has been reported (51;52). Di and tri block copolymers of PEO-*b*-poly(β-benzyl-L-glutamate) (PEO-*b*-PBLG) were prepared and self-assembled. The dimensions of the colloidal system was in the range of nanoparticles rather than micelles (200-300 nm) possibly due to the formation of secondary aggregates. This system has been utilized to solubilize clonazepam and norfloxacin.

Yokoyama *et al.* engineered the chemical structure of the core-forming block in PEO-*b*-PBLA through partial replacement of its benzyl group by an aliphatic chain, cetyl ester residue, PEO-*b*-P(BLA,C16) to encapsulate a cytotoxic agent, KRN5500, which has an aliphatic moiety (Figure 1.10) (31). The average diameter of the colloidal system was found to be above 100 nm, which was reduced to 70 nm by sonication without any loss in the drug content. Similar to free drug, cytotoxic effect of KRN 5500 encapsulated in PEO-*b*-P(BLA,C16) micelles was not strongly time dependent in *in vitro* and *in vivo* assessments. This contrast previous findings for formulation of DOX in PEO-*b*-P(Asp)-DOX micelles implying the possibility of a rapid drug release or a direct interaction of the micellar system with tumor cells (118).

32

CH₃(OCH₂CH₂)ₙ̄ NH(COCHNH)ₘ̄ H   **PEO-*b*-PBLA**
                          |
                    CH₂COOCH₂〈◯〉

                          |
                          | **Hydrolysis or ester exchange**
                          ▼

CH₃(OCH₂CH₂)ₙ̄-NH(COCHNH)ₓ̄-(COCHNH)ₘ̄₋ₓ H   **PEO-*b*-P(BLA,C16)**
                          | |
              CH₃(CH₂)₁₅COOCH₂   CH₂COOCH₂ 〈◯〉

KRN5500

Figure 1.10. Synthesis of PEO-*b*-P(BLA,C16) and chemical structure of KRN5500.

The physical encapsulation of hydrophobic molecules in polymeric micelles is usually carried out through dialysis or O/W emulsion methods (32;70;72;73). In the dialysis method polymer and drug are both dissolved in an organic solvent. The solution is then dialyzed against distilled water to remove the free drug and organic solvent. In the O/W emulsion method, drug is dissolved in a volatile solvent, which is also immiscible with water, such as chloroform, and added to an aqueous solution of polymeric micelles. The mixture is hemogenized by sonication and chloroform is evaporated in an air open system. Free drug is removed by ultra-filtration.

33

The choice of solvent and loading process seems to be important factors affecting micellar stability, size and drug encapsulation. Optimized conditions of loading for each drug in its polymeric carrier have been explored and the results have been reported in a few cases. For instance, for the encapsulation of KRN5500 in PEO-*b*-P(BLA,C16) by dialysis, *N,N*-dimethylsulfoxide (DMSO) is found to be a better choice than *N,N*-dimethylformamide (DMF) as the selective solvent leading to an improved solubilization, smaller size and enhanced stability of polymeric micelles (31). The encapsulation of indomethacin and DOX in PEO-*b*-PBLA was slightly improved when an O/W emulsion method of drug incorporation was used instead of dialysis (70;72).

1.7.3. Polyion complex micelles – Depending on the type of amino acid, PEO-*b*-PLAA block copolymers may bear positive or negative charge at their side chains. Therefore, oppositely charged therapeutic molecules such as DNA or peptides can form poly ion complexes with the PLAA segment of the block copolymer, neutralize the charge and induce required amphiphilicity for micellization of the complex. The incorporation of DNA and peptides in polymeric micelles may lead to their stabilization against digestive enzymes such as nuclease and facilitate their penetration in cells. The polyion complex micelles are salt-sensitive. They will fall apart and release their content as the salt concentration increases above a certain value (141). There has been a rising interest on this novel application of PEO-*b*-PLAA micelles over the past few years (Table 1.1) with promising results for the use of polyion complex micelles in the areas of diagnosis, biotechnology and gene therapy. These delivery systems have been described elsewhere (11;12;27;142).

34

1.8. Amphotericin B (AmB)

Amphotericin B has been the main choice in antifungal therapy for over 30 years (143). It was originally derived from *Streptomyces nodosus* in 1953 (144). Its total synthesis process was reported just a few years ago, in 1987 (145).

The chemical structure of AmB is shown in Figure 1.11. It is characterized by a large 38-membered lactone ring linked covalently to an amino sugar moiety. The ring itself is made up of two chains. The chain that contains the polyene chromophore is completely hydrophobic, whereas the chain that contains the hydroxyl groups has a hydrophilic face and a hydrophobic face, rendering it amphiphilic. The asymmetrical distribution of hydrophobic and hydrophilic groups in AmB confers an exceptionally low solubility for the drug in water and in many organic solvents (146). Instead, due to the amphiphilic nature, AmB is prone to an open self-association process at levels above 1 μM in water (146;147).
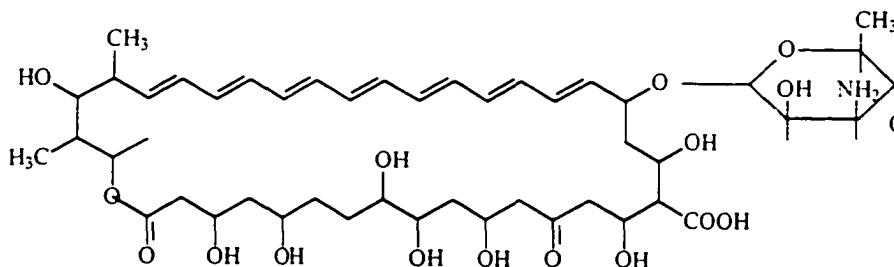
Figure 1.11. Chemical structure of amphotericin B

Formation of aggregates is evidenced by changes in the absorption as well as circular dichroism (CD) spectrum of AmB. At concentrations as low as 10^{-8} M AmB is solubilized in water in a monomeric state, characterized by its absorption at 409 nm. At higher concentrations, AmB self associates in to oligomers and aggregates of oligomers.

35

As a result, in its absorption and CD spectra, the bands are slightly shifted to the red side and a new band appears at the blue site (340 nm) (148). In the presence of proteins, lipids or even lipoproteins, the higher wavelength absorption bands of amphotericin B in water are shifted to 414 nm (149;150). This effect has been used to monitor the interaction of amphotericin B with phospholipids, sterols, surfactants and polymers (147;148;151-153). The absorption spectra of monomeric and aggregated AmB are shown in Figure 1.12.
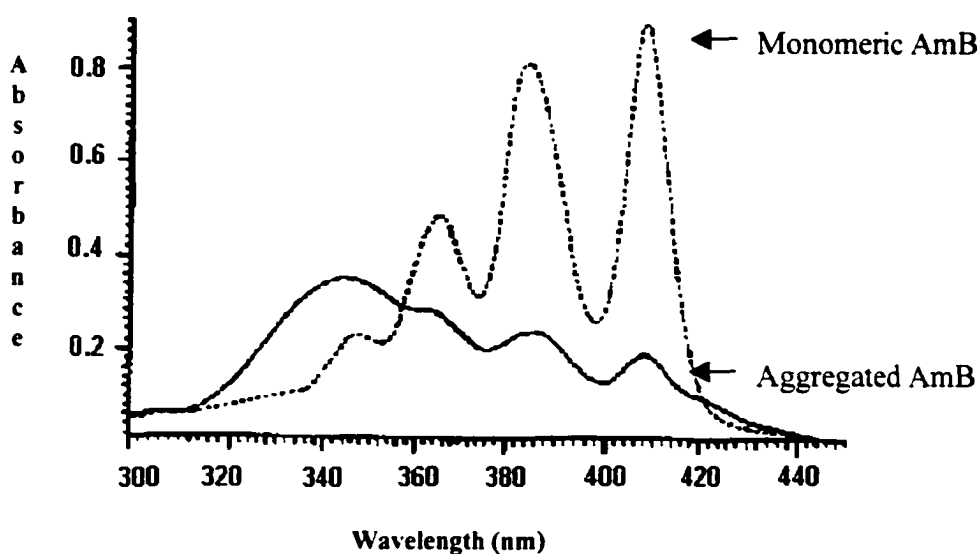
Figure 1.12. Absorption spectrum of AmB in an aggregated and monomeric state.

The amphiphilic nature of AmB is the reason behind its membrane activity. AmB binds to sterols and forms pores in the membrane. The pore permits the transfer of ions leading to an osmotic imbalance and cell lysis. The selectivity of AmB for fungal cells versus mammalian cells is explained by a higher affinity for ergosterol, found in fungal cell membranes, than for cholesterol, the main sterol of the mammalian cells (146;154). Other mechanisms involved in cell toxicity of AmB include inhibition of membrane

36

enzymes, induction of lipid peroxidation of the cell membrane and internalization of AmB-LDL complex by receptor-mediated endocytosis (54;154;155). Several studies suggest a role for the aggregation state of AmB for its toxicity (152;156;157). Based on Bolard's model (Figure 1.13), AmB can form a complex with ergosterol leading to a barrel shape pore in cell membranes, which is partly walled by ergosterol molecules. The complex is not formed with cholesterol, therefore, formation of channels traversing membranes require more AmB molecules when cholesterol is present in the membrane. As a result, AmB in an aggregated state is toxic to both mammalian and fungal cell membranes, while just toxic to fungal cells in a monomeric state (154). From this prospective, AmB delivery in a monomeric state might be desired to reduce its toxicity.
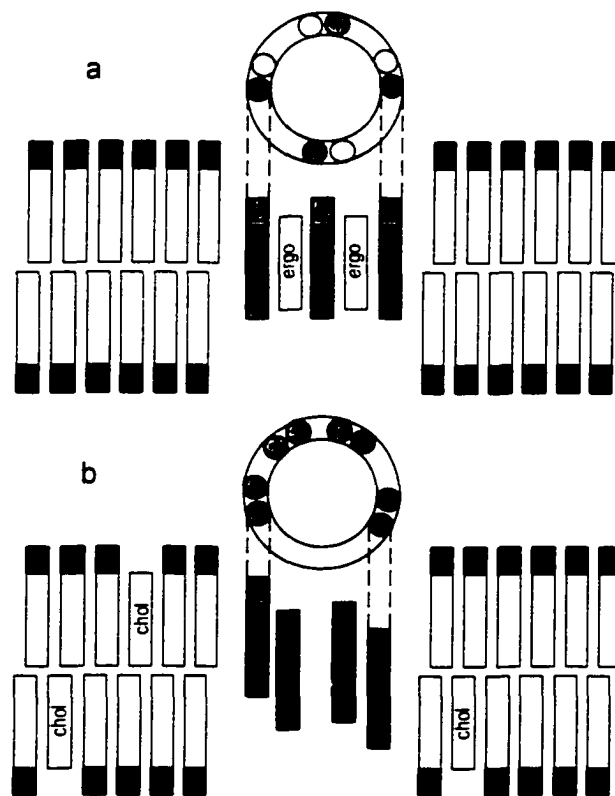
Figure 1.13. Schematic representation of AmB pores inducing K⁻ leakage by one-sided action through a) ergostrol and b) cholesterol membranes.

37

Amphotericin B is poorly soluble in water. The most common formulation of AmB in the clinic, Fungizone®, is prepared with the aid of a low molecular weight surfactant to induce water solubility. Despite great effectiveness against a broad spectrum of fungi strains, the use of Fungizone® is restricted due to severe side effects associated with its administration, including fever, chills, nausea, vomiting, electrolyte abnormalities and nephrotoxicity (154). There have been attempts to circumvent the poor water solubility and toxic side effects of AmB by synthesizing new derivatives (158-160) or preparing novel carriers for AmB (147). This has led to the development of three lipid-based formulations, which are commercially available at present. Selected characteristics of clinical formulations of AmB are summarized in Table 1.2.

Table 1.2. Selective characteristics of clinical formulations of AmB (144).

AmB preparation	Carrier composition	Diameter (nm)	Common dose (mg/kg/day)	Cost (US $/day)
Fungizone®	Sodium deoxycholate	400	1	34
Ablect® (ABLC)	DMPC/DMPG ª	1600-11,000	5	693
Amphocil® (ABCD)	Cholesteryl sulfate	120-140	3-4	447
Ambisome®	HSPC/DSPG/CHOL ᵇ	80	3-5	1036

a. DMPC: Dimyristoyl phosphatidylcholine, DMPG: Dimyristoyl phosphatidylglycerol
b. HSPC: Hydrogenated soy phosphatidylcholine, DSPG: Distearoylphosphatidylglycerol, CHOL: cholestrol.

Lipid based formulations are able to reduce toxicity of AmB. This has been attributed to relative stability of lipid carriers opposed to the low stability of AmB carriers in Fungizone®. The sodium deoxycholate micelles in Fungizine® are not stable

38

and tend to dissociate rapidly upon IV administration. In contrast, AmB dissociates slowly from its lipid complex (161). Upon dilution in blood, free AmB dissociated rapidly from deoxycholate micelles and binds to low-density lipoproteins (LDL). The AmB-LDL complex can be internalized by receptor-mediated endocytosis into cells bearing LDL receptors, such as kidney cells, and cause toxicity. Stable carriers can simply prevent LDL binding by protecting AmB or shifting the AmB distribution toward safe components in the blood stream such as high-density lipoproteins (HDL) (162-165) or albumin (166-168). At a cellular level, rapid release of AmB from sodium deoxycholate micelles leads to its release in an aggregated state, which is toxic towards mammalian cells. Lipid carriers may release monomeric AmB, which is only toxic toward fungal cells. A difference between aggregated and monomeric AmB may exist in their distribution in protein components of the serum (150). The issue has not been addressed in most of the studies, however.

Despite a reduced toxicity, lipid formulations of AmB failed to replace Fungizone® in the clinic because of their high cost, high dose and risk of long-term toxicities (Table 1.2). The use of long circulating carriers has been suggested as an alternative approach to lower the dose of therapy (169-172). Recently, AmB in long circulating liposomes was shown superior efficacy in a murine model of candiasis in comparison to standard liposomes (173).

1.9. Thesis proposal

1.9.1. Rationale

The chemical structure of the core-forming block in PEO-*b*-PLAA micelles could be tailored to modify micellar properties, drug solubilization and release. We explored this concept for a membrane-acting drug, AmB. As Fungizone®, AmB is very potent but causes rupture of both fungal and mammalian cell membranes, leading to severe side effects. Instability of the low molecular weight micelle used for AmB solubilization and a rapid drug release in Fungizone®, leading to AmB delivery in an aggregated state are believed to be the primary cause of toxicity. Lipid formulations of AmB are less toxic but not as effective *in vivo* and very expensive. Polymeric micelles with tailored core structures are expected to encapsulate AmB and release it in a monomeric state, leading to an enhanced therapeutic index for AmB. Long circulating carriers with sufficient stability and control over the rate of drug release may lower the dose and cost of AmB therapy. From pharmaceutical perspective, a polymeric micellar formulation is advantageous since it can be freeze-dried, reconstituted and easily sterilized by filtration.

1.9.2. Objective

The objective of this study was to achieve a novel formulation based on tailor-made micelle-forming block copolymers of PEO-*b*-PLAA for the solubilization and delivery of AmB.

40

1.9.3. Hypothesis

Tailoring the core structure of PEO-*b*-PLAA micelles through the attachment of saturated fatty acids will enhance the delivery of AmB in terms of encapsulation, release pattern, toxicity and antifungal activity.

1.9.4. Specific aims

1. To prepare micelles based on poly(ethylene oxide)-*b*-poly(hydroxyalkyl-L-aspartamide) (PEO-*b*-PHAA) that have fatty acid side chains on the core-forming block.

2. To assess the effect of alkyl core structure on the properties of micelles composed of PEO-*b*-PHAA derivatives.

3. To assess a solvent evaporation method for the encapsulation of AmB by micelles of poly(ethylene oxide)-*b*-poly[*N*-(6-hexyl stearate)-L-aspartamide)] (PEO-*b*-PHSA).

4. To assess the effect of stearic acid substitution on the *in vitro* toxicity and antifungal activity of AmB encapsulated in PEO-*b*-PHSA micelles.

5. To assess the effect of stearic acid substitution on the *in vitro* release of AmB from PEO-*b*-PHSA micelles.

41

1.10. References

1. Ehrich, P., *Collected Studies on Immunity* John Wiley & Sons, New York (1906).

2. Kataoka, K., Kwon, G., Yokoyama, M., Okano, T., and Sakurai, Y., Block copolymer micelles as vehicles for drug delivery. *Journal of Controlled Release* 24:119-132 (1993).

3. Yokoyama, M., Block copolymers as drug carriers, *Critical Reviews in Therapeutic Drug Carrier Systems* 9:213-248 (1992).

4. Kataoka, K., Design of nanoscopic vehicles for drug targeting based on micellization of block copolymers, *Journal of Macromolecular Science Pure and Applied Chemistry* 11:1759-1769 (1994).

5. Kwon, G. S., and Kataoka, K., Block copolymer micelles as long circulating drug vehicles, *Advanced Drug Delivery Reviews* 16:295-309 (1995).

6. Yokoyama, M. and Okano, T., Targetable drug carriers: present status and a future perspective, *Advanced Drug Delivery Reviews* 21:77-80 (1996).

7. Kwon, G.S. and Okano, T., Polymeric micelles as new drug carriers, *Advanced Drug Delivery Reviews* 21:107-116 (1996).

8. Kwon, G.S., Diblock copolymer nanosparticles for drug delivery, *Critical Reviews in Therapeutic Drug Carrier Systems*, 15:481-512 (1998).

9. Allen, C., Maysinger, D., and Eisenberg, A., Nano-engineering block copolymer aggregates for drug delivery, *Colloids & Surfaces B: Biointerfaces* 16:3-27 (1999).

10. Allen, C., Eisenberg, A., and Maysinger, D., Copolymer drug carriers: conjugates, micelles and microspheres, *S.T.P. Pharma Sciences* 9:139-151 (1999).

11. Kabanov, A. V. and Kabanov, V. A., Interpolyelectrolyte and block ionomer complexes for gene delivery: physico-chemical aspects, *Advanced Drug Delivery Reviews* 30:49-60 (1998).

12. Alexandridas P. and Lindman, B., In *Amphiphilic block copolymers: self assembly and applications* ELSEVIER, Amesterdam (2000).

13. Jones, M-C. and Leroux, J. C., Polymeric micelles- a new generation of colloidal drug carriers, *European Journal of Pharmaceutics & Biopharmaceutics* 48:101-111 (1999).

14. Torchilin, V. P., Structure and design of polymeric surfactant-based drug delivery systems, *Journal of Controlled Release* 73:137-172 (2001).

42

15. Dunn, S.E., Brindley, A., Davis, S.S., Davies, M.C. and Illum, L., Polystyrene-poly (ethylene glycol) (PS-PEG2000) particles as model systems for site specific drug delivery. 2. The effect of PEG surface density on the *in vitro* cell interaction and *in vivo* biodistribution, *Pharmaceutical Research* 11:1016-1022 (1994).

16. Stolnik, S., Illum, L., and Davis, S. S., Long circulating microparticulate drug carriers, *Advanced Drug Delivery Reviews* 16:195-214 (1995).

17. Litzinger, D.C., Buiting, A.M., Van Rooijen, N., and Huang, L., Effect of liposome size on the circulation time and intraorgan distribution of amphipathic poly(ethylene glycol)-containing liposomes, *Biochimica et Biophysica Acta* 1190:99-107 (1994).

18. Jain, R. K., Delivery of molecular and cellular medicine to solid tumors, Advanced *Drug Delivery Reviews* 26:71-90 (1997).

19. Yuan, F., Dellian, M., Fukumura, D., Leunig, M., Berk, D. A., Torchilin, V. P. and Jain, R. K., Vascular permeability in a human tumor xenograft: molecular size dependence and cutoff size, *Cancer Research* 55:3752-3756 (1995).

20. Yuan, F., Leuning, M., Huang, S. K., Berk, D. A., Papahadjopoulos, D. and Jain. R. K., Microvascular permability and interstitial penetration of sterically stabilized (stealth) liposomes in human tunor xenograft, *Cancer Research* 54:3352-3356 (1994).

21. Kabanov, A., Batrakova, E. V., Melik-Nubarov, N. S., Fedoseev, N. A., Dorodnich, T. Y., Alakhov, V., Chekhonin, V. P., Nazarova, I. R. and Kabanov, V. A., A new class of drug carriers: micelles of poly(oxyethylene)-poly(oxypropylene) block copolymers as microcontainerrs for drug targeting from blood in brain, *Journal of Controlled Release* 22:141-158 (1992).

22. Scholz, C., Iijima, M., Nagasaki, Y. and Kataoka, K., A novel reactive polymeric micelles with aldehyde groups on its surfaces, *Macromolecules* 28:7295-7297 (1995).

23. Yamamoto, K., Nagasaki, Y., Kato, M. and Kataoka, K., Surface charge modulation of poly(ethylene glycol)-poly(D,L-lactide)block copolymer micelles: conjugation of charged peptides, *Colloids & Surfaces B: Biointerfaces* 16:135-146 (1999).

24. Vinogradov, S. V., Baratkova, EV., Li, S. and Kabanov, A. V., Polyion complex micelles with protein-modified corona for receptor-mediated delivery of oligonucleotides into cells, *Bioconjugate Chemistry* 10:851-860 (1999).

25. Jeong, B., Bae, Y.H., Lee, D.S. and Kim, S.W., Biodegradable block copolymers as injectable drug-delivery systems, *Nature* 388:860-862 (1997).

43

26. Taillefer, J., Jones, M.-C., Brasseur, N., Van lieer, J. e. and Leroux, J. C., Preparation and characterization of pH-responsive polymeric micelles for the delivery of photosensitizing anticancer drugs, *Journal of Pharmaceutical Sciences* 89:52-62 (2000).

27. Kataoka, K., Harada, A. and Nagasaki, Y., Block copolymer micelles for drug delivery: design, characterization and biological significance, *Advanced Drug Delivery Reviews* 47:113-131 (2001).

28. Yokoyama, M., Kwon, G.S., Okano, T., Sakurai, Y., Sato, T. and Kataoka, K., Preparation of micelle-forming polymer-drug conjugates, *Bioconjugate Chemistry* 3:295-301 (1992).

29. Yokoyama, M., Okano, T., Sakurai, Y., Suwa, S. and Kataoka, K., Introduction of cisplatin into polymeric micelle, *Journal of Controlled Release* 39:351-356 (1996).

30. Li, Y. and Kwon, G. S., Micelle-like structures of poly(ethylene oxide)-*block*-poly(2-hydroxyethyl aspartamide)-methotrexate conjugates, *Colloids & Surfaces B: Biointerfaces* 16:217-226 (1999).

31. Yokoyama, M., Satoh, A., Sakurai, Y., Okano, T., Matsumura, Y., Kakizoe, T. and Kataoka, K., Incorporation of water-insoluble anticancer drug into polymeric micelles and control of their particle size, *Journal of Controlled Release* 55:219-229 (1998).

32. Yokoyama, M., Fukushima, S., Uehara, R., Okamoto, K., Kataoka, K., Sakurai, Y. and Okano, T., Characterization of physical entrapment and chemical conjugation of adriamycin in polymeric micelles and their design for *in vivo* delivery to a solid tumor, *Journal of Controlled Release* 50:79-92 (1998).

33. Yokoyama, M., Kwon, G.S., Okano, T., Sakurai, Y., Naito, M. and Kataoka, K., Influencing factors on *in vitro* micelle stability of adriamycin-block copolymer conjugates, *Journal of Controlled Release* 28:59-65 (1994).

34. Li, Y. and Kwon, G. S., Methotrexate esters of poly(ethylene oxide)-*block*-poly(2-hydroxyethyl-L-aspartamide). part I: effects of the level of methotrexate conjugation on the stability of micelles and on drug release, *Pharmaceutical Research* 17:607-611 (2000).

35. Plestil, J., Luong, T. T. and Florence, A. T., Small angle x-ray scattering of the block copolymer polystyrene/polybutadiene/polystyrene in ethyl methyl ketone, *Makromolecule Chemistry* 174:183-191 (1973).

36. Cammas, S., Suzuki, K., Sone, C., Sakuri, Y., Kataoka, K. and Okano, T., Thermo-responsive polymer nanoparticles with a core-shell micelle structure as site-specific drug carriers, *Journal of Controlled Release* 48:157-164 (1997).

44

37. Xu, R., Winnik, M., Hallett, F. R., Riess, G. and Croucher, M. D., Light scattering study of the association behavior of styrene-ethylene oxide block copolymers in aqueous solution, *Macromolecules* 24:87-93 (1991).

38. Khan, T. N., Mobbs, R. H., Price, C., Quintana, J. R. and Stubbersfield, R. B., Synthesis and colloidal behavior of a polystyrene-*b*-poly(ethylene oxide) block copolymer, *European Polymer Journal* 23:191 (1987).

39. Hagan, S. A., Coombes, A. G., Garnett, M. C., Davies, M. C., Illum, L. and Davis, S. S., Polylactide-poly(ethylene glycol) copolymers as drug delivery systems. 1. characterization of water dispersible micelle forming systems, *Langmuir* 12:2153-2161 (1996).

40. Tanford, C., In *The hydrophobic effect: formation of micelles and biological membranes,* Wiley-Intescience, New York (1980).

41. Zhou, Z. and Chu, B., Light scattering study on the association behavior of triblock copolymers of ethylene oxide and propylen oxide in aqueous solution, *Journal of Colloid & Interface Science* 126:171-180 (1988).

42. Jones, J. L., Marques C.M. and Joanny J.F., Shear induced micellization of diblock copolymers, *Macromolecules* 28:136-142 (1995).

43. I. R. Schmolka. In *Polymers for Controlled Drug Delivery* CRC Press, Boca Raton (1991).

44. Johnston, T. P. and Miller, S. C., Toxicological evaluation of poloxamer vehicles for intramuscular use, *Journal of Parenteral Science & Technology* 39:83-89 (1985).

45. Drobnik, J., Biodegradable soluble macromolecules as drug carriers, *Advanced Drug Delivery Reviews* 3:229-245 (1989).

46. Chiu, H.-C., Kopeckova, P., Deshmane, A. S. and Kopecek J., Lysosomal degradability of poly(α-amino acids), *Journal of Biomedical Material Research* 34:381-392 (1997).

47. McCormick-Thomson, L. A., Sgouras, D. and Duncan, R., Poly(amino acid) copolymers as potential soluble drug delivery system. 2. Body distribution and preliminary biocompatibility testing *in vitro* and *in vivo, Journal of Bioactive Compatible Polymers* 4:252-268 (1989).

48. Shen, W. C. and Ryser, H. J. P., Poly(L-lysine) and poly(D-lysine) conjugates of methotrexate: different inhibitory effect on drug resistant cells, *Molecular Pharmacology* 16: 614-622 (1979).

49. Seymour, L. W., Duncan, R., Strohalm, J. and Kopecek, J., Effect of molecular weight (Mw) of *N*-(2-hydroxypropyl)methacrylamide copolymers on body

45

distribution and rate of excretion after subcutaneous, intraperitoneal, and intravenous administration to rats, *Journal of Biomedical Material Research* 4:253-264 (1987).

50. Kwon, G.S., Naito, M., Yokoyama, M., Okano, T., Sakurai, Y. and Kataoka, K., Micelles based on AB block copolymers of poly(ethylene oxide) and poly(β-benzyl L-aspartate), *Langmuir* 9:945-949 (1993).

51. Jeong, Y.-I, Cheon, J.-B, Kim, S.-H. Nah, J.-W, Lee, Y.-M, Sung , Y.-K, Akaike, T. and Cho, C.-S., Clonazepam release from core-shell type nanoparticles *in vitro*, *Journal of Controlled Release* 51:169-178 (1998).

52. Nah, J.-W, Jeong, Y.-I. and Cho, C.-S., Norfloxacin release from polymeric micelle of poly(γ-benzyl L-glutamate)/polyethylene oxide)/poly(γ-benzyl L-glutamate) block copolymer, *Bulletin of Korean Chemical Society* 19:962-967 (1998).

53. Rolland, A., O'Mullane, J., Goddard, P., Brookman, L. and Petrak, K., New macromolecular carriers for drugs, I. preparation and characterization of poly(oxyethylene-*b*-isoprene-*b*-oxyethylene) block copolymer aggregates, *Journal of Applied Polymer Science* 44:1195-1199 (1992).

54. Papahadjopoulos, D. and Gabizon, A., Liposomes designed to avoid the reticuloendothelial system, *Progress in Clinical & Biological Research* 343:85-93 (1990).

55. Siegal, T., Horowitz, A. and Gabizon, A., Doxorubicin encapsulated in sterically stabilized liposomes for the treatment of a brain tumor model: biodistribution and therapeutic efficacy, *Journal of Neurosurgery* 83:1029-1037 (1995).

56. Gabizon, A., Price, D.C., Huberty, J., Bresalier, R.S. and Papahadjopoulos, D.. Effect of liposome composition and other factors on the targeting of liposomes to experimental tumors: biodistribution and imaging studies, *Cancer Research* 50:6371-6378 (1990).

57. Batrakova, E.V., Han, H.Y., Alakhov, V.Y., Miller, D.W. and Kabanov, A.V., Effects of pluronic block copolymers on drug absorption in caco-2 cell monolayers. *Pharmaceutical Research* 15:850-855 (1998).

58. Batrakova, E.V., Han, H.Y., Miller, D.W. and Kabanov, A.V., Effects of Pluronic p85 unimers and micelles on drug permeability in polarized BBMEC and caco-2 cells, *Pharmaceutical Research* 15:1525-1532 (1998).

59. Miller, D.W., Batrakova, E.V., Waltner, T.O., Alakhov, V.Y. and Kabanov, A.V., Interactions of pluronic block copolymers with brain microvessel endothelial cells: evidence of two potential pathways for drug absorption, *Bioconjugate Chemistry* 8:649-657 (1997).

46

60. Pratten, M.K., Lioyd, J.B., Horpel, G. and Ringsdorf, H., Micelle-forming block copolymers: pinocytosis by macrophages and interaction with model membranes, *Makromolecule Chemistry* 186:725-733 (1985).

61. Garnett, M.C., Stolnik, S., Dunn, S.E., Armstrong, D., Lin, W., Schacht, E., Ferutti, P., Vert, M., Davies, M.C., Illum, L. and Davis, S. S., Application of novel biomaterials in colloid drug delivery systems, *MRS Bulletin* 49-56 (1999).

62. Gref, R., Minamitake, Y., Peracchia, M.T., Trubetskoy, V., Torchilin, V.P. and Langer, R., Biodegradable long-circulating nanospheres, *Science* 263:1600-1603 (1994).

63. Kim, I-S, Jeong, Y.-I., Cho, C.-S. and Kim, S.-H., Thermo-responsive self assembled polymeric micelles for drug delivery *in vitro*, *International Journal of Pharmaceutics* 205:165-172 (2000).

64. Mortensen, K. and Yashayahu, T., Cryo-TEM and SANS microstructural study of pluronic polymer solution, *Macromolecules* 28:8829-8834 (1995).

65. Nagasaki, Y., Okada, T., Scholz, C., Iijima, M., Kato, M. and Kataoka, K., The reactive polymeric micelles based on an aldehyde-ended poly(ethylene glycol)/poly(lactide) block copolymer, *Macromolecules* 31:1473-1479 (1998).

66. Mortensen, K., Structural properties of self assembled polymeric micelles, *Current Opinion in Colloid & Interface Science* 3:12-19 (1998).

67. Nagarajan, R., Barry, M. and Ruckenstein, E., Unusual selectivity in solubilization by block copolymer micelles, *Langmuir* 2:210-215 (1986).

68. Nagarajan R. and Ganesh, K., Comparison of solubilization of hydrocarbons in (peo-ppo) diblock versus (PEO-PPO-PEO) triblock copolymer micelles, *Journal of Colloid & Interface Science* 184:489-499 (1996).

69. Hurter, P.N. and Hatton, T.A., Solubilization of polycyclic aromatic hydrocarbons by poly(ethylene-propylene oxide) block copolymer micelles: effects of polymer structure, *Langmuir* 8:1291-1299 (1992).

70. La, S. B., Okano, T. and Kataoka, K., Preparation and characterization of the micelle-forming polymeric drug indomethacin-incorporated poly(ethylene oxide)-poly(β-benzyl L-aspartate) block copolymer micelles, *Pharmaceutical Science* 85:85-90 (1996).

71. Cao, T., Munk, P., Ramireddy, C., Tuzar, Z. and Webber, S.E., Fluorescence studies of amphiphilic poly(methacrylic acid)-*block*-polystyrene-*block*-poly(methacrylic acid) micelles, *Macromolecules* 24:6300 (1991).

47

72. Kwon, G.S., Naito, M., Yokoyama, M., Okano, T., Sakurai, Y. and Kataoka, K., Block copolymer micelles for drug delivery: loading and release of doxorubicin, *Journal of Controlled Release* 48:195-201 (1997).

73. Kwon, G.S., Naito, M., Yokoyama, M., Okano, T., Sakurai, Y. and Kataoka, K., Physical entrapment of adriamycin in ab block copolymer micelles, *Pharmaceutical Research* 12:192-195 (1995).

74. Piskin, P., Kaitian, X., Denkbas, E.B. and Kucukyavuz, Z., Novel pdlla/peg copolymer micelles as drug carriers, *Journal of Biomaterials Science, Polymer Edition* 7:359-373 (1995).

75. Allen, C., Han, J., Yu, Y., Maysinger, D. and Eisenberg, A., Polycaprolactone-*b*-poly(ethylene oxide) copolymer micelles as a delivery vehicle for dihydrotestostrone, *Journal of Controlled Release* 63:275-286 (2000).

76. Kim, S.Y., Shin, I.G., Lee, Y.-M., Cho, C.-S. and Sung, Y.-K., Methoxy poly(ethylene glycol) and ε-caprolactone amphiphilic block copolymeric micelle containing indomethacin: micelle formation and drug release behavior, *Journal of Controlled Release* 51:13-22 (1998).

77. Teng, Y., Morrison, M.E., Munk, P. and Webber, S.E., Release kinetics studies of aromatic molecules into water from block copolymer micelles, *Macromolecules* 31:3578-3587 (1998).

78. Gadelle, F., Koros, W.J. and Schechter, R.S., Solubilization of aromatic solutes in block copolymers, *Macromolecules* 28:4883-4892 (1995).

79. Tancrede, P., Barwicz, J., Jutras, S. and Gruda, I., The effect of surfactants on the aggregation state of amphotericin B, *Biochimica et Biophysica Acta - Biomembranes* 1030:289-295 (1990).

80. Kwon, G.S. and Okano, T., Soluble self assembled block copolymers for drug delivery, *Pharmaceutical Research* 16:597-600 (1999).

81. Trubetskoy V.S. and Torchilin, V.P., Use of polyoxyethylene-lipid conjugates as long-circulating carriers for delivery of therapeutic and diagnostic agents, *Advanced Drug Delivery Reviews* 16:311-320 (1995).

82. Allen, C., Yu, Y., Maysinger, D. and Eisenberg, A., Polycaprolactone-*b*-poly(ethylene oxide) block copolymer micelles as a novel drug delivery vehicle for neurotrophic agents FK506 and L-685,818, *Bioconjugate Chemistry* 9:564-572 (1998).

83. Batrakova, E.V., Dorodnich, T.Y., Klinskii, E.Y., Kliushnenkova, E.N., Shemchukova, O.B., Goncharova, O.N., Arjakov, V.Y., Alakhov, V. and Kabanov, A.V., Anthracycline antibiotics noncovalently incorporated into the block

48

copolymer micelles: in vivo evaluation of anticancer activity, *British Journal of Cancer* 74:1545-1552 (1996).

84. Torchilin V.P. and Trubetskoy, V.S., Micellar carriers for therapeutic and diagnostic agents, *Farmacevtski Vestnik*, 48:232-233 (1997).

85. Inoue, T., Chen, G., Nakamae, K. and Hoffman, A.S., An ab block copolymer of oligo(methyl methacrylate) and poly(acrylic acid) for micellar delivery of hydrophobic drags, *Journal of Controlled Release* 51:221-229 (1998).

86. Chung, J.E., Yokoyama, M., Aoyagi, T., Sakurai, Y. and Okano, T., Effect of molecular architecture of hydrophobically modified poly(N- isopropylacrylamide) on the formation of thermoresponsive core-shell micellar drug carriers, *Journal of Controlled Release* 53:119-130 (1998).

87. Quirion, F. and St-Pierre, S., Reduction of the *in vitro* hemolytic activity of soybean lecithin liposomesby treatment with a block copolymer, *Biophysical Chemistry* 40:129-134 (1991).

88. Kabanov, A.V., Chekhonin, V.P., Alakhov, V., Betrakova, E.V., Lebedev, A.S., Mellik-Nubarov, N.S., Arzakov, S.A., Levashov, A.V., Morozov, G.V., Severin, E.S. and Kabanov, V.A., The neuroleptic activity of haloperidol increases after its solubilization in surfactant micelles, *FEBS Letters* 258:343-345 (1989).

89. Lin, S. and Kawashima, Y., Kinetic studies on the stability of indomethacin in alkaline aqueous solutions containing poly(oxyethylene)poly(oxypropylene)surface active block copolymers, *Pharmaceutica Acta Helvetiae* 60:345-350 (1985).

90. Forster, D., Washington, C. and Davis, S. S., Toxicity of solubilized and colloidal amphotericin b formulations to human erythrocytes, *Journal of Pharmacy & Pharmacology* 40:325-328 (1988).

91. Hunter, R., strickland, F. and Kezdy, F, The adjuvant activity of nonionic block polymer surfactants, *Journal of immunology* 127:1244-1250 (1981).

92. Hunter, R. L. and Bennett, B., The adjuvant activity of nonionic block copolymer surfactants, *Scandinavian Journal of Immunology* 23:287- (1986).

93. Vitalias, E. A. US Patent No. 2 917410. (1959).

94. Bazile, D., Prud'Humme, C., Bassoullet, M-T, Marlard, M., Spenlehauer, G. and Veillard, M., Stealth Me.peg-pla nanoparticles avoid uptake by the mononuclear phagocytes system, *Journal of Pharmaceutical Sciences* 84:493-498 (1995).

95. Govender, T., Riley, T., Ehtezazi, T., Garnett, M.C., Stolnik, S., Illum,L. and Davis, S. S., Defining the drug incorporation properties of pla-peg nanoparticles, *International Journal of Pharmaceutics* 199: 95-110 (2000).

49

96. Burt, H.M., Zhang, X., Toleikis, P., Embree, L. and Hunter, W.L., Developement of copolymers of poly(D,L-lactide) and methoxypolyethylene glycol as micellar carriers of paclitaxol, *Colloids & Surfaces B: Biointerfaces* 16:161-171 (1999).

97. Zhang, X., Jackson, J.K. and Burt, H.M., Development of amphiphilic diblock copolymers as micellar carriers of taxol, *International Journal of Pharmaceutics* 132:195-206 (1996).

98. Zhang, X., Burt, H.M., von Hoff, D., Dexter, D., Mangold, D., Degen, D., Oktaba, M. and Hunter, W.L., An investigation of the antitumour activity and biodistribution of polymeric micellar paclitaxel, *Cancer Chemotherapy & Pharmacology* 40:81-86 (1997).

99. Ramaswamy, M., Zhang, X., Burt, H.M. and Wasan, K.M., Human plasma distribusion of free palclitaxel and pclitaxel associated with diblock copolymers, *Journal of Pharmaceutical Sciences* 86:460-464 (1997).

100. Zhang, X., Burt, H.M., Mangold, D., Dexter, D., Von Hoff, D., Mayer, L. and Hunter, W.L., Anti-tumor efficacy and biodistributionn of intravenous polymeric micellar taxol, *Anti-Cancer Drugs* 8:696-701 (1997).

101. Shin, I.G., Kim, S.Y., Lee, Y.M., Cho, C.S. and Sung, Y.K., Methoxy poly(ethylene glycol)/ε-caprolactone amphiphilic block copolymeric micelle containing indomethacin: I. preparation and characterization, *Journal of Controlled Release* 51:1-11 (1998).

102. Kim, S. Y. and Lee, Y.-M., Taxol-loaded block copolymer nanospheres composed of methoxy poly(ethylene glycol) and poly(ε-caprolactone) as novel anticancer drug carriers, *Biomaterials* 22:1697-1704 (2001).

103. Allen, C., Eisenberg, A. and Maysinger, D., PCL-*b*-PEO micelles as a delivery vehicle for fk506: assessment of a functional recovery of crushed peripheral nerve, *Drug Delivery: Journal of Delivery & Targeting of Therapeutics* 7:139-145 (2000).

104. Kim, S.Y., Shin, I.G., and Lee, Y.-M. Amphiphilic diblock copolymer nanospheres composed of methoxy poly(ethylene glycol) and glycolide: properties, cytotoxicity and drug release behavior, *Biomaterials* 20:1033-1042 (1999).

105. Yoo, H.S. and Park, T.G., Biodegradable polymeric micelles composed of doxorubicin conjugated PLGA-PEG block copolymer, *Journal of Controlled Release* 70:63-70 (2001).

106. Kim, S. Y., Shin, I. G. and Lee, Y.-M., Preparation and characterization of biodegradable nanospheres composed of methoxy poly(ethylene glycol) and DL-lactide block copolymer as novel drug carriers, *Journal of Controlled Release* 56:97-208 (1998).

50

107. Emoto, K., Nagasaki, Y., Iijima, M., Kato, M. and Kataoka, K., Preparation of non-fouling surface through the coating with core-polymerized block copolymer micelles having aldehyde-ended PEG shell, *Colloids & Surfaces B: Biointerfaces* 18:337-346 (2000).

108. Yasugi, K., Nakamura, T., Nagasaki, Y., Kato, M. and Kataoka, K., Sugar-installed polymer micelles: synthetesis and micellization of poly(ethylene glycol)-poly(D, L-lactide) block copolymers having sugar groups at the PEG chain end, *Macromolecules* 32:8024-8032 (1999).

109. Cammas, S., Okano, T. and Kataoka, K., Functional and site-specific macromolecular micelles as high potential drug carriers, *Colloids & Surfaces B: Biointerfaces* 16:207-215 (1999).

110. Dorn, K., Hoerpel, G. and Ringsdorf, H., Polymeric antitumor agents on a molecular and cellular level. In C. G. Gebelein and Jr. C. E. Carraher (eds), *Bioactive Polymer Systems: An Overview*, Plenum Press, New York. 531-585 (1985).

111. Yokoyama, M., Inoue, S., Kataoka, K., Yui, N. and Sakurai, Y., Preparation of adriamycin-conjugated poly(ethylene glycol)-poly(aspartic acid) block copolymer, *Macromulecular Chemistry Rapid Communications* 8:431-435 (1987).

112. Nishiyama, N., Yokoyama, M., Aoyagi, T., Okano, T., Sakurai, Y. and Kataoka, K., Preparation and characterization of self-assembled polymer-metal complex micelle from cis-dichlorodiammineplatinum (II) and poly(ethylene glycol)-poly(α, β-aspartic acid) block copolymer in an aqueous medium, *Langmuir* 15:377-383 (1999).

113. Yokoyama, M., Okano, T., Sakurai, Y., Seto, T. and Kataoka, K., Improved synthesis of adriamycin-conjugated poly(ethylene oxide)-poly(aspartic acid) block copolymer and formation of unimodal micellar structure with controlled amount of physically entrapped adriamycin, *Journal of Controlled Release* 32:269-277 (1994).

114. Kwon, G. S., Naito, M., Kataoka, K., Yokoyama, M., Sakurai, Y., and Okano, T., Block copolymer micelles as vehicles for hydrophobic drugs, *Colloids & Surfaces B: Biointerfaces* 2:429-434 (1994).

115. Kataoka, K., Matsumoto, T., Yokoyama, M., Okano, T., Sakurai, Y., Fukushima, S., Okamoto, K. and Kwon, G.S., Doxorubicin-loaded poly(ethylene glycol)-poly(β-benzyl-L-aspartate) copolymer micelles: their pharmaceutical characteristics and biological significance, *Journal of Controlled Release* 64:143-153 (2000).

116. Yu, B.G., Okano, T., Kataoka, K. and Kwon, G.S., Polymeric micelles for drug delivery: solubilization and hemolytic activity of amphotericine b, *Journal of Controlled Release* 33:131-136 (1998).

117. Yu, B. G., Sardari, S. and Kwon, G. S., Dissociated toxicity, but enhanced antifungal efficacy of amphotericin b loaded poly(ethylene oxide)-*block*-poly(β-benzyl L-aspartate) micelles, *Pharmaceutical Research* 14:S284 (1997).

118. Matsumura, Y., Yokoyama, M., Kataoka, K., Okano, T., Sakurai, Y., Kawaguchi, T. and Kakizoe, T., Reduction of the side effects of an antitumor agent km5500, by incorporation of the drug into polymeric micelles, *Japanese Journal of Cancer Research* 90:122-128 (1999).

119. Harada, A. and Kataoka, K., Formation of stable and monodispersive polyion complex micelles in aqueous medium from poly(L-lysine) and poly(ethylene glycol)-poly(aspartic asid) block copolymer, *Pure and Applied Chemistry* A34:2119-2133 (1997).

120. Harada, A. and Kataoka, K., Chain length recognition: core-shell supramolecular assembly from oppositely charged block copolymers, *Science* 283:65-67 (1999).

121. Katayose, D. and Kataoka, K., Water soluble polyion complex associates of DNA and poly(ethylene glycol)-poly(L-lysine) block copolymer, *Bioconjugate Chemistry* 8:702-707 (1997).

122. Harada, A. and Kataoka, K., Novel polyion complex micelles entrapping enzyme molecules in the core: preparation of narrowly distributed micelles from lysozyme and poly(ethylene glycol)-poly(aspartic acid) block copolymer in aqueous medium, *Macromolecules* 31:288-294 (1998).

123. Harada, A. and Kataoka, K., Novel polyion complex micelles entrapping enzyme molecules in the core [II]: characterization of the micelles prepared at non-stoichiometric mixing ratios, *Langmuir* 15:4208-4212 (1999).

124. Kabanov, A., Vinogradov, S.V., Suzdaltseva, Yu. and Alakhov, V.Y., Cationic copolymers for dna delivery, *Pharmaceutical Research* 13:S214 (1996).

125. Yokoyama, M., Miyauchi, M., Yamada, K., Okano, T., Sakurai, Y., Kataoka, K. and Inoue, S., Polymer micelles as novel drug carrier: adriamycin-conjugated poly(ethylene glycol)-poly(aspartic acid) block copolymer, *Journal of Controlled Release* 11:269-278 (1990).

126. Yokoyama, M., Miyauchi, M., Yamada, N., Okano, T., Sakurai, Y., Kataoka, K. and Inoue, S., Characterization and anticancer activity of the micelle forming polymeric anticancer drug adriamycin-conjugated poly(ethylene glycol)-poly(aspartic acid) block copolymer, *Cancer Research* 50:1693-1700 (1990).

127. Yokoyama, M., Sugiyama, T., Okano, T., Sakurai, Y., Naito, M. and Kataoka, K., Analysis of micelle formation of an adriamycin-conjugated poly(ethylene glycol)-poly(aspartic acid) block copolymer by gel permeation chromatography, *Pharmaceutical Research* 10:895-899 (1993).

52

128. Kwon, G.S., Yokoyama, M., Okano, T., Sakurai, Y. and Kataoka, K., Biodistribution of micelle-forming polymer-drug conjugates, *Pharmaceutical Research* 10:970-974 (1993).

129. Kataoka, K., Kwon, G. S., Yokoyama, M., Okano, T. and Sakurai, Y., Polymeric micelles as novel drug carriers and virus mimicking vehicles, *Macromolecules* 25:267-276 (1992).

130. Yokoyama, M., Okano, T., Sakurai, Y., Ekimoto, H., Shibazaki, C. and Kataoka, K., Toxicity and antitumor activity against solid tumors of micelle-forming polymeric anticancer drug and its extremely long circulation in blood, *Cancer Research* 51:3229-3236 (1991).

131. Kwon, G.S., Suwa, S., Yokoyama, M., Okano, T., Sakurai, Y. and Kataoka, K., Enhanced tumor accumulation and prolonged circulation times of micelle-forming poly(ethylene oxide-aspartate) block copolymer-adriamycin conjugates, *Journal of Controlled Release* 29:17-23 (1994).

132. Yokoyama, M., Kwon, G. S., Okano, T., Sakurai, Y., Ekimoto, H., Okamoto, K., Mashiba, H., Seto, T. and Kataoka, K., Composition-dependent *in vivo* antitumor activity of adriamycin-conjugated polymeric micelle against murine colon adenocarcinoma, *Drug Delivery* 1:11-19 (1993).

133. Mizumura, Y., Matsumura, Y., Hamaguchi, T., Nishiyama, N., Kataoka, K., Kawaguchi, T., Saito, T. and Kakizoe, T., Cisplatin-incorporated polymeric micelles reducing nephrotoxicity, while maintaining antitumor activity, *Japanese Journal of Cancer Research* 92:328-336 (2001).

134. Nishiyama, N., Kato, Y., Sugiyama, Y. and Kataoka, K., Development of cisplatin-loaded polymeric micelles with a prolonged circulation in the bloodstream and an enhanced accumulation in the solid tumor, *Proceedings of the Controlled Release Society* 28:5155-5156 (2001).

135. Feijen, J., Gregonis, D., Anderson, C., Peterson, V. and Anderson, J., Coupling of steroid hormones to biodegradable poly(α-amino acids) I: norethindrone coupled to poly-N5-(3-hydroxypropyl)-L-glutamine, *Journal of Pharmaceutical Sciences* 69:871-872 (1980).

136. Baratkova, EV., Miller, D.W., Li, S., Alakhov, V., Kabanov, A.V. and Elmquist, W.F., Pluronic P85 enhances the delivery of digoxin to the brain: *in vitro* and *in vivo* studies, *Journal of Pharmacology & Experimental Therapeutics* 296:551-557 (2001).

137. Miller, D.W. and Kabanov, A.V., Potential applications of polymers in the delivery of drugs to the central nervous system, *Colloids & Surfaces B: Biointerfaces* 16:321-330 (1999).

53

138. Yokoyama, M., Okano, T., Sakurai, Y., Fukushima, S., Okamoto, K. and Kataoka, K., Selective delivery of adriamycin to a solid tumor using a polymeric micelle carrier system, *Journal of Drug Targeting* 7:171-186 (1999).

139. Fukushima, S., Machida, M., Akutsu, T., Shimizu, K., Tanaka, S., Okamoto, K., Mashiba, H., Yokoyama, M., Okano, T., Sakurai, Y. and Kataoka, K., Roles of adriamycin and adriamycin dimer in antitumor activity of the polymeric micelle carrier system, *Colloids & Surfaces B: Biointerfaces* 16:227-236 (1999).

140. Liaw, J., Aoyagi, T., Kataoka, K., Sakurai, Y. and Okano, T., Visualization of peo-pbla-pyrene polymeric micelles by atomic force microscopy, *Pharmaceutical Research* 15:1721-1726 (1998).

141. Kabanov, A.V., Bronich, TK., Kabanov, V.A., Yu, K. and Eisenberg, A., Soluble stoichiometric complexes from poly(N-ethyl-4-vinylpyridinium) cations and poly(ethylene oxide)-*block*-polymethacrylate anions, *Macromolecules* 29:6797-6802 (1996).

142. Lemieux, P., Vinogradov, SV., Gebhart, CL., Guerin, N., Paradis, G., Nguyen, HK., Ochietti, B., Suzdaltseva, YG., Baratkova, EV., Bronich, TK., St-Pierre, Y., Alakhov, V.Y. and Kabanov, A.V, Block and graft copolymers and nanogel copolymer networks for dna delivery into cell, *Journal of Drug Targeting* 8:91-105 (2000).

143. Bekersky, I., Fielding, R.M., Buell, D. and Lawrence, I., Lipid-based amphotericin b formulations: from animals to man, *PSTT* 2:230-236 (1999).

144. Slain, D., Lipid based amphotericin b for the treatment of fungal infection, *Pharmacotherapy* 19:306-323 (1999).

145. Nicolau, K.C., Danies, R.A., Chakraborty, T.K. and Ogawa, Y., Total synthesis of amphotericin b, *Journal of American Chemical Society* 109:2821-2822 (1987).

146. Szoka, Jr. F.C.T. and Tang, M., Amphotericin b formulated in liposomes and lipid based systems: A review, *Journal of Liposome Research* 3:363-375 (1993).

147. Abu-saleh, K.M., Amphotericin b: an update, *British Journal of Biomedical science* 53:122-133 (1996).

148. Espuelas, M.S., Legrand, P., Cheron, M., Barratt, G., Puisieux, F., Devissaguet, J.-P. and Irache, J M., Interaction of amphotericin b with polymeric colloids: a spectroscopic study, *Colloids & Surfaces B: Biointerfaces* 11:141-151 (1998).

149. Bolard, J., How do the polyene macrolide antibiotics affect the cellular membrane properties? *Biochimica et Biophysica Acta* 864:257-304 (1986).

150. Barwicz, J., Gareau, R., Audet, A., Morisset, A., Villiard, J. and Gruda, I., Inhibition of the interaction between lipoproteins and amphotericin b by some

54

delivery systems, *Biochemical & Biophysical Research Communications* 181:722-728 (1991).

151. Gruda, I., Milette, D., Brother, M., Kobayashi, G.S., Medoff, G. and Brajtburg, J., Structure-activity study of inhibition of amphotericin B (Fongizone) binding to sterols, toxicity to cells and lethality to mice by esters of sucrose, *Antimicrobial Agents & Chemotherapy* 35:24-28 (1991).

152. Barwicz, J., Christian, S. and Gruda, I., Effects of aggregation state of amphotericin b on its toxicity to mice, *Antimicrobial Agents & Chemotherapy* 36:2310-2315 (1992).

153. Tasset, A., Preat, V. and Roland, M., The influence of Myrj 59 on the solubility, toxicity and activity of amphotericin b, *Journal of Phamacy & Pharmacology* 43:297-302 (1991).

154. Brajtburg, J. and Bolard, J., Carrier effects on biological activity of amphotericin b, *Clinical Microbiolgy Reviews* 9:512-531 (1996).

155. Brajtburg, J., Elberg, S., Schwartz, D.R., Vertut-Croquin, A., Schlessinger, D., Kobayashi, D. and Medoff, G., Involvement of oxidative damage in erythrocyte lysis induced by amphotericin b, *Antimicrobial Agents & Chemotherapy* 27:172-176 (1985).

156. Bolard, J., Legrand, P., Heitz, F. and Cybulska, B., One-sided action of amphotericin b on cholesterol-containing membranes is determined by its self-association in the medium, *Biochemistry* 30:5707-5715 (1991).

157. Legrand, P., Romero, E.A., Cohen, B.E. and Bolard, J., Effect of aggregation and solvent on the toxicity of amphotericin b to human erythrocytes, *Antimicrobial Agents & Chemotherapy* 36:2518-2522 (1992).

158. Reuhl, k. R., Vapiwala, M., Ryzlak, M. T. and Schaffner, C. P., Comparative neurotoxicities of amphotericin b and its mono methyl ester derivatives in rats, *Antimicrobial Agents & Chemotherapy* 37:419-428 (1993).

159. Saint-Julien, L., Joly, V., Seman, M., Carbom, C. and Yeni, P., Activity of MS-8209, a nonester amphotericin b derivative, in treatment of experimental systemic mycosis, *Antimicrobial Agents & Chemotherapy* 36:2722-2728 (1992).

160. Taylor, A.W., Costello, B.J., Hunter, P.A., Maclanand, W.S. and Shanks, C.T., Synthesis and antifungal selectivity of new derivatives of amphotericin b modified at the C [13] position, *Journal of Antibiotics* 46:486-493 (1993).

161. Legrand, P., Cheron, M., Leroy, L. and Bolard, J., Release of amphotericin b from delivery systems and its action against fungal and mammalian cells, *Journal of Drug Targeting* 4:311-319 (1997).

162. Lee, S. C., Chang, Y., Yoon, J., Kim, C., Kwon, I. C., Kim, Y. and Jeong, S. Y., Synthesis and micellar characterization of amphiphilic diblock copolymers based on poly(2-ethyl-2-oxazoline) and aliphatic polyesters, *Macromolecules* 32:1847-1852 (1999).

163. Wasan, K.M., Morton, R.E., Rosenblum, M.G. and Lopez-Berestein, G., Decreased toxicity of liposomal amphotericin b due to association of amphotericin b with high-density lipoproteins: role of lipid transfer protein, *Journal of Pharmaceutical Sciences* 83:1006-1010 (1994).

164. Wasan, K.M. and Lopez-Berestein, G., The interaction of liposomal amphotericin b and serum lipoproteins within the biological milieu, *Journal of Drug Targeting* 2:373-380 (1994).

165. Wasan, K.M., Brazeau, G.A., Keyhani, A, Hayman, A.C. and Lopez-Berestein, G., Roles of liposome composition and temperature in distribusion of amphotericin b in serum lipoproteins, *Antimicrobial Agents & Chemotherapy* 37:246-250 (1993).

166. Brajtburg, J., Elberg, S., Bolard, J., Kobayashi, G.S., Levy, R.A., Ostlund, R.E., Schlessinger, D. and Medoff, G., Interaction of plasma proteins and lipoproteins with amphotericin b, *The Journal of Infectious Diseases* 149:986-997 (1984).

167. Brezis, M., Heyman, S.N. and Sugar, A.M., Reduced amphotericin toxicity in an albumin vehicle, *Journal of Drug Targeting* 1:185-189 (1993).

168. Aramwit, P., Yu, B. G., Lavasanifar, A., Samuel, J. and Kwon, G. S., The effect of serum albumin on the aggregation state and toxicity of amphotericin b, *Journal of Pharmaceutical Sciences* 89:1589-1593 (2000).

169. Fukui, H., Koike, T., Saheki, A., Sonoke, S., Yoshikawa, H., Sasaki, H., Tomii, Y. and Seki, J. Characteristics of NS-718, a low-dose therapeutic system for amphotericin B with lipid nanosphere (LNS), *Proceedings of the Controlled Release Society* 25:388-389 (1998).

170. Van Etten, EWM., Viani, P., Tijhuis, R.H.G., Storm, G. and Bakker-Woudenberg, I.A., Sterically stabilized amphotericin b-liposomes: toxicity and biodistribution in mice, *Journal of Controlled Release* 37:123-129 (1995).

171. Van Etten, EWM., Kate, M.T., Stearne, L.E.T. and Bakker-Woudenberg, I.A., Amphotericin b liposomes with prolonged circulation in blood: *in vitro* antifungal activity, toxicity and efficacy in systemic candidiasis in leukopenic mice, *Antimicrobial Agents & Chemotherapy* 39:1954-1958 (1995).

172. Van Etten, E.M., Van Vianen, W., Hak, J. and Bakker-Woudenberg, I.M., Activity of liposomal amphotericin b with prolonged circulation in blood versus those of AmBisome and Fungizone against intracellular Candida albicans in murine peritoneal macrophages, *Antimicrobial Agents & Chemotherapy* 42:2437-2439 (1998).

173. Van Etten, E.M., Snijders, S.V., Van Vianen, W. and Bakker-Woudenberg, I.M., Superior efficacy of liposomal amphotericin b with prolonged circulation in blood in the treatment of severe candidiasis in leukopenic mice, *Antimicrobial Agents & Chemotherapy* 42:2431-2433 (1998).

Chapter 2

Micelles of poly(ethylene oxide)-*b*-poly(*N*-alkyl stearate-L-aspartamide):

synthetic analogues of lipoproteins for drug delivery

ı

2.1. Introduction

Compatibility between the micelle core and solubilizate is shown to be an important factor influencing encapsulation and release properties in micellar nanocontainers (1-5). With this in mind, we replaced the aromatic side chain of PEO-*b*-poly(β-benzyl-L-aspartate) (PEO-*b*-PBLA) with aliphatic structures, i.e., saturated fatty acid esters of an alkyl spacer group, to achieve a polymeric micellar carrier for solubilization and delivery of a model aliphatic drug, amphotericin B. We hypothesized that PEO-*b*-PLAA bearing fatty acid side chains self-assemble into micelles that mimic aspects of serum lipoproteins. Serum lipoproteins traverse the vascular system carrying water-insoluble molecules to destinations in the human body. Many water-insoluble drugs have been solubilized by serum lipoproteins, especially anti-cancer drugs (6;7). However, as a blood product serum lipoproteins express a lack of safety and poor stability. Polymeric micelles based on PEO-*b*-PLAA are expected to function like biological carriers due to their nanoscopic size, core/shell architecture, hydrophobicity of the core and stealth properties induced by the PEO shell. Mimicking structural aspects of lipoproteins, i.e., incorporation of fatty acid esters is hypothesized to improve the encapsulation of aliphatic drugs such as polyene macrolides within the micellar core and control their rate of release from the delivery system. As a result, PEO-*b*-PLAA micelles may play an analogous role to lipoproteins in terms of drug delivery, but with the ease of structural modifications, preparation and scale up (8).

The preparation of PEO-*b*-PLAA derivatives with fatty acid ester structures on the core-forming block, characterization of polymeric micelles and preliminary studies on the effect of the tailoring process on AmB encapsulation are discussed in this chapter.

59

The results shed light on functional properties of tailored polymeric micelles as synthetic analogues of lipoproteins.

2.2. Experimental section

2.2.1. Materials

2.2.1. Materials - Dicyclocarbodiimide (DCC), Dimethylaminopyridine (DMAP), 6-aminohexanol, fatty acids, and pyrene were purchased from Sigma. 2-hydroxypyridine (2-HP) and 2-aminoethanol were purchased from ICN. 1,3-(1,1'-dipyrenyl)propane) was purchased from Molecular Probes. All other chemicals were reagent grade.

2.2.2. Synthesis of stearic acid esters of PEO-b-poly(hydroxyalkyl-L-aspartamide)

2.2.2. Synthesis of stearic acid esters of PEO-b-poly(hydroxyalkyl-L-aspartamide) - The synthesis of PEO-b-poly(β-benzyl-L-aspartate) (PEO-b-PBLA) has been described in detail elsewhere (9). Briefly, PEO-b-PBLA has been synthesized by ring-opening polymerization of β-benzyl-L-aspartate N-carboxyanhydride, using α-methoxy-ω-amino-PEO as an initiator (M_n = 12,000 gmol^{-1}, M_w/M_n = 1.05, amine functionality = 0.96). After removal of PBLA oligomers, ^{1}H-NMR has established that the degree of polymerization of the PBLA block is 15.

PEO-b-PBLA (100 mg, 0.10 mmol BLA units) was dissolved in dried N,N-dimethylformamide (DMF) (5.0 ml) with the aid of stirring and slight heating. Subsequently, 2-aminoethanol (130 µl, 2.2 mmol) or 6-amino-hexanol (255 mg, 2.2 mmol.) and 2-hydroxypyridine (2-HP) (27 mg, 0.3 mmol) were added. The reaction mixture was stirred for 24 hs at 25°C and poured into vigorously stirred cold isopropanol (50 ml). The white precipitate was washed with isopropanol and ether and dried under

60

vacuum. The complete removal of benzyl groups was evidenced by ^{1}H-NMR in chloroform-d (AM- 300 MHz) and by absorption spectroscopy (Milton-Roy 3000).

Stearic acid (75 mg, 0.30 mmol), dicyclohexylcarbodiimide (DCC) (11 mg, 0.60 mmol) and dimethylamino-pyridine (DMAP) (3 mg, 0.020 mmol) were added to a solution of PEO-b-poly(hydroxyalkyl-L-aspartamide) (50 mg) in dried dichloromethane (5.0 ml) for 24 hs at 25°C. The product was precipitated in cold isopropanol (50 ml), collected by centrifugation and dried under vacuum. The product was characterized by ^{1}H-NMR in chloroform-d (AM-300 MHz).

2.2.3. Transmission electron microscopy of polymeric micelles - Samples for transmission electron microscopy (TEM) were prepared by placing an aqueous droplet of polymeric micelles (20 μL) on a membrane-coated grid, adding a droplet of 2 % phosphotungestic acid (negative stain). After 1 min excess fluid was removed, and images were obtained at a magnification of 18000 times (HITACHI H 7000).

2.2.4. Estimation of critical micelle concentration and core polarity - The critical micelle concentration (CMC) of the block copolymers and the polarity of the micelle cores were determined by following changes in the fluorescence excitation and the emission spectra of pyrene, respectively, in the presence of varied levels of block copolymers (10). Pyrene was dissolved in acetone and aliquots of this solution were added to 5.0 mL volumetric flask to provide final pyrene concentrations of 6×10^{-6} M. Acetone was evaporated and replaced with aqueous solutions of polymer having different concentrations. This solution was heated at 65-70 °C for an h and left at room

61

temperature overnight for the pyrene to equilibrate between the aqueous media and the micellar core. To monitor the excitation and emission spectrum of pyrene, emission and excitation wavelengths of the Fluoromax DM-3000 were set at 390 and 339 nm, respectively. The excitation and emission bandwidth were both chosen to be 4.25 nm.

2.2.5. Estimation of the core viscosity in PEO-b-PHSA micelles - The viscosity of the micelle cores above CMC was estimated by measuring the excimer to monomer intensity ratio (I_e/I_m) of 1,3-(1,1'-dipyrenyl) propane at 376 and 480 nm, respectively, from its fluorescence emission spectra (11). 1,3-(1,1'-dipyrenyl) propane was dissolved in chloroform and transferred to volumetric flasks providing concentrations of 2×10^{-7} M in the final solution. The concentration of block copolymer was 500 µg/ml (above CMC). Samples were then heated like what has been explained for pyrene experiment and the emission spectrum of the fluorescent probe was measured using an excitation wavelength and emission bandwidth of 333 nm and 4.25 nm, respectively. The same method was used to determine CMC, core polarity and viscosity in micelles of sodium dodecyl sulfate (SDS).

2.2.6. Encapsulation of amphotericin B (AmB) by polymeric micelles - The loading of AmB into polymeric micelles was accomplished by dissolving AmB (2.5 mg) and polymer (20 mg) in N,N-dimethylacetamide (4.0 ml). Water was added to the solution in a drop-wise manner (1 drop/10 sec) until the water content reached 10-15 % v/v. The solutions were dialyzed against water overnight and filtered (0.45 µm). An identical method was used to self-assemble the amphiphilic block copolymers without drug. The

62

drug content in an aliquot of the micellar solution diluted with an equal volume of DMF was measured from the UV/VIS (Milton Roy 3000) absorbance of AmB at 412 nm in the same solvent mixture.

2.3. Results and discussion

The scheme used to synthesize stearic acid esters of PEO-b-poly(hydroxyalkyl-L-aspartamide) is shown in Figure 2.1. The aminolysis of PEO-b-PBLA with 2-aminoethanol or 6-aminohexanol using 2-HP as a catalyst replaced benzyl groups with either a C_2 or C_6 spacer group containing a reactive hydroxyl group. Subsequently, the hydroxyl groups reacted with stearic acid to form an ester bond, using DCC and DMAP as a coupling reagent and catalyst, respectively. Purified product was shown to be free of unreacted stearic acid by thin layer chromatography using bromocresol as an indicator.

^{1}H-NMR was used to estimate the level of attached stearic acid on PEO-b-poly(N-ethyl stearate)-L-aspartamide (PESA) or PEO-b-poly(N-hexyl stearate)-L-aspartamide (PHSA) (Figure 2.2). Since the molecular weight of PEO block was known (12,000 gmol^{-1}) comparison of characteristic peak intensities of stearic acid (-CH$_3$, δ = 0.8 ppm) to that of PEO (-C$\underline{H}_2$-C$\underline{H}_2$O-, δ = 3.65 ppm) provided an estimate of fatty acid content (Table 2.1). An analysis of the data by unpaired t-test showed that the C_6 spacer group increases the degree of stearic acid substitution, i.e. ratio of fatty acid to aspartic acid, (P < 0.05). This could be attributed to the reduced steric hindrance, owing to the arrangement of hydroxyl groups away from the PHAA backbone.

PEO-b-PESA and PEO-b-PHSA self-assembled into spherical micelles based on TEM images, with low polydispersity and no evidence of secondary association (Figure

63

2.3). The average diameters of PEO-*b*-PESA and PEO-*b*-PHSA micelles were 17.9 nm to

21.6 nm in the dry state, respectively. The difference was found to be significant

(unpaired t-test, P < 0.001). The difference in diameter may be due to the varied degree

of stearic acid substitution, although the effect of the difference in the length of the spacer

group cannot be ruled out. Based on TEM photographs PEO-*b*-PBLA micelles had an

average diameter of 17.4 nm. Block copolymers of PEO-*b*-PBLA with the same

molecular dimensions were found to form micelles with an average diameter of 21 nm in

water using dynamic light scattering technique (5). The difference in the size measured

by these two methods (around 3.6 nm) is due to the hydration of the PEO chain in

aqueous medium. Therefore, a similar increase in size is expected for PEO-*b*-PESA and

PEO-*b*-PHSA polymeric micelles when introduced to water.

Fluorescent probe studies with pyrene and 1,3-(1,1'-dipyrenyl) propane on PEO-

b-PESA and PEO-*b*-PHSA micelles revealed low CMC, low core polarity and high core

viscosity characteristic of an aliphatic domain. At levels above the CMC, the probes

preferentially partitioned into micelle cores, altering their photophysical properties. A red

shift was observed in the excitation spectrum of pyrene with a rise in the level of PEO-*b*-

PESA or PEO-*b*-PHSA (Figure 2.4A). A plot of the ratio of peak intensities at 339 nm

over 334 nm versus polymer concentrations rises sharply at the CMC (Figure 2.4B).

PEO-*b*-PESA and PEO-*b*-PHSA had average CMCs of 39 and 23 µg/ml, whereas the

CMC of PEO-*b*-PBLA was 38 µg/ml. CMC of PEO-*b*-PHSA polymeric micelles was

found to be significantly lower than that of PEO-*b*-PESA (unpaired t-test, P < 0.05),

reflecting higher tendency for self association for copolymers having longer spacers or

higher levels of fatty acid attachment. The low CMCs of polymeric micelles reflect their

64

thermodynamic stability, contrasting with many low molecular weight surfactant micelles (Table 2.1).

A decrease in the relative intensity of the first (I_1) to the third (I_3) bands in the pyrene monomer emission spectrum was also revealed at the onset of micelle formation (Figure 2.4C and D). The I_1/I_3 of pyrene is a function of polarity. The I_1/I_3 ratio of pyrene above the CMCs of PEO-*b*-PESA and PEO-*b*-PHSA was about 1.0. This value corresponds to that of pyrene partitioned into sodium dodecyl sulfate micelles and to that of pyrene in *n*-butanol (12). The I_1/I_3 ratio of pyrene was noticeably lower for PEO-*b*-PESA and PEO-*b*-PHSA micelles than PEO-*b*-PBLA micelles, reflecting a lower polarity of an alkyl core than an aromatic core. The polarity of cores of polymeric micelles can be adjusted by polymeranalogous reaction, impacting interactions with drugs and drug solubilization.

Lastly, 1,3-(1,1'-dipyrenyl) propane partitioned into PEO-*b*-PESA and PEO-*b*-PHSA micelle cores displayed little excimer fluorescence (Figure 2.5, Table 2.1). The low value of the excimer to monomer intensity ratios, I_e/I_m, indicated that the cores in PEO-*b*-PLAA micelles have a high viscosity, which may prevent the dissociation of micellar structure to polymeric unimers. PEO-*b*-PBLA micelles also have cores with high viscosity. In contrast, the I_e/I_m ratio for sodium dodecyl sulfate micelles is quite high and consistent with a liquid-like core. At low viscosity, free rotation around carbon-carbon bonds in 1,3-(1,1'-dipyrenyl) propane favors excimer formation.

AmB partitioned into PEO-*b*-PESA and PEO-*b*-PHSA micelles, increasing its solubility to 137 and 332 μg/mL from 1.0 μg/mL (Table 2.1). PEO-*b*-PBLA micelles increased the solubility of AmB to 25 μg/ml. The increase in AmB solubility reflects

65

preferential interaction of the drug with alkyl group, as opposed to benzyl group. AmB interacts favorably with serum lipoproteins, which have cores rich in triglycerides, and with lipid bilayer membranes. The solubility of AmB increased as the degree of fatty acid substitution and/or micellar size was increased.

2.4. Conclusion

PEO-b-PESA and PEO-b-PHSA self-assemble into nanoscopic supramolecular core-shell architectures, mimicking structural features of serum lipoproteins. Owing to a core of stearic acid, solubilization of AmB is effectively improved in PEO-b-PESA and PEO-b-PHSA micelles. PEO-b-PESA and PEO-b-PHSA micelles may also solubilize other drugs solubilized by serum lipoproteins and have the potential to alter the biodistribution of the incorporated drugs.

Table 2.1. Characteristic properties of micelles based on PEO-*b*-PLAA block copolymer with aromatic and aliphatic side chains in comparison to sodium lauryl sulfate.

Polymer	Side chain substitution level (%)	Micellar diameter ± SD (nm)	CMC (μg/ml)	I_1/I_3	I_e/I_m	AmB solubility (μg/ml)	AmB / polymer (molar ratio)
PEO-*b*-PBLA	100	17.4 ± 3.9	38 ± 5	1.14	0.25 ± 0.06	25	0.1
PEO-*b*-PESA	44.6 ± 8.6	17.9 ± 5.9	39 ± 7	1.04	0.15 ± 0.05	137	1.5
PEO-*b*-PHSA	63.8 ± 13.9	21.6 ± 4.0	23 ± 5	1.00	0.15 ± 0.04	332	4.2
SDS	-	-	2500	0.96	0.93	-	-

67

	hydrophilic block	hydrophobic block

CH₃O(CH₂CH₂O)ₓ(CH₂)₃S(CH₂)NH⁺COCHNH₎H
                  |
                  CH₂
                  |
                  CO₂—H₂C—⟨ ⟩

PEO- b -PBLA

aromatic groups

↓ H₂N(CH₂)₆OH

CH₃O(CH₂CH₂O)ₓ(CH₂)₃S(CH₃)NH⁺COCHNH₎H
                  |
                  CH₂
                  |
                  CONH(CH₂)₆OH

PEO- b -PHAA

alkyl spacer groups

↓ CH₃(CH₂)₁₆CO₂H

CH₃O(CH₂CH₂O)ₓ(CH₂)₃S(CH₂)NH⁺COCHNH₎ₓCOCHNH₎₋₂H
                        CH₂   CH₂
                        | |
CH₃(CH₂)₁₆CO₂⁻(CH₂)₆⁻NH—CO   CONH(CH₂)₆OH

PEO- b -PHSA

fatty acid side chains
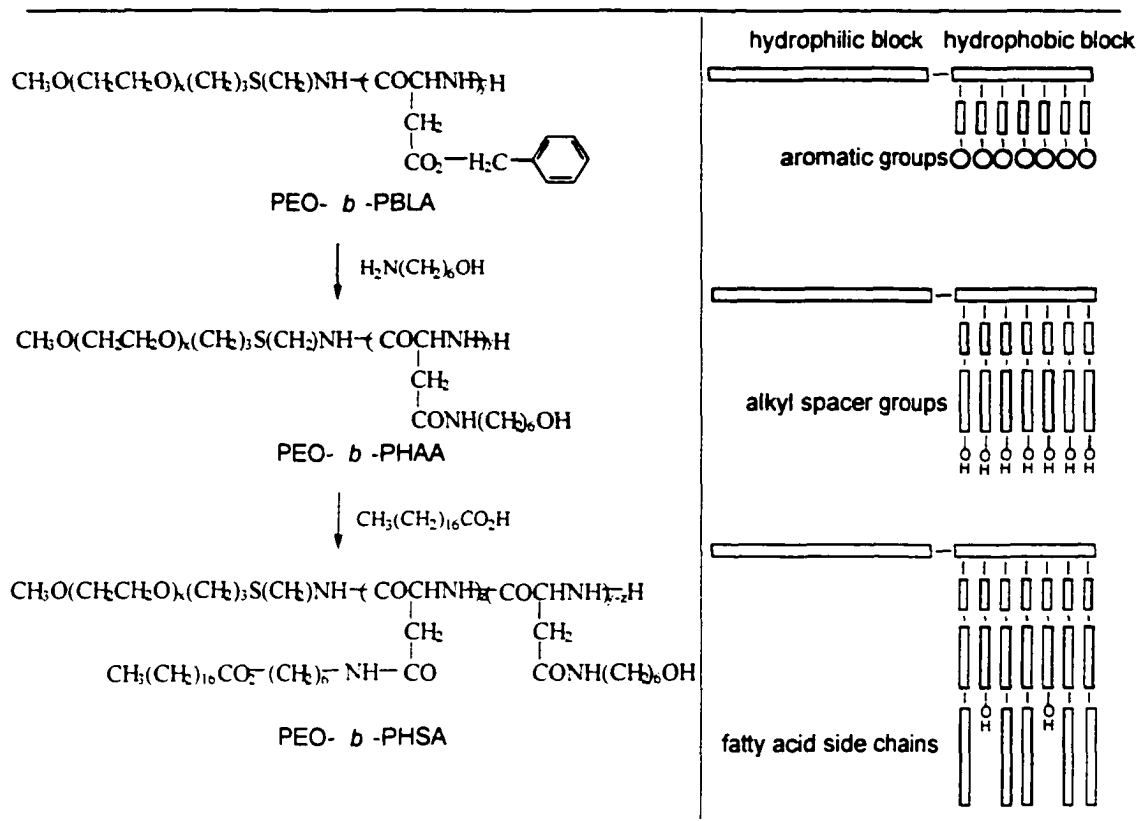
Figure 2.1. Synthetic scheme for PEO-b-PHSA from PEO-b-PBLA and models.

CH3O(CH2CH2O)n-(COCHNH)mH

1, 2   3

4 CH2
   CO
   NH
5 CH2
6 (CH2)4
7 CH2
   CO2
8 CH2
9 (CH2)15
10 CH3

1, 2

6, 9

10

7, 8

3 5

4

Figure 2.2. ^{1}H NMR spectrum of PEO-b-PHSA in chloroform-d and peak assignments.

69
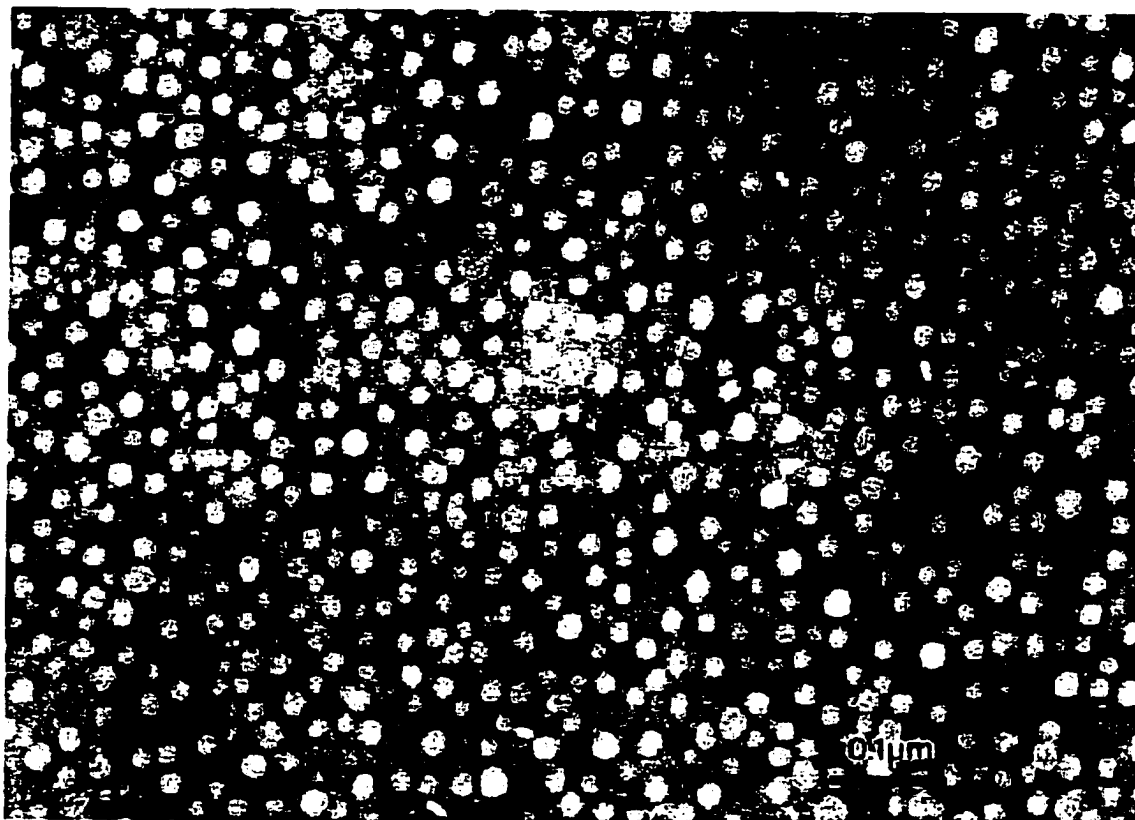
Figure 2.3. TEM photograph of PEO-*b*-PHSA micelles (magnification 18000 × 5.9).

70
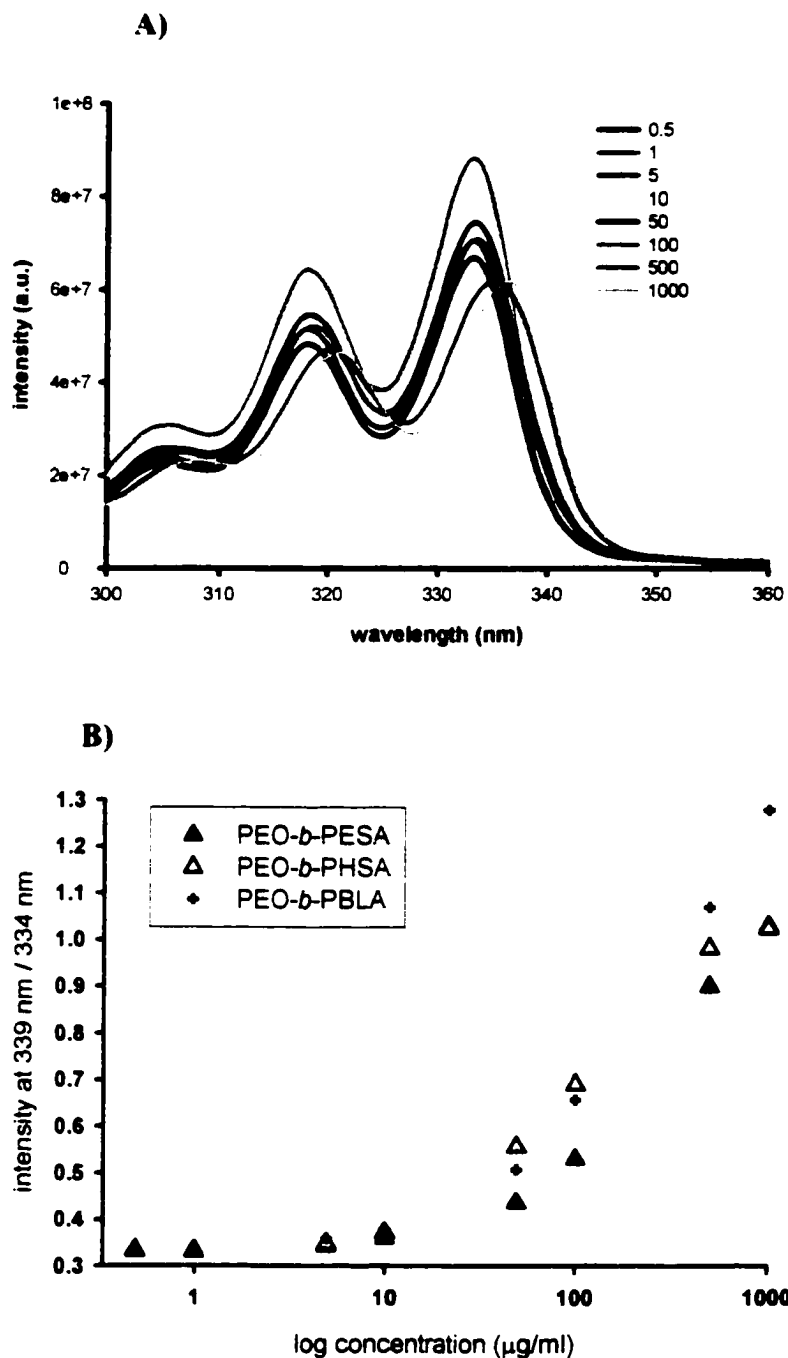
Figure 2.4. A) Florescence excitation spectra of pyrene in the presence of different

concentrations of PEO-*b*-PESA block copolymer **B)** Intensity ratio (339 nm/334 nm) of

pyrene (6×10^{-7} M) from excitation spectrum as a function of polymer concentration

71

B)
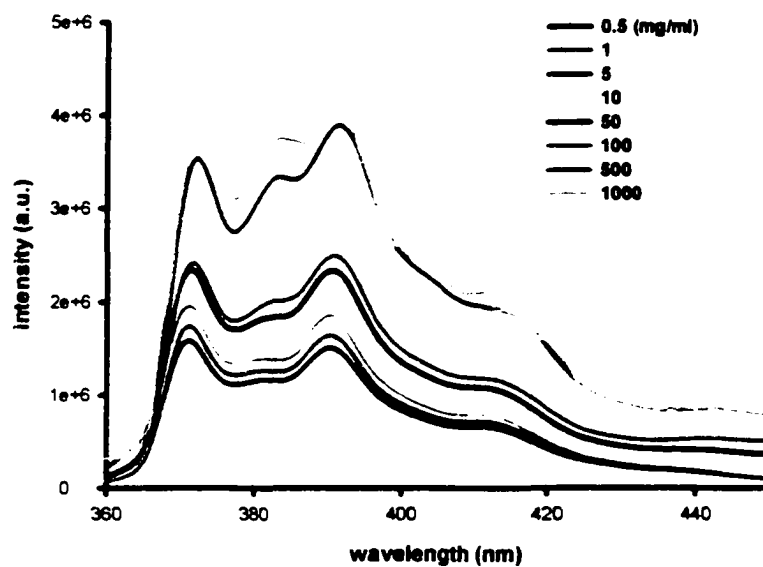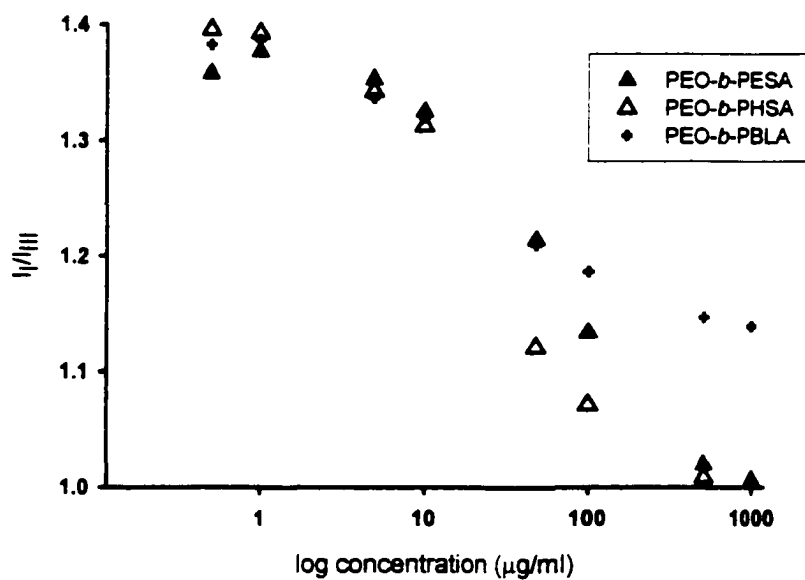
Figure 2.5. A) Florescence emission spectra of pyrene in the presence of different

concentrations of PEO-*b*-PESA block copolymer B) Intensity ratio (I_1/I_3) of pyrene (6×10^{-7}

M) from emission spectrum as a function of polymer concentration.

72
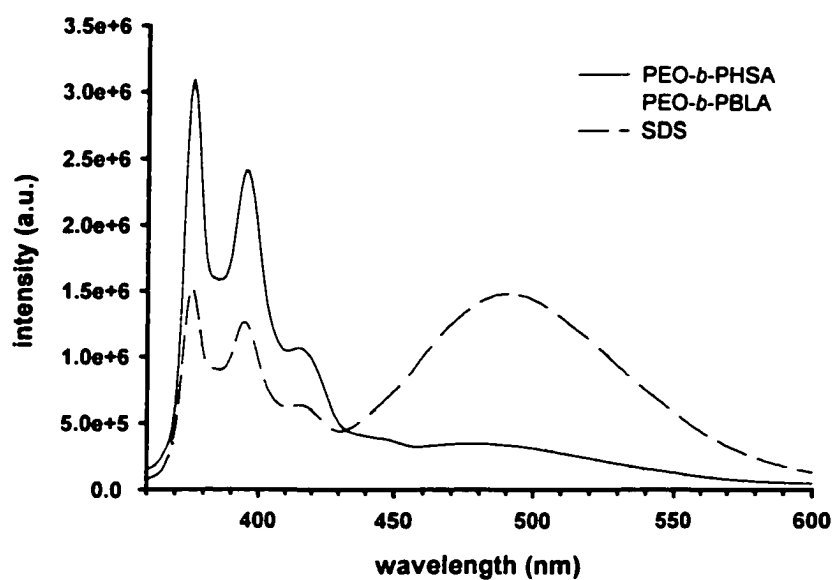
Figure 2.6. Fluorescence emission spectrum of 1,3-(1,1'-dipyrenyl)propane in micellar solutions of PEO-*b*-PBLA and PEO-*b*-PHSA in comparison to SDS.

73

2.5. References

1. Nagarajan, R., Barry, M. and Ruckenstein, E., Unusual selectivity in solubilization by block copolymer micelles, *Langmuir* 2:210-215 (1986).

2. Hurter, P.N. and Hatton, T.A., Solubilization of polycyclic aromatic hydrocarbons by poly(ethylene-propylene oxide) block copolymer micelles: effects of polymer structure, *Langmuir* 8:1291-1299 (1992).

3. Kwon, G.S. and Kataoka, K., Block copolymer micelles as long circulating drug vehicles, *Advanced Drug Delivery Reviews* 16:295-309 (1995).

4. Yokoyama, M., Fukushima, S., Uehara, R., Okamoto, K., Kataoka, K., Sakurai, Y. and Okano, T., Characterization of physical entrapment and chemical conjugation of adriamycin in polymeric micelles and their design for *in vivo* delivery to a solid tumor, *Journal of Controlled Release* 50:79-92 (1998).

5. Yokoyama, M., Satoh, A., Sakurai,Y., Okano, T., Matsumura, Y., Kakizoe, T. and Kataoka, K., Incorporation of water-insoluble anticancer drug into polymeric micelles and control of their particle size, *Journal of Controlled Release* 55:219-229 (1998).

6. Bijsterbosch, M.K. and Van Berkel, T.C., Native and modified lipoproteins as drug delivery systems, *Advanced Drug Delivery Reviews* 5:231-251 (1990).

7. Firestone, R. A., Low-density lipoprotein as a vehicle for targeting antitumor compounds to cancer cells, *Bioconjugate Chemistry* 5:105-113 (1994).

8. Kwon, G. S. and Okano, T., Soluble self assembled block copolymers for drug delivery, *Pharmaceutical Research* 16:597-600 (1999).

9. Yokoyama, M., Kwon, G.S., Okano, T., Sakurai, Y., Sato, T. and Kataoka, K., Preparation of micelle-forming polymer-drug conjugates, *Bioconjugate Chemistry* 3:295-301 (1992).

10. Kwon, G.S., Naito, M., Yokoyama, M., Okano, T., Sakurai, Y. and Kataoka, K., Micelles based on ab block copolymers of poly(ethylene oxide) and poly(β-benzyl-L-aspartate), *Langmuir* 9:945-949 (1993).

11. Georges, J., Molecular fluorescence in micelles and microemulsions: micellar effects and analytical applications, *Spectochimica Acta Reviews* 13:27-45 (1990).

12. Lianos, P., Viriot, M. and Zana, R., Study of the solubilization of aromatic hydrocarbons by aqueous micellar solutions, *Journal of Physical Chemistry* 88:1098-1101 (1984).

74

Chapter 3

The effect of alkyl core structure on micellar properties of poly(ethylene

oxide)-*b*-poly(L-aspartamide) derivatives

3.1. Introduction

The alteration of the core structure in PEO-*b*-poly(L-aspartic acid) (PEO-*b*-P(Asp)) based micelles to aliphatic ones enhanced the solubilization of a model aliphatic drug, AmB, as reported in the first chapter. In this chapter, we intend to elaborate on the effect of different alkyl core structures on crucial micellar properties for an efficient drug delivery.

Block copolymers with various dimensions of the P(Asp) block, different chain lengths of fatty acid and alkyl spacer groups and varied levels of fatty acid substitution on the polymeric backbone have been prepared. Micellar properties such as size, critical micelle concentration, core polarity and viscosity have been measured by transmission electron microscopy (TEM) and fluorescent probe techniques. Amphiphilic polymers that self assemble at very low concentrations (μM levels) in an aqueous environment and form spherical micelles with nanoscopic dimensions could mimic aspects of natural transport systems *in vivo* (1). While compatibility of the core-forming block and solublizate is essential for polymeric micelles to solubilize the hydrophobic molecules effectively (2-5), the existence of rigid cores provides kinetic stability for the micellar structure. Besides, slow release of the solubilized molecules from the polymeric micelles with very rigid cores can be achieved, as the diffusion coefficients are very low in temperatures below glass transition temperatures (Tg) (1).

3.2. Experimental section

3.2.1. Synthesis of fatty acid esters of PEO-b-poly(hydroxy-alkyl-L-aspartamide) - The synthesis of PEO-*b*-poly(hydroxy-alkyl-L-aspartamide) with fatty acid ester side chains

76

from PEO-*b*-poly(β-benzyl-L-aspartate) (PEO-*b*-PBLA) has been carried out in two steps. Based on ^{1}H NMR spectroscopy, the degree of polymerization of the PBLA block in the samples used was either 15 or 24. To differentiate between these samples, a nomenclature of 12-15 or 12-24 is defined based on molecular weight of the PEO block (12000 gmol^{-1}) and the degree of polymerization of the PLAA block (15 or 24). For a detailed description of the first step refer to chapter 2, section 2.2.2. For the current study, in the second step, PEO-*b*-PHAA (12-15) was esterified with hexanoic (C=6), capric (C=10), myristic (C=14), stearic (C=18) or behenic acid (C=22) using the procedure explained under section 2.2.2 in chapter 2.

3.2.2. Micelle formation from fatty acid esters of PEO-b-PHAA - Micellization of polymers was achieved by dissolving 15 mg of each polymer in 4.0 mL of DMF with the aid of slight heat. Doubly distilled water was then added to this solution in a drop-wise manner (one drop per 20 s) until the final water concentration was 10-15 % (v/v). A dialysis membrane with a molecular cutoff of 12,000-14,000 gmol^{-1} was used to replace the organic solvent with distilled water overnight at room temperature replacing the medium three times. Micelles were then passed through 0.22 μM filters.

3.2.3. Determination of the micellar shape and size by transmission electron microscopy (TEM) - Method of sample preparation for TEM is described under section 2.2.3 in chapter 2. Prepared samples were loaded into a HITACHI H 7000 transmission electron microscope. Images were obtained at a magnification of 18,000 times (75 kV). Apparent diameters of micelles were measured and mean diameter ± SD was calculated

77

for each species based on at least 120 measurements. For micelles with an elepsoid shape, the diagonal of the ellipsoid is reported as the micellar size.

3.2.4. Estimation of the critical micelle concentration and micellar core polarity by fluorescent probe techniques - By following changes in the fluorescence excitation and emission spectra of pyrene in the presence of varied concentrations of block copolymers, according to a method described in section 2.2.4 in Chapter 2, the critical micelle concentration (CMC) and the polarity of the micellar core for each block copolymer were determined, respectively.

3.2.5. Estimation of the core viscosity by fluorescent probe measurements - The viscosity of the micelle cores above the CMC was estimated by measuring excimer to monomer intensity ratio (I_e/I_m) of 1,3-(1,1'-dipyrenyl)propane at 376 and 480 nm, respectively, based on a procedure explained in section 2.2.5 in chapter 2.

3.2.6. Statistical analysis - Data obtained from CMC and micellar size measurements were subjected to analysis of variance or unpaired t test by Statistical Analysis Software (SAS). For ratios obtained in the polarity and viscosity measurements inverse sin transformed data were subjected to analysis of variance. Differences among treatment means were tested for statistical significance using the Duncan multiple mean procedure at a significance level of 0.05.

3.3. Results

The preparation of fatty acid esters of PEO-*b*-PHAA from PEO-*b*-PBLA with either 15 or 24 degrees of polymerization in the PBLA block was accomplished in two steps. In the first step, 2-HP was used as a catalyst to remove the benzyloxy group of PEO-*b*-PBLA and replace it with either 2-aminoethanol or 6-aminohexanol. As a result, PEO-*b*-poly(hydroxyethyl-L-aspartamide) PEO-*b*-PHEA) and PEO-*b*-poly(hydroxyhexyl-L-aspartamide) (PEO-*b*-PHHA) were formed, respectively. PEO-*b*-PHEA and PEO-*b*-PHHA were then reacted with saturated fatty acids of various chain lengths ranging from 6 to 22 carbons in the presence of DCC and DMAP as coupling agent and catalyst, respectively. The general structure of the final product is shown in Figure 3.1. Thin layer chromatography using diethyl ether:dichloromethane (20:80) as the mobile phase and 0.1 % solution of bromocresol in ethanol as an indicator confirmed the purity of block copolymers from free fatty acids.

^{1}H NMR was used to estimate the level of fatty acid substitution on PEO-*b*-PHAA. Since the molecular weight of the PEO block was known and the purity of the synthesized copolymers was confirmed by TLC, comparison of characteristic peak intensities of fatty acid substitutents (CH_3-, δ = 0.8 ppm) to that of PEO (-CH_2-CH_2-O-, δ = 3.6 ppm) provides an estimation of the degree of fatty acid attachment. The substitution of fatty acid is expressed as the percentage of conjugated stearic acid to hydroxyl groups of PEO-*b*-PHAA throughout the thesis. Statistical analysis (ANOVA, Duncan's test) of the data obtained for different batches of synthesized polymers (with varied fatty acid chain lengths) reveals that the use of longer spacer groups significantly (P < 0.01) increases the level of fatty acid substitution on the PHAA block.

79

Micellization of the fatty acid conjugates of PEO-*b*-PHAA having different core structures was achieved using a dialysis method, and the formation of micelle like structures was investigated by TEM. The TEM images clearly indicate the presence of spherical particles with nanoscopic dimensions. However, a tendency towards the formation of ellipsoids is seen when longer fatty acids (myristic and stearic) attached to C_6 spacer group with higher degrees of substitution (ca. 65 %) were used (Figure 3.2).

The average diameter of the prepared micelles measured from TEM images for 12-15 samples was found to be between 14.7 - 21.8 nm (Table 3.1). Increasing the substitution level of fatty acid on the polymeric backbone caused a significant increase (P < 0.001) in micellar size as it is shown for PEO-*b*-poly[*N*-(6-hexyl caprate)-L-aspartamide] (PEO-*b*-PHCA) in Figure 3.3A (7 % vs. 44%). The length of the spacer group showed no significant effect when micellar size was compared in capric acid conjugates of PEO-*b*-PHEA and PEO-*b*-PHHA with the same degree of fatty acid attachment (Figure 3.3A). Increasing the length of fatty acid chain was shown to cause a significant raise in micellar size (P < 0.001) when polymer batches with similar degree of fatty acid attachment were compared (Table 3.1). The average diameter of stearic acid conjugates of PEO-*b*-PHEA and PEO-*b*-PHHA for 12-24 samples was measured to be between 23.3 to 25.3 nm. An increase in the length of the PLAA block from 15 to 24 also showed an enhancing influence (unpaired t test, P < 0.001) on micellar size when block copolymers with the same degree of stearic acid substitution on the PHEA or PHHA blocks were compared (Figure 3.3B). The substitution level of stearic acid on the PHEA and PHHA block was calculated to be 45 and 60 %, respectively in both 12-15 and 12-24 samples.

80

Pyrene was used as a fluorescent probe to determine the CMCs and the micropolarities of the core for micelles formed from fatty acid esters of PEO-*b*-PHAA. Following partitioning of pyrene into the micellar core at polymer levels above CMC, a red shift is seen in the excitation spectrum of pyrene. Therefore, the ratios of peak intensities at 339 nm over 334 nm can be plotted vs. the logarithm of polymer concentration to determine CMC (Figure 3.4A). The CMC is measured from a sharp rise in the intensity ratios at the onset of micellization (6-8). The average CMCs for the polymeric micelles under study ranged from 9 to 50 µg/mL. The elongation of the fatty acid chain did not change CMC values obtained from this method of measurement (Table 3.1). As it is shown in Figure 3.4B and 3.4C, no significant effect ($P > 0.05$) on CMC was observed when block copolymers with longer PHAA block or spacer group but similar level of fatty acid substitution were used, respectively, whereas the substitution level of fatty acid on the PHAA block seems to be the major factor controlling the onset of micellization. As it is illustrated in Figure 3.4C, a decrease in the level of capric acid attachment from 44 to 7 % results in a reduced tendency for self-association in PEO-*b*-PHCA. The mean CMC value rose from 29 to 57 µg/mL in PEO-*b*-PHCA with 7 % of capric acid substitution.

The fluorescence emission spectrum of pyrene was also affected by the polarity of its environment. A sharp decrease in the relative intensity of the first (I_1) to the third band (I_3) was observed at the CMC as pyrene partitions to the non-polar core of the micelles (Figure 3.5A). The I_1/I_3 ratios obtained from emission spectra of pyrene in the presence of 500 µg/mL of fatty acid ester of PEO-*b*-PHAA (12-15) are reported in Table 3.1. In water, a ratio of 1.4 was observed for pyrene, which is in agreement with previous

81

observations (7). At low polymer concentrations, this ratio was close to what has been found for water. As the concentration of the polymer increased, the I_1/I_3 ratio dropped to about 1.0. The reduced value of I_1/I_3 ratio is an indication of the existence of non-polar microdomains in micelles with polarities similar to n-pentanol in the pyrene scale (9). No significant effect on I_1/I_3 was detected when different structural factors were altered in fatty acid conjugates of PEO-b-PHAA, $P > 0.05$ (Table 3.1, Figure 3.5B). A decrease in the level of fatty acid substitution caused a significant decrease in I_1/I_3 ratio, $P < 0.01$ (Figure 3.5C).

Evidence for the limited motion of fatty acid esters in the micellar core was obtained from the fluorescence emission spectrum of 1,3-(1,1'-dipyrenyl)propane in the presence of 500 μg/mL of polymeric micelles (Figure 3.6A). Like pyrene, 1,3-(1,1'-dipyrenyl)propane is a hydrophobic fluorescent probe that preferentially partitions into the hydrophobic micro-domains of micelles at polymer concentrations above the CMC. By changing its conformation, 1,3-(1,1'-dipyrenyl)propane forms intramolecular pyrene excimers that emit light at 480 nm when excited at 390 nm. The conformational change in 1,3-(1,1'-dipyrenyl)propane probe is being restricted by a local friction imposed by the viscosity of its environment. Therefore, the ratio of the intensity of the light emitted from excited dipyrene excimer (I_e) to that of isolated pyrene monomer (I_m) in its emission spectrum could be used as a measure of effective viscosity (7). As shown in Table 3.1 and Figure 3.6, I_e/I_m ratios are found to be very low for all the copolymers under study, reflecting rigid structures for the polymeric micellar cores. In contrast, a high incidence of excimer formation in sodium lauryl sulfate (SDS) reflects the liquid like core of a low molecular weight surfactant (Figure 3.6A). No significant change ($P > 0.05$) in I_e/I_m ratios

82

was detected for different fatty acids attached to the polymeric backbone in 12-15 samples (Table 3.1). However, behenic acid conjugates of PEO-b-PHHA with substitution levels of 65 % showed lowered I_e/I_m ratio (0.08) in comparison to other copolymers (Table 3.1). In addition to this specific structure, lower average I_e/I_m ratios in 12-24 samples of PEO-b-poly[N-(2-ethyl stearate)-L-aspartamide] (PEO-b-PESA) PEO-b-poly[N-(6-hexyl stearate)-L-aspartamide] (PEO-b-PHSA) compared to 12-15 species indicates the elongation of the PHAA block cause more restricted motions in the micellar core environment as well (Figure 3.6B).

3.4. Discussion

It is known that amphiphilic block copolymers can form supramolecular core/shell structures in aqueous environment through the expulsion of their hydrophobic segments from water and further hydrophobic association of these blocks. Supramolecular self-assembled structure plays an analogous role to natural carriers with several advantages such as ease of chemical modification, stability and safety (10; 11). To achieve optimized micellar properties and drug loading capacities we pursue the chemical tailoring of the core structure in PEO-b-PLAA in our recent research studies. Compatibility between the solubilizate and the core-forming block is proven to be necessary for efficient solubilization of water insoluble molecules in micellar systems (2; 3; 5; 12). With this in mind, the chemical structure of the core-forming block in PEO-b-PLAA was tailored to aliphatic ones to enhance the solubilization of compatible drugs. This issue is investigated for a model drug, AmB, and the preliminary results are emphasized in the first chapter. The purpose of the current study was to investigate the

83

role of structural modifications on the key micellar properties, which determine the effectiveness of the drug delivery system.

Chemical modification of the core structure in PEO-*b*-PLAA block copolymers was carried out through replacement of benzyloxy group in PEO-*b*-PBLA with hydrophobic spacers having hydroxyl termini. These products were further conjugated with different fatty acids to form fatty acid conjugates of PEO-*b*-PHAA (Figure 3.1). ^{1}H NMR was used to measure the degree of fatty acid substitution. Attachment of a hydrophobic spacer was proposed to introduce hydroxyl functional moieties to the side chains, which could react with the carboxyl groups of the fatty acids. The conjugation of fatty acid was increased as the length of the spacer was raised from 2 to 6 carbons. Using the same method of synthesis, block copolymers with different structures of the core-forming block were prepared, purified, dissolved in DMF and dialyzed against water to form micellar structures. Micellar properties were determined for each structure by TEM and fluorescent probe techniques.

Our data suggests that PEO-*b*-PLAAs with alkyl core structures are potential candidates to mimic aspects of biological carriers for delivery of hydrophobic molecules. They self-assemble into nanoscopic, supramolecular core/shell structure where the core is rich in fatty acid esters. The shape of the micellar system was shown to be spherical by TEM in most of the cases with the exception of highly substituted ($\geq$ 65 %) myristic, stearic and behenic conjugates of PEO-*b*-PHHA. In those species a tendency toward the formation of ellipsoids is observed (Figure 3.2), which could be attributed to the larger dimensions of the hydrophobic block in those constituents. Low CMC values measured for fatty acid conjugates of PEO-*b*-PHAA indicate a high tendency of these amphiphilic

84

structures toward self-association in aqueous environment, i.e., their thermodynamic stability. The aliphatic core of polymeric micelles prepared in this study also appeared to be highly viscous. Micelles with glassy cores tend to disassemble more slowly than those with a mobile core (1). As a result the micellar system may show kinetic stability surviving for some period of time *in vivo*.

The alkyl core of the polymeric micelles in our studies was essentially varied in four structural aspects: a) The length of the PLAA block, b) the length of the alkyl spacer, c) the length of the attached fatty acid and d) the substitution level of fatty acid on the polymeric backbone.

The substitution level of fatty acid on the polymeric backbone was revealed to be the major factor affecting micellar size, shape, CMC and micropolarity. The effect of the fatty acid substitution level was investigated in PEO-*b*-PHCA block copolymers with two different degrees of capric acid attachment. An increase in the fatty acid content of the micellar core caused an increase in micellar size (P < 0.0001, unpaired t test) and a decrease in CMC (P < 0.05, unpaired t test) as it is illustrated in Figures 3.3 and 3.4, respectively. Average micellar size was enhanced when capric acid content of the core was increased from 7 to 44 %. Enhancement of the micellar size in the dry state is assumed to be a consequence of larger dimensions of the hydrophobic block in those structures. Owing to the hydration of the PEO surface, micellar size is expected to show an increase in aqueous environment. However, enhanced hydrophobicity of the core-forming block may restrict this hydration and affect the final size of the polymeric micelles *in vivo*. Therefore, the results obtained from the TEM measurements cannot simply be extrapolated to micellar dimensions in aqueous environment.

85

Reduced CMC values for block copolymers with higher levels of capric acid attachment reflect reduced free energy of micellization for those polymers. Preferential expulsion of the copolymers with larger hydrophobic segments from water (greater entropic driving force) is assumed to be the reason behind this observation. PEO-b-PHCA with 7% of capric acid attachment exhibited greater micropolarities at 500 µg/mL concentration ($I_1/I_3 = 1.3$) (Figure 3.5C). The I_1/I_3 in this case is even higher than values measured for benzyl core in PEO-b-PBLA at the same concentration (Chapter 2, section 2.3). The higher I_1/I_3 ratios could result from high core polarities due to the expression of OH groups in the micellar core. However, incomplete localization of the pyrene probe in the micellar core can cause the same effect. This in turn is a result of reduced hydrophobicity in the core region when polymeric micelles with capric acid substitutions as low as 7 % are used. At 7 % substitution, the amount of fatty acid present is not high enough to overcome the high polarities induced by free hydroxyl groups present in the micellar core. Existence of polar groups in the micellar core is expected to make the delivery system more susceptible to dissociation and hydrolysis. It is interesting that no difference in micellar core viscosity was shown in the two species. The formation of the 1,3-(1,1'-dipyrenyl)propane excimer was considerably restricted in PEO-b-PHCA even with 7% of fatty acid substitution. This result is in contrast to SDS, which shows a 10 fold ratio of I_e/I_m in comparsion to polymeric micelles (Figure 3.6).

The application of block copolymers with different lengths of the PLAA block induced changes in micellar size and core viscosity. Average micellar size was increased when length of the PHEA and PHHA was increased at the similar level of stearic acid substitution as it is illustrated in Figure 3.3B. Increasing the hydrophobic block length

86

showed no detectable effect on CMC measured from partitioning of pyrene in micellar core (Figure 3.4B). This finding seems to contradict previous observations (6). However, in this case the presence of hydroxyl groups in the core-forming block might have caused the effects of the block elongation in reducing CMC to be hindered. Like CMC, micellar core polarity was not affected by this structural factor as it is shown in Figure 3.5B. Micellar core viscosity, however, was found to be influenced by the length of the P(Asp) block. More viscose cores were formed when the length of P(Asp) was elongated from 15 to 24 (Figure 3.6B). Side chain crystallization in the core caused by parallel arrangement of fatty acids is a possibility, but it requires further study. This may in turn, result in the formation of polymeric micelles with greater dynamic stability. At the same time, due to this effect particle movements into or out of the core region could be restricted.

The length of the spacer group showed no significant effect on micellar properties. Its effect on micellar size and CMC is compared in Figure 3.3A and 3.4C, respectively, for PEO-*b*-PECA and PEO-*b*-PHCA having similar degrees of capric acid attachment. The difference observed in micellar size (Figure 3.3B) and CMC (Figure 3.4B) between PEO-*b*-PESA and PEO-*b*-PHSA is, therefore, most likely a result of an increase in the level of stearic acid substitution from 45 to 60 percent.

Except for micellar size, other properties of the system were not affected when length of the fatty acid attached to the polymeric backbone was changed (Table 3.1), or at least the methods used were not sensitive enough to detect the possible differences. Attachment of behenic acid with 22-carbon chain to hexyl spacer in a high level of substitution was the only exception. This unique structure lowered the formation of dipyrene probe excimer reflecting higher local viscosity in micellar core in comparison to

87

other polymeric micelles in this study (Table 3.1). The same structure with 50 % of behenic acid attachment showed similar I_e/I_m ratios in comparison to other structures reflecting similar microviscosities.

3.5. Conclusions

Fatty acid esters of PEO-*b*-PHAA can be used for drug delivery as they form nanoscopic, core/shell micellar structures at very low concentrations where the core is solid like at room temperature. Owing to the possibility of structural modifications in the core-forming block, polymeric micelles with selected structures for the purpose of drug delivery can be designed and prepared. Our results indicate varying the level of fatty acid side chain and the length of the PHAA block are the major factors by which the micellar structure can be tailored. Changing the level of fatty acid attachment will affect micellar size, thermodynamic stability and micropolarity, whereas varying the length of the PHAA block in PEO-*b*-PLAA copolymers can be used to achieve desired micellar core viscosity. Increasing the core viscosity can also be achieved by conjugation of fatty acids having long chains (>22 carbon) in a high level to the polymeric backbone.

88

Table 3.1. The effect of fatty acid chain length on micellar properties in PEO-*b*-PHAA (12-15) derivatives.

Spacer group	Fatty acid chain length	Substitution level (%)	Size ± SD (nm)[†] n=120	CMC ± SD (μg/mL)[†] n=3	I_1/I_3 ± SD[†] n=3	Ie/Im ± SD[†] n=3
	6	44	16.4 ± 3.2^A	39 ± 5^A	1.05 ± 0.01^A	0.16 ± 0.01^A
	10	43	17.6 ± 3.3^B	32 ± 2^A	1.00 ± 0.02^A	0.15 ± 0.02^A
Ethyl	14	42	17.7 ± 3.9^C	34 ± 16^A	1.03 ± 0.02^A	0.15 ± 0.01^A
	18	47	18.0 ± 5.9^D	39 ± 7^A	1.06 ± 0.03^A	0.15 ± 0.05^A
	10	57	18.1 ± 3.3^E	26 ± 3^B	1.01 ± 0.03^A	0.12 ± 0.01^A
	14	65	21.3 ± 5.9^F	14 ± 6^B	1.02 ± 0.01^A	0.12 ± 0.01^A
Hexyl	18	60	21.6 ± 3.4^G	23 ± 5^B	1.02 ± 0.01^A	0.15 ± 0.04^A
	22	65	21.8 ± 7.4^H	9 ± 2^C	1.08 ± 0.01^A	0.08 ± 0.01^B
	22	48	NA*	27 ± 4^B	1.03 ± 0.01^A	0.12 ± 0.01^A

[†] The difference between data with the same superscripts in one column is not significant ($P > 0.05$). The difference betweem data with different superscripts in one column is significant ($P < 0.05$).

* Not available

CH₃O(CH₂CH₂O)ₓ(CH₂)₃ S(CH₂) NH—(COCHNH)ᵧ(COCHNH)z H

$$CH_3O(CH_2CH_2O)_x(CH_2)_3\ S(CH_2)\ NH\!-\!\!(COCHNH)_y(COCHNH)_z\ H$$

$$\begin{array}{cc} & \quad CH_2 \qquad\qquad\qquad CH_2 \\ CH_3(CH_2)_nCO_2(CH_2)_mHNCO & \qquad CONH(CH_2)_mOH \end{array}$$

x	y + z	m	n
270	15	2	4
270	15	2	8
270	15	2	12
270	15	2	16
270	15	6	8
270	15	6	12
270	15	6	16
270	15	6	20
270	24	2	16
270	24	6	16

Figure 3.1. Chemical structure of fatty acid conjugates of PEO-*b*-PHAA.

90

A)

B)

Figure 3.2. TEM images of (A) PEO-b-poly[N-(2-ethyl myristate)-L-aspartamide] PEO-b-PEMA

(12-15) , substitution level = 42 %; (B) PEO-b-poly[N-(6-hexyl myristate)-L-aspartamide] PEO-

b-PHMA (12-15), substitution level = 65 % (Magnification 18,000 × 6.0).

91

A)

B)
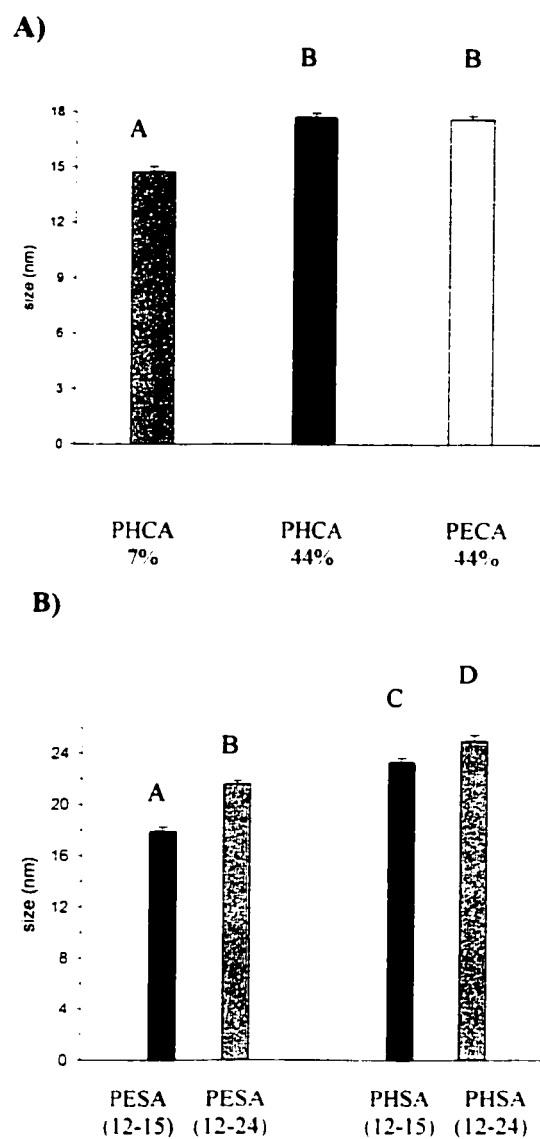
Figure 3.3. The effect of alkyl core structure on micellar size (mean ± SE). A) The effect of spacer group and level of fatty acid conjugation in capric acid conjugates of PEO-b-PHAA. B) The effect of PHAA block length in stearic acid conjugates of PEO-b-PHAA. The difference between bars presented with the same letter in each graph is not significant (P > 0.05). The difference betweem bars presented with different letters in each graph is significant (P < 0.05).

92
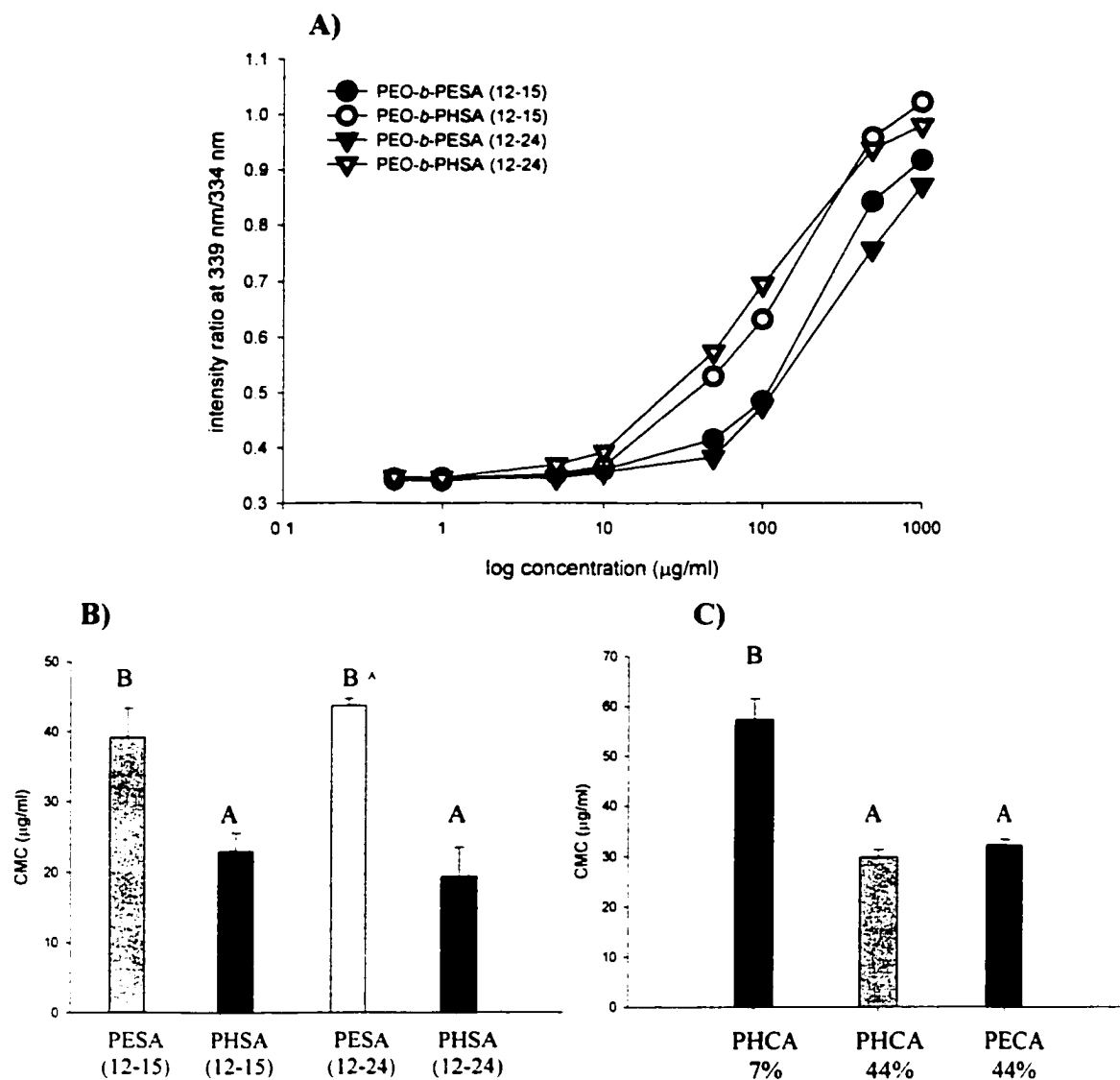
Figure 3.4. A) Intensity ratio (339 nm/334 nm) of pyrene (6×10^{-7} M) from excitation spectrum as a function of block copolymer concentration. B) The effect of PHAA block length in stearic acid conjugates of PEO-b-PHAA on CMC (mean ± SE) C) The effect of spacer group and level of fatty acid conjugation in capric acid conjugates of PEO-b-PHAA on CMC (mean ± SE). The difference between bars presented with the same letter in each graph is not significant (P > 0.05). The difference betweem bars presented with different letters in each graph is significant (P < 0.05).

93

A)

B)   C)
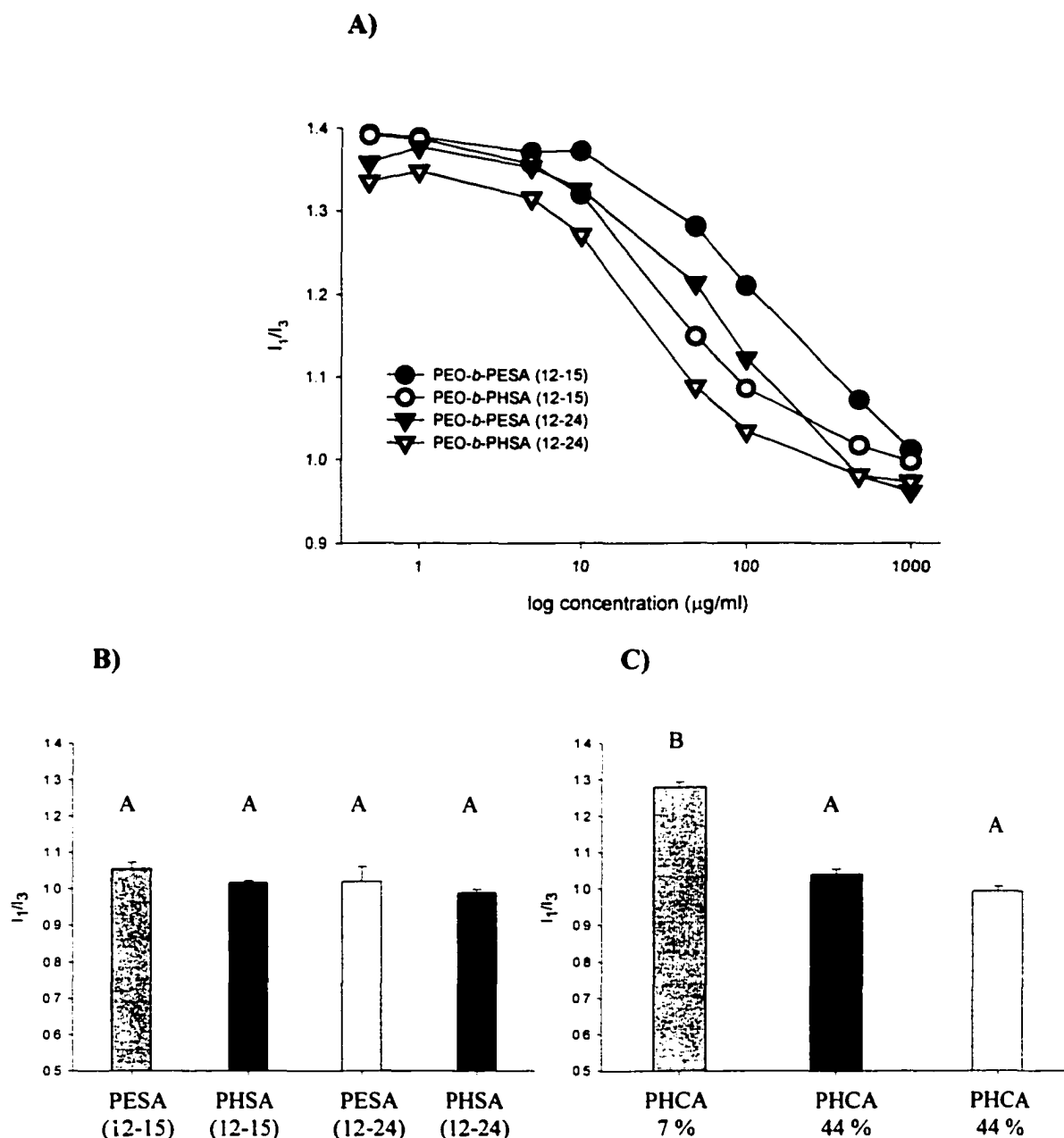
Figure 3.5. A) Intensity ratio (I_1/I_3) of pyrene (6×10^{-7} M) from emission spectrum as a function

of block copolymer concentration B) The effect of PHAA block length in stearic acid conjugates

of PEO-b-PHAA on I_1/I_3 ratio (mean ± SE) C) The effect of spacer group and level of fatty acid

conjugation in capric acid conjugates of PEO-b-PHAA on I_1/I_3 ratio (mean ± SE). The difference

between bars presented with the same letter in each graph is not significant ($P > 0.05$). The

difference betweem bars presented with different letters in each graph is significant ($P < 0.05$).

94
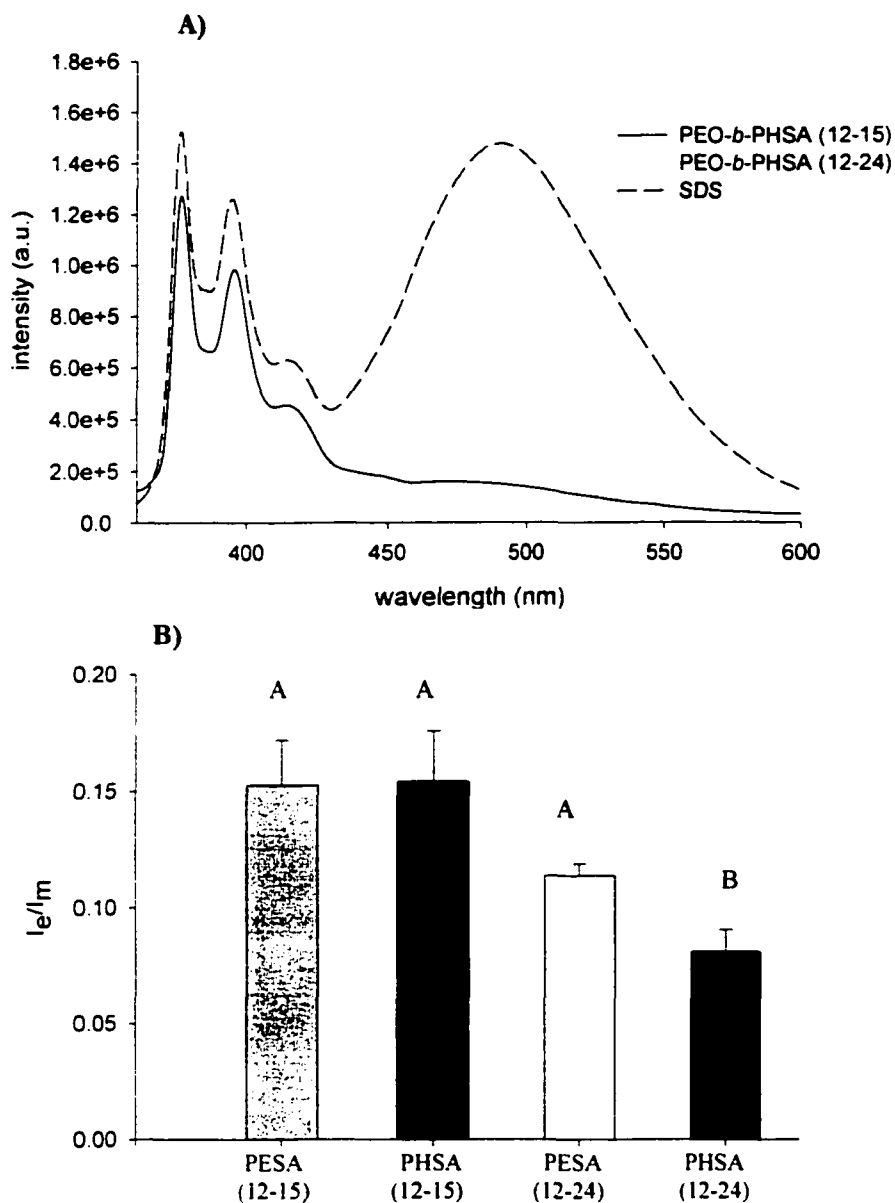
Figure 3.6. A) Fluorescence emission spectrum of 1,3-(1,1'-dipyrenyl)propane in micellar solutions of PEO-*b*-PHSA in comparison to SDS. **B)** The effect of PHAA block length on microviscosity in stearic acid conjugates of PEO-*b*-PHAA. The difference between bars presented with the same letter in each graph is not significant ($P > 0.05$). The difference betweem bars presented with different letters in each graph is significant ($P < 0.05$).

95

3.6. References:

1. Kataoka, K., Kwon, G.S., Yokoyama, M., Okano, T. and Sakurai, Y., Block copolymer micelles as vehicles for drug delivery, *Journal of Controlled Release* 24:119-132 (1993).

2. Yokoyama, M., Satoh, A., Sakurai, Y., Okano, T., Matsumura, Y., Kakizoe, T. and Kataoka, K., Incorporation of water-insoluble anticancer drug into polymeric micelles and control of their particle size, *Journal of Controlled Release* 55:219-229 (1998).

3. Yokoyama, M., Fukushima, S., Uehara, R., Okamoto, K., Kataoka, K., Sakurai, Y. and Okano, T., Characterization of physical entrapment and chemical conjugation of adriamycin in polymeric micelles and their design for *in vivo* delivery to a solid tumor, *Journal of Controlled Release* 50:79-92 (1998).

4. Hurter, P.N. and Hatton, T.A., Solubilization of polycyclic aromatic hydrocarbons by poly(ethylene-propylene oxide) block copolymer micelles: effects of polymer structure, *Langmuir* 8:1291-1299 (1992).

5. Nagarajan, R., Barry, M. and Ruckenstein, E., Unusual selectivity in solubilization by block copolymer micelles, *Langmuir* 2:210-215 (1986).

6. Kwon, G.S., Naito, M., Yokoyama, M., Okano, T., Sakurai, Y. and Kataoka, K., Micelles based on ab block copolymers of poly(ethylene oxide) and poly(β-benzyl-L-aspartate), *Langmuir* 9:945-949 (1993).

7. Georges, J., Molecular fluorescence in micelles and microemulsions: micellar effects and analytical applications, *Spectochimica Acta Reviewes* 13:27-45 (1990).

8. Winnik, M. and Regismond, S.T.A., Fluorescence methods in the study of the interactions of surfactants with polymers, *Colloids & Surfaces A: Physicochemical & Engineering Aspects* 118:1-39 (1996).

9. Dong, D. C. and Winnik, M., The py scale of solvent polarities, *Canadian Journal of Chemistry* 62:2560-2565 (1984).

10. Kwon, G.S., Diblock copolymer nanoparticles for drug delivery, *Critical Reviews in Therapeutic Drug Carrier Systems* 15:481-512 (1998).

11. Kwon, G. S. and Okano, T., Soluble self assembled block copolymers for drug delivery, *Pharmaceutical Research* 16:597-600 (1999).

12. Allen, C., Maysinger, D. and Eisenberg, A., Nano-engineering block copolymer aggregates for drug delivery, *Colloids & Surfaces B: Biointerfaces* 16:3-27 (1999).

96

Chapter 4

Micelles self-assembled from poly(ethylene oxide)-*b*-poly(*N*-hexyl stearate-L-aspartamide) by a solvent evaporation method: effect on solubilization and haemolytic activity of amphotericin B

4.1. Introduction

PEO-*b*-poly(L-aspartic acid) (PEO-*b*-P(Asp)) derivatives with aliphatic core-forming structures may form micelles that may effectively solubilize aliphatic or water-insoluble drugs, such as amphotericin B (AmB) (1). In addition, PEO-*b*-P(Asp) based micelles may potentially be tailored to increase the encapsulation of AmB by alteration in the side chain structure. A family of amphiphilic PEO-*b*-P(Asp) derivaives, which have aliphatic fatty acid side chains have been prepared (Figure 4.1) and assessed the functional properties of their self-assembled structures for an efficient drug delivery (2). Micelles composed of PEO-*b*- poly[*N*-(6-hexyl stearate)-L-aspartamide] (PEO-*b*-PHSA) with a polymerization degree of 24 in the PHSA block were selected as optimized structures for AmB delivery. Based on a higher core viscosity, we speculate an improved stability and release properties for PEO-*b*-PHSA (12-24) micelles.

In this context, we are interested in finding an optimal method for drug loading in PEO-*b*-PHSA micelles. The encapsulation of AmB by PEO-*b*-PHSA micelles by a dialysis method of drug loading has been (1). In this chapter, a solvent evaporation method for AmB encapsulation in PEO-*b*-PHSA micelles is described which may diminish AmB toxicity significantly as a result. The solvent evaporation method has been used widely for liposomes, but not polymeric micelles (3). Drug loading in polymeric micelles is usually accomplished by either dialysis or O/W emulsion methods (4-7). The solvent evaporation method may have advantages in drug loading at a large scale.

98

4.2. Experimental section

4.2.1. Synthesis of PEO-b-PHSA - PEO-b-PHSA was prepared from PEO-b-poly(β-benzyl-L-aspartate) (PEO-b-PBLA) as described previously (Chapter 2, section 2.2.2). The molecular weight of PEO and the number of BLA units in PEO-b-PBLA were 12,000 g mol^{-1} (M_w/M_n = 1.05) and 24, respectively. Briefly, PEO-b-PBLA was reacted with 6-aminohexanol at 25° C in the presence of 2-hydroxypyridine as a catalyst. PEO-b-poly(hydroxyhexyl-L-aspartamide) (PEO-b-PHHA) was formed, providing hydroxyl groups in the side chains. Stearic acid was then reacted with PEO-b-PHHA in dry dichloromethane with the aid of dicyclohexylcarbodiimide and dimethylaminopyridine. The degree of fatty acid substitution was 50%, based on ^{1}H-NMR in chloroform-d (AM-300 MHz).

4.2.2. Encapsulation of AmB by PEO-b-PHSA micelles - A) Dialysis method. The dialysis method was optimized for AmB encapsulation in PEO-b-PHSA micelles. AmB (400 μg) and PEO-b-PHSA (20 mg) were dissolved in 1.2 mL of N,N-dimethylsulfoxide. Water was added to the solution in a drop-wise manner (1 drop/20 sec) until its content reached 80 % v/v. The solution was dialysed against water overnight, filtered (0.22 μm) and freeze-dried.

B) Solvent evaporation method. AmB (470 μg) and PEO-b-PHSA (20 mg) were dissolved in methanol (5.0 ml) in a round bottom flask. Methanol was evaporated under vacuum at 40°C in 15 min. Distilled water was added to the polymer/drug film, the solution was incubated at 40°C for 10 min and vortexed for 30 sec afterwards. The micellar solution was filtered (0.22 μm) and freeze-dried.

99

The freeze-dried samples of AmB in PEO-*b*-PHSA micelles were reconstituted in water and filtered (0.22 μm). An aliquot of the micellar solution in water was diluted with an equal volume of *N*, *N*-dimethylformamide and the drug content was determined from the UV/VIS absorbance of AmB at 412 nm (Pharmacia Biotech Ultraspec 3000).

4.2.3. Transmission electron microscopy (TEM) - Samples for TEM were as described in Chapter 2 under section 2.2.3 and images were obtained at a magnification of 18,000 times (75 kV) (HITACHI H 7000). Apparent micellar diameters were measured, and a mean diameter ± SD was calculated based on at least 120 measurements.

4.2.4. Size exclusion chromatography (SEC) - AmB was dissolved in 0.10 M phosphate buffer solution, pH = 7.4, with the aid of DMSO, providing levels at 1.0 to 100 μg/ml. The amount of DMSO in the final samples was less than 1 % (v/v). Freeze-dried PEO-*b*-PHSA micelles with or without AmB were dissolved in a 0.10 M phosphate buffer to provide a level of 0.5 mg/mL for polymer. Samples of 125 μLwere injected into a Hydrogel 2000 (Waters) column after it was equilibrated with phosphate buffer 0.10 M (pH = 7.4) at a flow rate of 0.8 ml/min (Waters B15 LC system). Elutions were done with a UV/VIS detector (Waters 486) set at 210 and 410 nm for PEO-*b*-PHSA and AmB, respectively. The column was calibrated with dextran standards (8.05×10^5 –9.11×10^6 gmol^{-1}) using refractive index detection (Precision Detectors 2000).

4.2.5. Haemolytic activity of AmB toward human red blood cells - Human blood was collected and centrifuged. The supernatant and the buffy coat were pipetted off and the

100

red blood cells (RBCs) were diluted with an isotonic phosphate buffer, pH 7.4. The proper dilution factor was estimated from the UV/VIS absorbance of haemoglobin at 576 nm in the supernatant after red blood cells were lysed by 20 μg/mL of AmB. A properly diluted sample of RBCs gave an absorbance of 0.4-0.5 in this condition. Solutions of diluted RBCs (2.5 ml) with varied levels of AmB in different samples were incubated at 37°C for 30 min. Samples were then placed in ice to stop the haemolysis. The unlyzed RBCs were removed by centrifugation at 20,000 G for 20 sec. The supernatant was collected and analyzed for haemoglobin by UV/VIS spectroscopy at 576 nm. The percent of haemolysed RBCs was determined using the following equation: % haemolysis = $100(Abs - Abs_o)/(Abs_{100} - Abs_o)$, where Abs, Abs_o and Abs_{100} are the absorbance for the sample, control with no AmB and control in the presence of 20 μg/mL AmB, respectively.

4.3. Results and Discussion

A scheme for the dialysis and solvent evaporation methods used to encapsulate AmB in PEO-*b*-PHSA micelles is shown in Figure 4.2. The level of AmB in PEO-*b*-PHSA micelles by solvent evaporation method was 0.35 mol drug/mol polymer, and the yield of AmB encapsulation was 73 % (Table 4.1). In contrast, the dialysis method provided 0.25 mol AmB/mol PEO-*b*-PHSA, and the yield of AmB encapsulation was 60 %. In both cases of drug loading, reconstitution of freeze-dried samples yielded aqueous solutions having AmB levels greater than 250 μg/ml. The solubility of AmB itself in water is 1 μg/ml, and it is administered at 100 μg/ml.

101

TEM provided evidence for the formation of spherical micelles from PEO-*b*-PHSA when solvent evaporation method was used for micelle formation and drug loading (Figure 4.3A). The average diameter of PEO-*b*-PHSA micelles was 15.2 ± 4.0 nm before freeze-drying. An increase in the micellar size to 22.3 ± 4.7 nm was observed for the reconstituted samples. PEO-*b*-PHSA micelles prepared by the dialysis method were also spherical (Figure 4.3B), but significantly larger (average diameter of 25.0 ± 4.9 nm) than PEO-*b*-PHSA micelles prepared by the solvent evaporation (P< 0.0001, unpaired t test).

SEC provided evidence for the encapsulation of AmB in PEO-*b*-PHSA micelles and levels of free AmB below detectable limits (Figure 4.4A). Free AmB eluted from the column at 17.4 to 16.5 min depending on its concentration and aggregation state (Figure 4.4B). PEO-*b*-PHSA micelles formed by dialysis and solvent evaporation methods eluted at 10.6 ± 0.1 and 10.8 ± 0.0 min, respectively, corresponding to a molecular weight of 2.9 × 10^6 and 2.4 × 10^6 g mol $^{-1}$ based on dextran standards. This reflects formation of significantly larger micelles by the dialysis method (unpaired t test, P< 0.05) consistent with TEM. Using either the solvent evaporation or the dialysis method of drug loading, AmB loading at levels of 0.25-0.35 drug to polymer molar ratio caused no significant change in the elution time of PEO-*b*-PHSA micelles (unpaired t test, P>0.05) (Table 4.1).

The primary advantage of the solvent evaporation method was a reduction in haemolysis owing to free AmB (Figure 4.5). AmB itself caused 100 % haemolysis at about 1 μg/ml. After encapsulation of AmB in PEO-*b*-PHSA micelles by the dialysis method, the drug was less toxic than AmB itself, causing 80% haemolysis at 4.5 μg/ml and 100 % haemolysis at 6 μg/ml. In contrast, AmB encapsulated by the solvent

102

evaporation method in PEO-*b*-PHSA micelles was completely nonhaemolytic at 15 μg/ml.

The results contrast with earlier findings, where Pluronics, PEO-*b*-poly(propylene oxide)-*b*-PEO, successfully solubilized AmB after encapsulation through a solvent evaporation method, but failed to protect red blood cells from haemolysis (8). PEO-*b*-PHSA micelles may reduce haemolysis by the slow release of AmB over the 30 min time period of incubation of drug with red blood cells or release of AmB in an unaggregated state, unimers, which are known to be non-toxic for mammalian cells (9; 10). In either situation, AmB encapsulated in PEO-*b*-PHSA micelles by the solvent evaporation method is expected to be much less toxic than AmB alone in an *in vivo* system.

4.4. Conclusions

PEO-*b*-PHSA self assembles into micelle like structures and encapsulate AmB through a solvent evaporation method. As a result, the concentration of AmB in solution can be increased to levels that are clinically relevant and the toxicity of the drug in terms of haemolysis can be reduced dramatically.

Table 4.1. The effect of loading process on encapsulation of AmB by PEO-*b*- PHSA micelles.

Loading method	PEO-*b*-PHSA (mg)	Initial level of AmB (µg)	Loaded AmB (µg)	AmB: PEO-*b*-PHSA (mol:mol)	Yield (%)	Elution time of polymeric micelles without AmB (min ± SD)	Elution time of polymeric micelles with AmB (min ± SD)
Dialysis	20	406	244	0.25	60	10.6 ± 0.1	10.6 ± 0.0
Solvent evaporation	20	470	340	0.35	73	10.8 ± 0.0	10.7 ± 0.0

104

CH$_3$O(CH$_2$CH$_2$O)$_x$(CH$_2$)$_3$ S(CH$_2$) NH —(COCHNH)$_y$(COCHNH)$_z$ H

                                    CH$_2$ CH$_2$

                                    CO   CO

                                    NH   NH

                                  (CH$_2$)$_6$ (CH$_2$)$_6$

                                    O   OH

                                    CO

                                  (CH$_2$)$_{16}$

                                    CH$_3$
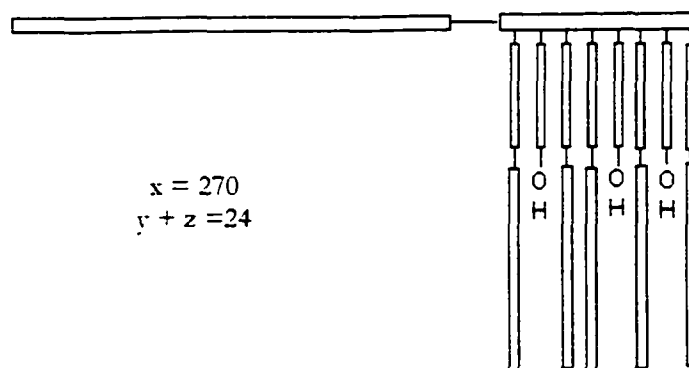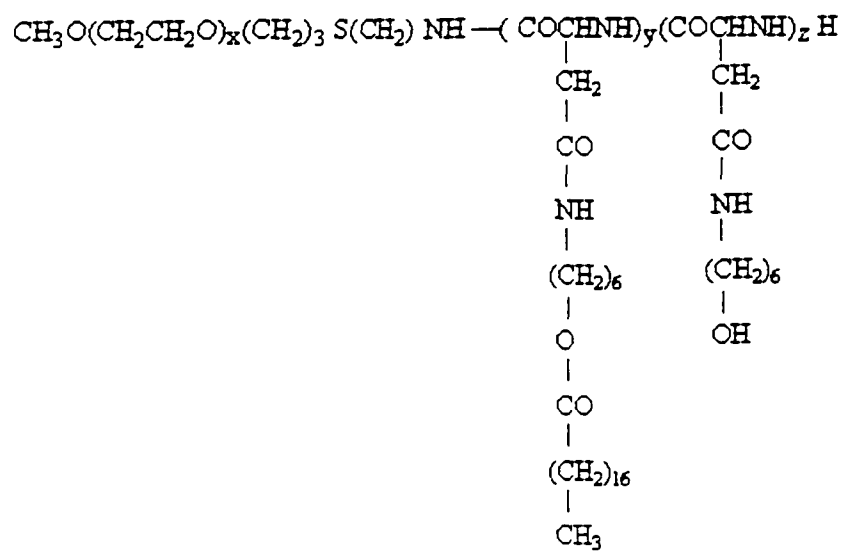
$x = 270$
$y + z = 24$

Figure 4.1 . Chemical structure of PEO-b-PHSA block copolymer and molecular model.

105
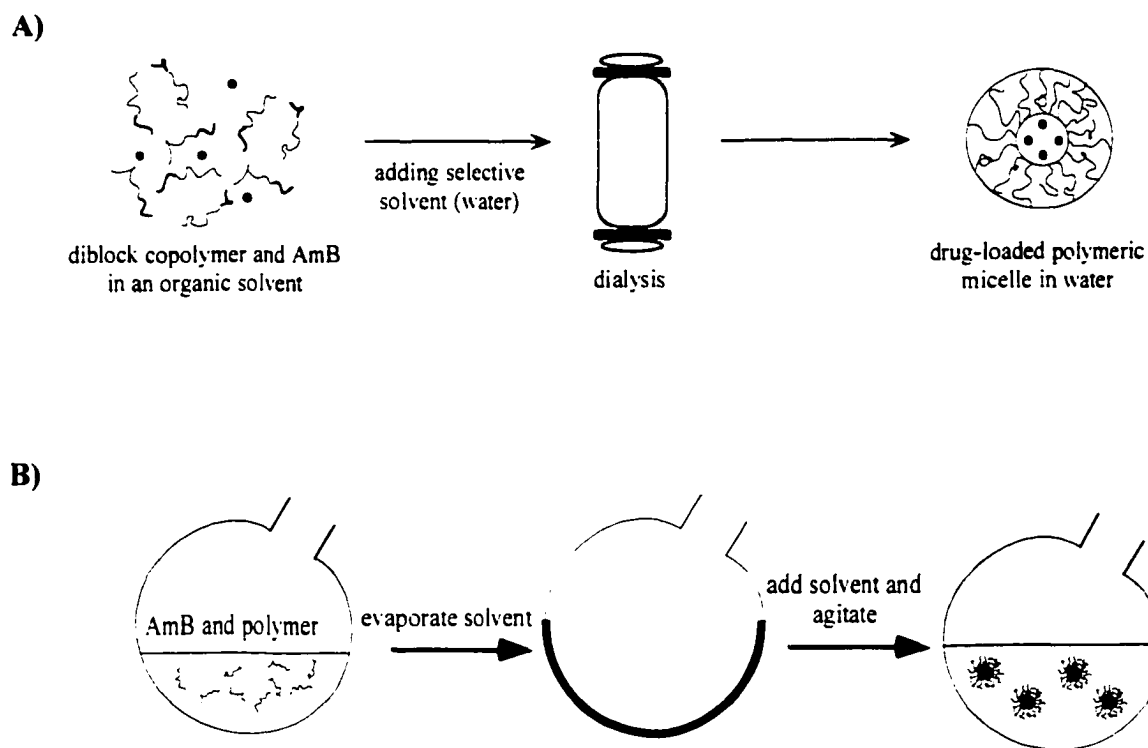
Figure 4.2 . Schematic representation of A) dialysis and B) solvent evaporation method of drug loading in PEO-*b*-PHSA micelles.

106

A)
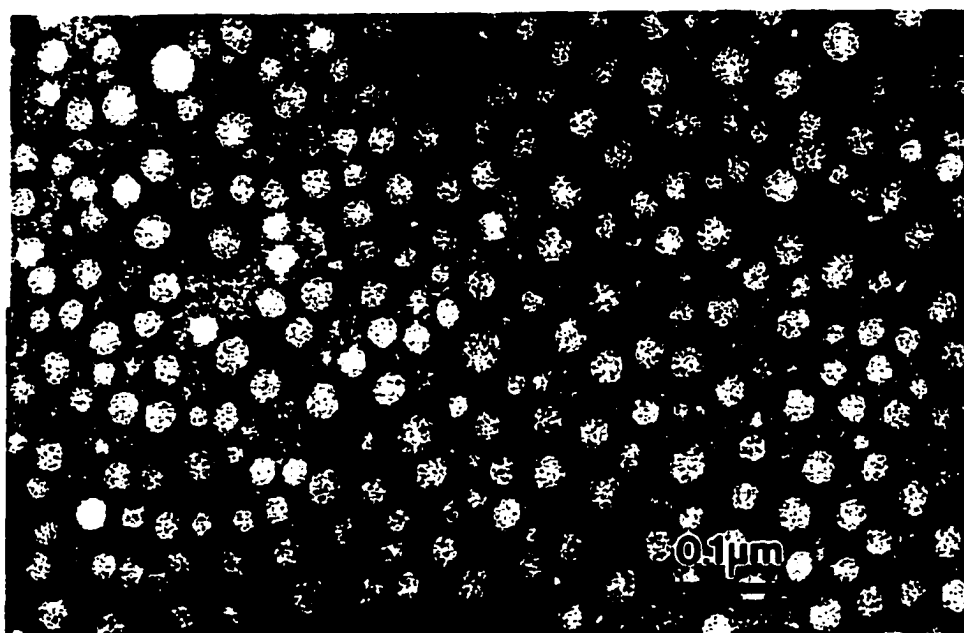
B)
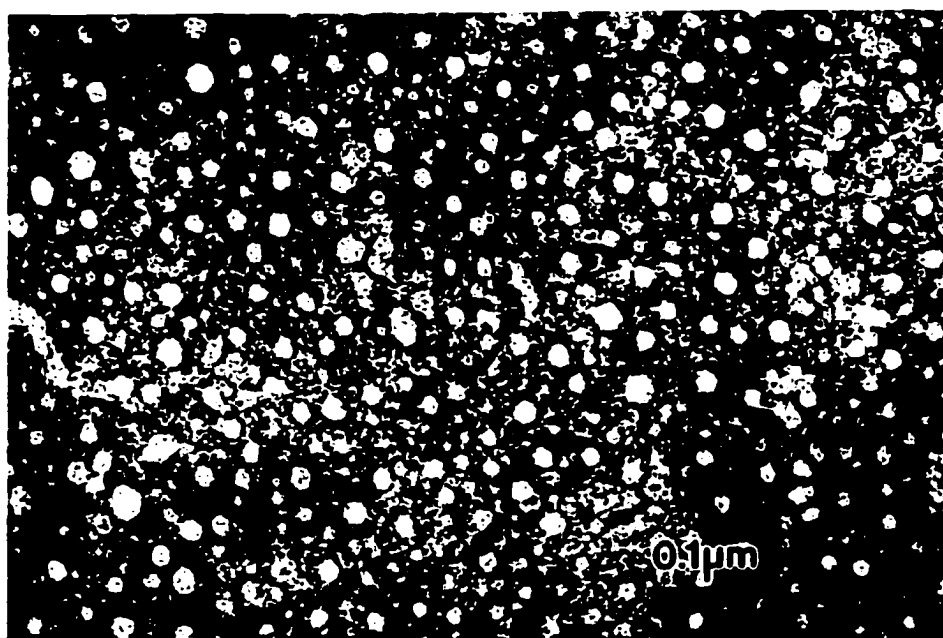
Figure 4.3. TEM images of PEO-b-PHSA micelles prepared by (A) dialysis and (B) solvent

evaporation method (magnification of 18,000 × 6).
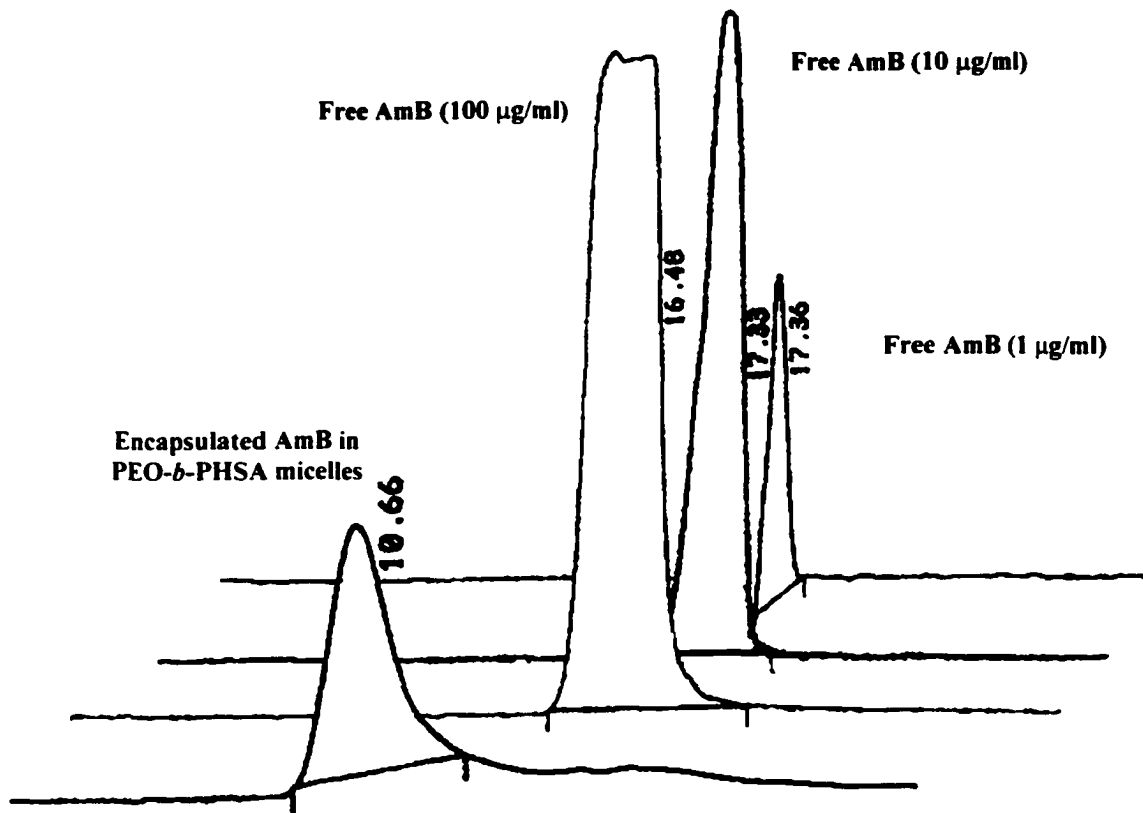
Figure 4.4. Size exclusion chromatograms of free AmB in phosphate buffer 0.1 M, pH 7.4 (1, 10 and 100 μg/mL AmB concentration) and encapsulated AmB in PEO-*b*-PHSA micelles by solvent evaporation (λ = 410).

108
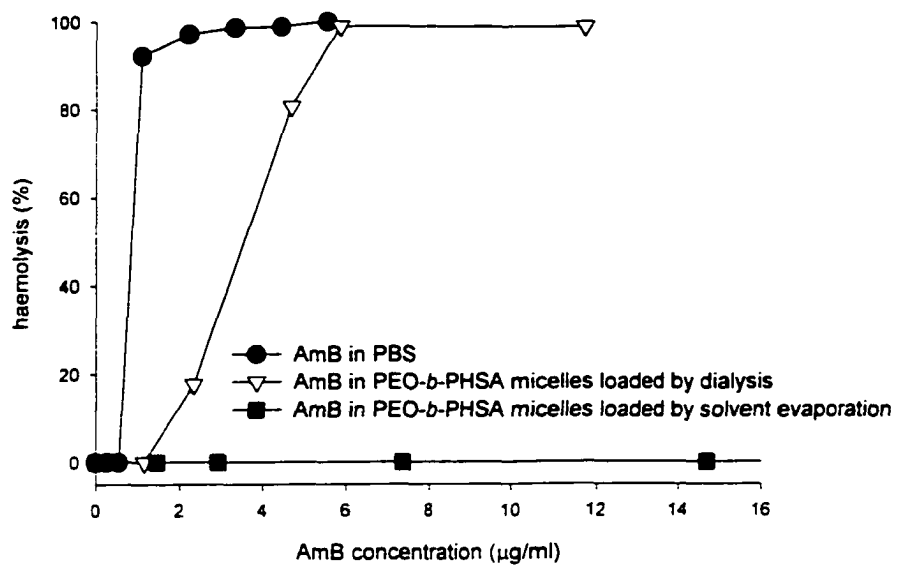
Figure 4.5. The effect of loading process on haemolysis induced by encapsulated AmB in PEO-b-PHSA micelles in comparison to free AmB.

109

4.5. References

1. Lavasanifar, A., Samuel, J. and Kwon, G. S., Micelles of poly(ethylene oxide)-block-poly(hydroxy alkyl-L-aspartamide): synthetic analogues of lipoproteins for drug delivery, *Journal of Biomedical Materials Research* 52:831-835 (2000).

2. Lavasanifar, A., Samuel, J. and Kwon, G. S., The effect of alkyl core structure on micellar properties of poly(ethylene oxide)-block-poly(L-aspartamide) derivatives, *Colloids & Surfaces B: Biointerfaces* 22:115-126 (2001).

3. Ostro, M.J. and Cullis, P.R., Use of liposomes as injectable-drug delivery systems, *American Journal of Hospital Pharmacy* 46:1576-1587 (1989).

4. La, S. B., Okano, T. and Kataoka, K., Preparation and characterization of the micelle-forming polymeric drug indomethacin-incorporated poly(ethylene oxide)-poly(β-benzyl-L-aspartate) block copolymer micelles, *Pharmaceutical Science* 85:85-90 (1996).

5. Kwon, G.S., Naito, M., Yokoyama, M., Okano, T., Sakurai, Y. and Kataoka, K., Physical entrapment of adriamycin in AB block copolymer micelles, *Pharmaceutical Research* 12:192-195 (1995).

6. Kwon, G.S., Naito, M., Yokoyama, M., Okano, T., Sakurai, Y. and Kataoka, K., Block copolymer micelles for drug delivery: loading and release of doxorubicin, *Journal of Controlled Release* 48:195-201 (1997).

7. Yokoyama, M., Fukushima, S., Uehara, R., Okamoto, K., Kataoka, K., Sakurai, Y. and Okano, T., Characterization of physical entrapment and chemical conjugation of adriamycin in polymeric micelles and their design for *in vivo* delivery to a solid tumor, *Journal of Controlled Release* 50:79-92 (1998).

8. Forster, D., Washington, C. and Davis, S. S., Toxicity of solubilized and colloidal amphotericin B formulations to human erythrocytes, *Journal of Pharmacy & Pharmacology* 40:325-328 (1988).

9. Brajtburg, J. and Bolard, J., Carrier effects on biological activity of amphotericin B, *Clinical Microbiology Reviews* 9:512-531 (1996).

10. Bolard, J., Legrand, P., Heitz, F. and Cybulska, B., One-sided action of amphotericin B on cholesterol-containing membranes is determined by its self-association in the medium, *Biochemistry* 30:5707-5715 (1991).

Chapter 5

Tailor-made polymeric micelles of poly(ethylene oxide)-*b*-poly(*N*-hexyl stearate-L-aspartamide) for the encapsulation and delivery of amphotericin B

A version of this chapter has been submitted to *Pharmaceutical Research* for

publication.

5.1. Introduction

To enhance the encapsulation of aliphatic drugs such as amphotericin B (AmB), we have synthesized micelle-forming PEO-*b*-poly(L-aspartic acid) derivatives with fatty acid side chains on the P(Asp) block and assessed the effect of polymer structure on micellar properties (1; 2). AmB has been encapsulated by PEO-*b*-poly(*N*-hexyl stearate-L-aspartamide) (PEO-*b*-PHSA) (12-24) micelles and its haemolytic activity was reduced, particularly after encapsulation by a solvent evaporation method (Chapter 4). This chapter focuses on the effect of polymer structure on the encapsulation, haemolytic and antifungal activity of AmB. We have pursued an optimum structure for PEO-*b*-PHSA micelles by changing the level of stearic acid conjugated as a side chain and obtained adequate encapsulation and reduced haemolytic activity of AmB. The latter is hypothesized to be due to a control over the rate of AmB release. AmB encapsulated in PEO-*b*-PHSA micelles having different levels of stearic acid substitution was active against fungal cells. The attachment of chemically compatible moieties of varied degrees of substitution onto a core-forming block may be used as a tailoring strategy to control the encapsulation and the release of water insoluble drugs from polymeric micelles (3; 4).

5.2. Experimental section

5.2.1 Synthesis of PEO-b-PHSA - PEO-*b*-PHSA was synthesized from PEO-*b*-poly(β-benzyl-L-aspartate) (PEO-*b*-PBLA) (PEO M_n = 12,000 g mol^{-1}; M_w/M_n = 1.05; number of BLA units = 24) as described in the previous chapters (1). Briefly, PEO-*b*-PBLA was reacted with 6-aminohexanol at 25°C in the presence of 2-hydroxypyridine, as a catalyst. Free hydroxyl groups on PEO-*b*-poly(hydroxyhexyl-L-aspartamide) (PEO-*b*-PHHA), were reacted with stearic acid in dry dichloromethane in the presence of

112

dicyclohexylcarbodiimide and dimethylaminopyridine. The reaction time was kept between 2 to 72 h to achieve varied substitution levels of stearic acid on the PHHA block (mol stearic acid: mol hydroxyl). The level of stearic acid substitution on PEO-*b*-PHSA was estimated by ^{1}H-NMR in chloroform-*d* (AM-300 MHz).

5.2.2. AmB encapsulation in PEO-b-PHSA micelles by a solvent evaporation method - AmB (470 μg or 2.0 mg) and PEO-*b*-PHSA (20 mg) were dissolved in methanol (5 or 10 mL depending on AmB level) in a round bottom flask. Methanol was evaporated under vacuum at 40°C. Distilled water was added to the PEO-*b*-PHSA/drug film, and the solution was incubated at 40°C for 10 min and vortexed for 30 sec afterwards. The micellar solution was filtered (0.22 μm) and freeze-dried. An aliquot of the micellar solution in water was diluted with an equal volume of *N*, *N*-dimethylformamide (DMF) and the drug content measured from the UV/VIS absorbance of AmB at 412 nm (Pharmacia Biotech Ultraspec 3000).

5.2.3. Size exclusion chromatography (SEC) - Freeze-dried PEO-*b*-PHSA micelles with encapsulated AmB were dissolved in 0.10 M phosphate buffer, pH = 7.4, at 0.50 mg/ml for the polymer and 6 to 10 μg/mLfor AmB. The samples at 125 μLwere injected into a SEC column (Hydrogel 2000, Waters) after having been equilibrated with 0.10 M phosphate buffer, pH = 7.4, at a flow rate of 0.80 ml/min (Waters B15 LC system). PEO-*b*-PHSA and AmB were detected by UV/VIS at 210 and 410 nm, respectively.

5.2.4. Aggregation state of AmB – UV/VIS spectroscopy - Freeze-dried samples of AmB in PEO-*b*-PHSA micelles with 11 and 70 % of stearic acid substitution were dissolved in PBS, pH = 7.4, at 4 μg/mL of AmB. DMSO was used to solubilize AmB in PBS, pH = 7.4, at a similar concentration. The level of DMSO in the final sample was < 1 % (v/v). The UV/VIS spectra of AmB in different samples were recorded from 300 nm to 450 nm (Milton Roy 3000).

5.2.5. Haemolytic activity of AmB toward human red blood cells - Haemolytic activity of encapsulated AmB was measured according to a method described in detail in section 4.2.5 of Chapter 4.

5.2.6. Minimal inhibitory concentration (MIC) of AmB - AmB in PEO-*b*-PHSA micelles was dissolved in isotonic sodium chloride solution giving an AmB level of 200 μg/ml. AmB was dissolved in DMSO and diluted further with sodium chloride solution to give the same concentration. The level of DMSO in the final solution was < 1 % v/v. Samples of PEO-*b*-PHSA micelles in sodium chloride solution were also used as a control. Solutions of 20 μL from these samples were diluted with the broth medium (RPMI 1640) (80 μl) in the first microwell. The next 11 microwells had two-fold diluted solutions. To each microwell, 100 μL of the inoculum containing 5×10^3 cfu/mL of fungal organisms (*Candida albicans*, *Aspergillous fumigatus* or *Cryptococos neoformans*) in broth medium was added, giving a total volume of 200 μL per well. Microwell containers were incubated at 35°C for 24 h. Organism and medium controls were performed simultaneously to check the growth of organisms and sterility of broth

114

medium, respectively. The MIC was defined as the minimum concentration of AmB that shows a full inhibition of the fungus growth in the well, examined by an inverted microscope (×40). All tests were repeated three times.

5.3. Results and discussion

PEO-b-PHSA was synthesized at three levels of stearic acid substitution (Figure 5.1). The level of fatty acid substitution was determined by ^{1}H NMR comparing the characteristic peak intensity of PEO (-C$\underline{H}_2$-C$\underline{H}_2$O-, δ = 3.65 ppm) to the peak intensity of the methyl group of stearic acid (-C$\underline{H}_3$, δ = 0.8 ppm). The levels of stearic acid substitution on PEO-b-PHSA were 11, 50 and 70 %. In an earlier study, the level of fatty acid substitution had a dramatic effect on the thermodynamic stability of micelles composed of fatty acid conjugates of PEO-b-PHHA (Chapter 3). This structural parameter was hypothesized to influence the encapsulation of AmB, the drug's toxicity in terms of haemolysis and its antifungal activity.

SEC confirmed the encapsulation of AmB by PEO-b-PHSA micelles. AmB eluted with PEO-b-PHSA micelles at 50 and 70 % stearic acid substitution at 10.7 and 10.6 min on average, respectively, with no evidence of unencapsulated drug. We were unable to directly confirm the encapsulation of AmB by PEO-b-PHSA micelles at 11 % by SEC, owing to its dissociation and elution as unimers.

The level of AmB encapsulated in PEO-b-PHSA micelles at 11 % stearic acid substitution was 0.22 mol drug: mol PEO-b-PHSA, and the level increased to 0.35 and 0.36 at 50 and 70 % of stearic acid substitution, respectively (Table 5.1). The yield of encapsulated AmB for PEO-b-PHSA micelles was 51, 73 and 77 %, respectively. In each

115

case, freeze-dried product could be reconstituted with an aqueous vehicle at 200 μg/mL of AmB, the initial level of drug used for the MIC experiments, indicating encapsulation of AmB at all three levels of stearic acid substitution. An increase in the initial amount of AmB used for encapsulation lead to a higher content of AmB encapsulated in PEO-*b*-PHSA micelles at 50 % stearic acid substitution (0.89 mol drug: mol PEO-*b*-PHSA).

Haemolysis of AmB encapsulated in PEO-*b*-PHSA micelles at 11 % stearic acid substitution was similar to AmB itself, causing 50 % haemolysis at 1 μg/mL and 100 % haemolysis at about 3 μg/mL (Figure 5.2 and 5.3). In contrast, AmB encapsulated in PEO-*b*-PHSA micelles at 50 and 70 % stearic acid substitution was completely non-toxic (no lysis) at levels reaching 22 μg/ml.

The effect on haemolysis, however, was dependent on the content of AmB in the PEO-*b*-PHSA micelles (Figure 5.3). PEO-*b*-PHSA micelles (50 % stearic acid substitution) at 0.36 mol drug: mol polymer were completely non-haemolytic at 22 μg/mL of AmB. On the other hand, PEO-*b*-PHSA micelles at 0.89 mol drug: mol polymer caused 80 % haemolysis at a similar level of drug. Notably, PEO-*b*-PHSA exerted no haemolytic effects.

While there was a decrease of haemolysis induced by AmB, the antifungal activity of encapsulated AmB was comparable to AmB itself or better based on measurements of MICs against the growth of three pathogenic fungi. Fungi growth was examined by an inverted microscope (×40). AmB in an isotonic solution inhibited the growth of *C. albicans, C. neoformans* and *A. fumigatus* at 0.30, 0.30 and 0.45 μg/ml, respectively (Table 5.2). AmB encapsulated in PEO-*b*-PHSA micelles was as effective as AmB itself in most of the cases. At 11 and 50 % of stearic acid substitution, encapsulated

116

AmB was even more effective than AmB itself, inhibiting the growth of *C. neoformans* at a level of 0.18 μg/mL (Unpaired t test, P < 0.01). PEO-*b*-PHSA micelles without AmB were unable to inhibit the fungal growth at 5 mg/mL level or below.

The reduction of haemolysis but with a maintenance or even improved antifungal activity in terms of MIC of AmB encapsulated in PEO-*b*-PHSA micelles may reflect the sustained release of the drug and/or the release of the drug in a monomeric (non-aggregated) state. Monomeric AmB is non-toxic toward mammalian cells, but causes leakage of fungal cells, presumably due to its selective interaction with ergosterol. Aggregated AmB, on the other hand, is non-selective, i.e., forms pores in both mammalian and fungal cell membranes (5-7)

Insight to the aggregation state of AmB can be obtained by UV/VIS spectroscopy (8; 9). AmB easily forms aggregates (its critical aggregation concentration is 1.0 μg/ml) (10; 11). The UV/VIS spectrum of aggregated AmB has four characteristic peaks: A broad peak at 334 and three other peaks at 364, 385, 409 nm (Figure 5.4A). The spectral features of AmB encapsulated in PEO-*b*-PHSA micelles at 11 % are quite similar to AmB alone (Figure 5.4B), indicating weak interaction with micelle core, which has little effect on the aggregation state of the drug. Thus, encapsulated AmB in PEO-*b*-PHSA micelles at 11 % of stearic acid substitution might be quickly released and/or released in an aggregated state. In contrast, there was a bathochromic shift for AmB encapsulated in PEO-*b*-PHSA micelles at 70 % stearic acid substitution (Figure 5.4C). The absorption peaks of AmB appeared at 351, 366, 387, and 418 nm. AmB exhibits a similar spectrum after its binding to serum lipoproteins, which have cores rich in triglycerides (8). While AmB is aggregated, its spectral features reflect a favorable interaction of the drug and the

117

micelle core at a high level of fatty acid substitution. Stably encapsulated AmB in PEO-*b*-PHSA micelles might be released gradually in a monomeric state, increasing the *in vitro* efficacy of this important antifungal drug. This hypothesis is under study.

5.4. Conclusion

The degree of fatty acid substitution of PEO-*b*-PHSA as a structure parameter can be altered to enhance the encapsulation of AmB and reduce the drug's toxic effects (haemolysis) while retaining its antifungal activity in terms of MIC. PEO-*b*-PHSA micelles at 50 and 70 % stearic acid substitution effectively encapsulate AmB and increase its efficacy *in vitro*.

Table 5.1. The effect of fatty acid substitution on the encapsulation of AmB by PEO-*b*-PHSA micelles by a solvent evaporation method.

Stearic acid substitution level (%)	PEO-*b*-PHSA (mg)	Initial level of AmB (μg)	AmB (μg)	AmB: PEO-*b*-PHSA (mol:mol)	Yield (%)
11	20	470	240	0.22	51
50	20	470	340	0.35	73
70	20	470	360	0.36	77
50	20	2000	942	0.89	53

119

Table 5.2. The effect of fatty acid substitution of the core-forming block on the *in vitro* antifungal activity of AmB encapsulated by PEO-*b*-PHSA micelles in comparison to AmB alone.

AmB in:	MIC ± SD (μg/ml) [†]		
	C. albicans	*C. neoformans*	*A. fumigatus*
PBS	0.30 ± 0.00^A	0.30 ± 0.00^A	0.45 ± 0.00^A
PEO-*b*-PHSA 11 % [*]	0.35 ± 0.09^A	0.18 ± 0.04^B	0.6 ± 0.00^A
PEO-*b*-PHSA 50 % [*]	0.27 ± 0.04^A	0.18 ± 0.05^B	0.6 ± 0.00^A
PEO-*b*-PHSA 70 % [*]	0.33 ± 0.11^A	0.23 ± 0.07^A	0.35 ± 0.09^A

[*] AmB was encapsulated in PEO-*b*-PHSA micelles by a solvent evaporation method

[†] The difference between data with the same superscripts in one column is not significant (P > 0.05). The difference betweem data with different superscripts in one column is significant (P < 0.05).

PEO-*b*-PHSA

$$CH_3O(CH_2CH_2O)_x(CH_2)_3\ S(CH_2)\ NH \overset{\displaystyle\diagup}{\diagdown}\ (CO\underset{|}{C}HNH)_y(CO\underset{|}{C}HNH)_z\ H$$
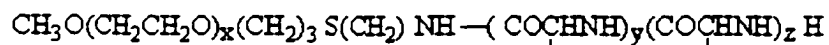
Stearic acid substitution level (%)	x	y	z
11	270	3	21
50	270	12	12
70	270	17	7

Side chains:

Column y:
CH_2 — CO — NH — $(CH_2)_6$ — O — CO — $(CH_2)_{16}$ — CH_3

Column z:
CH_2 — CO — NH — $(CH_2)_6$ — OH
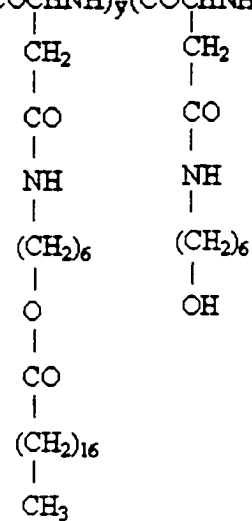
AmB
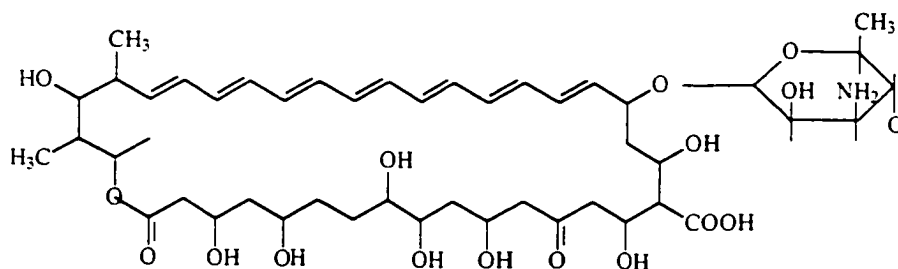
Figure 5.1. Chemical structure of PEO-*b*-PHSA and AmB.

121
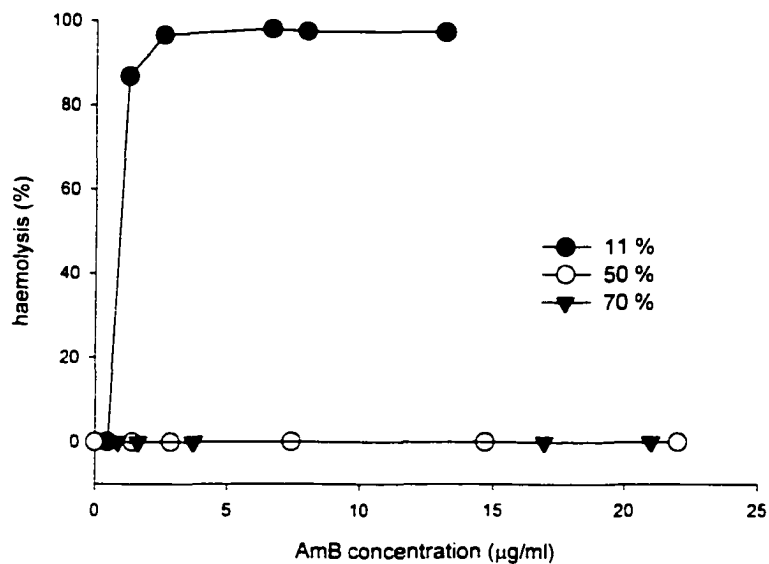
Figure 5.2. The effect of fatty acid substitution level in PEO-*b*-PHSA micelles on the haemolytic activity of AmB encapsulated by a solvent evaporation method.

122
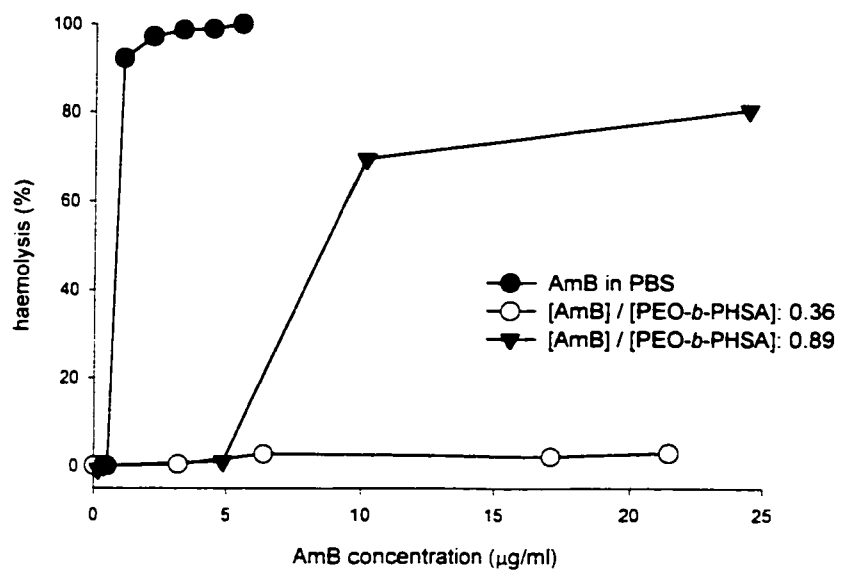
Figure 5.3. The effect of drug loading on the haemolytic activity of AmB encapsulated in PEO-*b*-PHSA micelles (50 % of stearic acid substitution) by a solvent evaporation method.

123
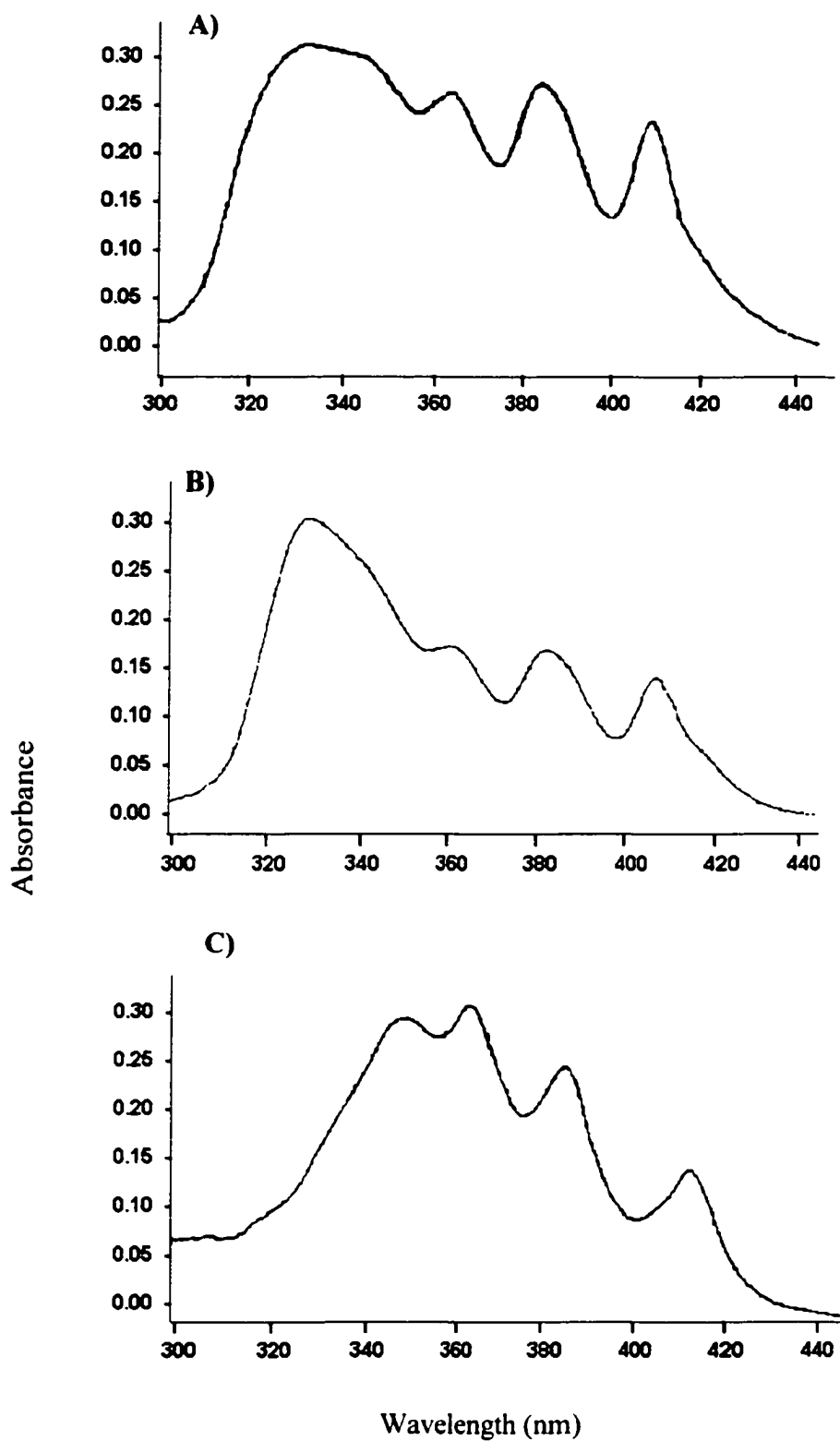
Figure 5.4. Absorption spectra of AmB (4 μg/ml) in **A)** PBS, pH = 7.4, **B)** PEO-*b*-PHSA at 11 %

stearic acid substitution and **C)** PEO-*b*-PHSA at 70 % stearic acid substitution.

124

5.5. References

1. Lavasanifar, A., Samuel, J. and Kwon, G. S., The effect of alkyl core structure on micellar properties of poly(ethylene oxide)-*b*-poly(L-aspartamide) derivatives, *Colloids & Surfaces B: Biointerfaces* 22:115-126 (2001).

2. Lavasanifar, A., Samuel, J. and Kwon, G. S., Micelles of poly(ethylene oxide)-*b*-poly(hydroxy alkyl-L-aspartamide): synthetic analogues of lipoproteins for drug delivery, *Journal of Biomedical Material Research* 52:831-835 (2000).

3. Yokoyama, M., Fukushima, S., Uehara, R., Okamoto, K., Kataoka, K., Sakurai, Y. and Okano, T., Characterization of physical entrapment and chemical conjugation of adriamycin in polymeric micelles and their design for *in vivo* delivery to a solid tumor, *Journal of Controlled Release* 50:79-92 (1998).

4. Yokoyama, M., Satoh, A., Sakurai, Y., Okano, T., Matsumura, Y., Kakizoe, T. and Kataoka, K., Incorporation of water-insoluble anticancer drug into polymeric micelles and control of their particle size, *Journal of Controlled Release* 55:219-229 (1998).

5. Bolard, J., Legrand, P., Heitz, F. and Cybulska, B., One-sided action of amphotericin b on cholesterol-containing membranes is determined by its self-association in the medium, *Biochemistry* 30:5707-5715 (1991).

6. Brajtburg, J. and Bolard, J., Carrier effects on biological activity of amphotericin B, *Clinical Microbiology Reviews* 9:512-531 (1996).

7. Storm, G. and van Etten. E., Biopharmaceutical aspects of lipid formulations of amphotericin B, *European Journal of clinical microbiology & infectious diseases* 16:64-73 (1997).

8. Barwicz, J., Gareau, R., Audet, A., Morisset, A., Villiard, J. and Gruda, I., Inhibition of the interaction between lipoproteins and amphotericin B by some delivery systems, *Biochemical & Biophysical Research Communications*, 181:722-728 (1991).

9. Espuelas, M.S., Legrand, P., Cheron, M., Barratt, G., Puisieux, F., Devissaguet, J.-P. and Irache, J.M., Interaction of amphotericin B with polymeric colloids: a spectroscopic study, *Colloids & Surfaces B: Biointerfaces* 11:141-151 (1998).

10. Barwicz, J., Christian, S. and Gruda, I., Effects of aggregation state of amphotericin B on its toxicity to mice, *Antimicrobial Agents & Chemotherapy* 36:2310-2315 (1992).

11. Aramwit, P., Yu, B.G., Lavasanifar, A., Samuel, J. and Kwon, G.S., The effect of serum albumin on the aggregation state and toxicity of amphotericin B, *Journal of Pharmaceutical Sciences* 89:1589-1593 (2000).

Chapter 6

The effect of fatty acid substitution on the *in vitro* release of

amphotericin B from micelles composed of poly(ethylene oxide)-*b*-

poly(*N*-hexyl stearate-L-aspartamide)

A version of this chapter has been submitted to *Journal of Controlled Release* for

publication.

126

6.1. Introduction

A polymeric micelle formulation is developed for amphotericin B (AmB) as reported in the previous chapters(1). AmB is the most potent antifungal agent in clinical practice (2). Despite great efficacy, severe side effects associated with the administration of its water-soluble formulation, Fungizone®, have restricted the clinical application of AmB. While three lipid-based carriers are available for AmB that circumvent its poor water solubility and reduce its toxicity (449, 414, 448), there are still concerns about high cost and high dose requirements and on whether the therapeutic index of the drug has been increased (3). Recently, AmB encapsulated in long circulating liposomes has been found to be more effective than AmB in standard liposomes in a murine model of candidiasis (4). Thus, long circulating carriers of AmB may be able to increase the therapeutic index of AmB at low dose with low risk of toxicity and low cost.

Poly(ethylene oxide)-b-poly[N-(6-hexyl stearate)-L-aspartamide] (PEO-b-PHSA) are synthesized, which self-assembles into nanoscopic micelles at very low concentration (Chapter 2 and 3) (1; 5). The goal was to prepare polymeric micelles that can effectively encapsulate AmB and circulate for long periods of time in blood, while functioning as a depot for AmB release. In other words, mimic the function of biological transport systems, i.e., low-density serum lipoprotein, but with a favourable effect on the biodistribution of AmB. Owing to favorable interaction between AmB and the fatty acid ester core, AmB encapsulated in PEO-b-PHSA micelles is non-toxic toward red blood cells, but active against fungal cells (Chapter 4 and 5). A low rate of drug release perhaps with the drug in a monomeric state has been hypothesized to be the basis of the reduced toxicity of encapsulated AmB.

127

The release of AmB from PEO-*b*-PHSA micelles and the stability of the micelles with respect to dissociation is studied. The results show the sustained release of AmB by PEO-*b*-PHSA micelles, which is dependent on the level of fatty acid substitution. A dependence of micelle stability on the level of fatty acid ester substitution has also been revealed. Owing to high micelle stability and the sustained release of AmB, PEO-*b*-PHSA micelles at a high level of fatty acid substitution may act as a long-circulating depot of AmB for increased drug efficacy.

6.2. Experimental section

6.2.1. Synthesis of PEO-b-PHSA - PEO-*b*-PHSA having different levels of stearic acid substitution was prepared from PEO-*b*-poly(β-benzyl-L-aspartate) (PEO-*b*-PBLA) and characterized as described previously under section 5.2.1, Chapter 5.

6.2.2. AmB encapsulation - AmB was encapsulated by PEO-*b*-PHSA micelles by dialysis and solvent evaporation according to methods described in Chapter 4, section 4.2.3.

6.2.3. Self-assembly of PEO-b-PHSA by solvent evaporation - PEO-*b*-PHSA (20 mg) were dissolved in methanol in a round bottom flask. Methanol was evaporated under vacuum at 40°C in 30 min. Distilled water was added to the polymer film, the solution was incubated at 40°C for 10 min and vortexed for 30 sec. The micellar solution was filtered (0.22 μm) and freeze-dried.

128

6.2.4. In vitro release study - Multilamellar lipid vesicles were prepared as previously reported (6). Dipalmitoyl phosphatidylcholine, cholesterol and dimyristoyl phosphatidylglycerol were dissolved in chloroform in 3:1:0.25 proportions. Chloroform was then evaporated using a rotary evaporator at 53°C within 5-10 min. The lipid layer was kept in a vacuum oven set at 43°C overnight to remove traces of solvent. Lipid vesicles were formed by adding the proper volume of PBS, pH = 7.4 to produce a 30 mM lipid concentration. The mixture was incubated at 53°C for 5 min and vortexed for another 5 min afterwards. The incubation and vortex steps were repeated until the entire lipid was removed from the flask. The solution was then transferred to a Bechman L8-55 ultracentrifuge and spun at 40,000 (100,000 G) for 20 min. The supernatant was removed and liposome pellets washed twice with the same volume of PBS at this condition. Lipid vesicles were diluted with PBS to achieve a 0.2 mM lipid concentration.

AmB was dissolved in PBS with the aid of DMSO in a way to give levels of 0.2, 5 and 8 µg/mL as measured from the UV absorbance of these solutions, diluted with equal volumes of methanol at 412 nm. The final concentration of DMSO was below 1%. PEO-*b*-PHSA micelles containing AmB were reconstituted in PBS, pH 7.4, to achieve a level of 0.5 mg/mL for the polymer and 6-10 µg/mL for AmB. Separate samples were prepared for each time point in the release study by adding 0.50 mL of a liposomal solution to 0.50 mL of a AmB solution in PBS. Samples were incubated at 37°C for 24 hs. A sample was taken at each time point and centrifuged at 20,000 G for 10 min to separate the lipid pellet. The level of AmB in the supernatant was determined from its UV absorbance at 412 nm after an aliquot of supernatant was diluted with the same volume of methanol. For time zero, 0.50 mL of AmB alone or encapsulated AmB was

129

added to 0.50 mL of PBS. An aliquot of this solution was diluted with an equal volume of methanol and its UV absorbance was measured at 412 nm. Lipid pellets were also dissolved in methanol and assayed for the amount of transferred AmB by UV spectroscopy. Each experiment was conducted in triplicate. The percentage of released AmB was calculated and plotted versus time. AmB was also incubated in PBS and its level in solution measured to assess its stability over time as a control. The association of AmB with PEO-*b*-PHSA micelles before and during the time of release (in the supernatant) was confirmed by size exclusion chromatography (SEC) at 410 nm by a method described below.

6.2.5. Stability of PEO-b-PHSA micelles -

Freeze-dried samples of PEO-*b*-PHSA micelles (without AmB) with varied levels of stearic acid substitution were dissolved in 0.1 M phosphate buffer, pH = 7.4 at a level of 0.5 mg/ml. The solutions containing PEO-*b*-PHSA micelles were filtered (0.22 μm) and incubated at 37°C for 4 weeks. Samples (125 μL) were taken at specified time intervals and injected into a SEC column (Hydrogel 2000, Waters), equilibrated with 0.1 M phosphate buffer, pH = 7.4, at a flow rate of 0.8 ml/min (Waters B15 LC). Micelle and unimer peaks were detected by UV/VIS (Waters 486) at 210 nm. The column was calibrated with dextran standards (8.05×10^5 – 9.11×10^6 gmol^{-1}) using a refractive index detector (Precision Detectors 2000).

6.3. Results

The chemical structure of PEO-*b*-PHSA samples used in this study is shown in Figure 6.1. AmB was encapsulated at three levels of stearic acid substitution (Table 6.1) and the release of drug for PEO-*b*-PHSA micelles assessed by measuring the transfer of

130

AmB to lipid vesicles. The lipid vesicles were used to maintain sink conditions for poorly soluble AmB and to separate the released drug from encapsulated drug. We assume the rate-determining step is the release of AmB from PEO-*b*-PHSA micelles. While the method needs to be validated by independent methods, it does provide an approach to assess the relative effect of fatty acid substitution on the release of AmB from PEO-*b*-PHSA micelles and insight into the rate and duration of drug release for these nanoscopic drug delivery systems.

Unencapsulated AmB quickly partitioned into the lipid vesicles at 5 and 8 μg/mL (ca., 90 % at 5 min), but more slowly at 0.2 μg/mL (Figure 6.2). On the other hand, AmB encapsulated in PEO-*b*-PHSA micelles at 6.0 μg/mL was gradually released, with less than 20 % release of AmB after one hour.

The effect of degree of stearic acid substitution on the *in vitro* release of AmB from PEO-*b*-PHSA micelles is shown in Figure 6.3. At all three levels of stearic acid substitution, the release of AmB from PEO-*b*-PHSA micelles was rapid at early times, ca., < 1 hour, and was much more gradual at longer times. PEO-*b*-PHSA micelles at 11 % stearic acid substitution gradually released AmB over the first 60 min. While 90 % of AmB itself in PBS at 5 μg/mL rapidly partitioned into lipid vesicles in 5 min (Figure 6.2), 35 % of AmB encapsulated in PEO-*b*-PHSA micelles was still in the supernatant. At a stearic acid substitution of 50 %, the release of AmB from PEO-*b*-PHSA micelles occurred more slowly, with 50 % release of AmB at ca., 30 min. At a stearic acid substitution of 70 %, the release of AmB from PEO-*b*-PHSA micelles was inordinately slow, and it took more than 360 min for 50 % release of AmB.

131

The release of AmB from PEO-*b*-PHSA micelles was also found to be dependent on the method of encapsulation – AmB encapsulated by a dialysis method released the drug more rapidly than AmB encapsulated by the solvent evaporation method, with 50 % release of AmB at ca., 20 min in the former case (Figure 6.3).

The effect of degree of stearic acid substitution on the stability of PEO-*b*-PHSA micelles is shown in Table 6.2. The intermediate block copolymer with no attached stearic acid (Figure 6.1, 0 % substitution), PEO-*b*-PHAA, completely eluted as unimers at 14.5 min (Table 6.2). Similarly, PEO-*b*-PHSA at 11 % eluted predominately as unimer at 14.1 min, but with a small fraction eluting as micelles at 11.7 min. The area under the curve (AUC) of the micelle peak was 1.7 %. In contrast, PEO-*b*-PHSA at 50 and 70 % stearic acid substitution formed micelles that eluted intact (100 % of AUC). PEO-*b*-PHSA eluted entirely as micelles independent of its concentration (63 μg/mL to 1.0 mg/mL). The average elution time of the micellar peak shortened from 11.5 to 10.6 min as the level of fatty acid substitution on the core-forming block increased from 20 to 70 %, indicating an increase in the size of the micelles. Lastly, PEO-*b*-PHSA micelles with 11, 20 and 40 % of stearic acid substitution were incubated in phosphate buffer 0.1 M, pH 7.4, for 28 days at 37°C. Only slight changes in the elution profiles were determined (Figure 6.4).

6.4. Discussion

The long-term objective of this study is to develop a novel long circulating nanoscopic carrier based on PEO-*b*-PLAA for AmB. To enhance the encapsulation of AmB, we attached a compatible moiety i.e., fatty acid, to the core-forming block (Figure

6.1). Through a solvent evaporation method PEO-*b*-PLAA micelles effectively encapsulated AmB, resulting in reduced toxicity (haemolysis), particularly in comparison to the more common dialysis method of drug loading. The degree of fatty acid substitution was the key structural factor of PEO-*b*-PHSA varied to enhance the thermodynamic stability of micelles raise the level of AmB encapsulation and reduce its haemolytic activity. Encapsulated AmB was as active as AmB itself against pathogenic fungi in terms of MIC.

The *in vitro* release studies clearly illustrate that PEO-*b*-PHSA micelles can release AmB in a sustained manner (Figures 6.2 and 6.3). We took advantage of the propensity of AmB to partition favorably into lipid vesicles to assess its release from PEO-*b*-PHSA micelles (7-9). Typically, the *in vitro* release of drugs from polymeric micelles has been assessed by methods based on SEC or dialysis. The sustained release of doxorubicin from PEO-*b*-PBLA micelles has also been revealed by changes in fluorescence quenching of the drug (10). These methods were found to be inappropriate for AmB, owing to its poor solubility in water and self-aggregation. Thus, we devised this new method using lipid vesicles to study the release of AmB.

The results support a growing body of evidence that show that polymeric micelles are capable of sustained drug release even though they have nanoscopic dimensions. The release of AmB from PEO-*b*-PHSA micelles depends on the method used to encapsulate AmB (Figure 6.3). More importantly, the results suggest that the release of AmB from PEO-*b*-PHSA micelles can be controlled, by varying the structure of the polymer, specifically the degree of fatty acid substitution (Figure 6.3). Particularly at a high level of stearic acid substitution (70 %), the release of AmB from PEO-*b*-PHSA micelles was

133

prolonged and incomplete even after 1400 min. This striking result is at odds with low molecular weight micelles, which rapidly release encapsulated molecules. But it is consistent with the highly stable rigid core structure of PEO-*b*-PHSA micelles revealed in earlier studies by fluorescence spectroscopy (Chapter 3) (1).

Notably, AmB encapsulated in PEO-*b*-PHSA micelles at 50 and 70 % caused no haemolysis at 20 µg/ ml, whereas AmB encapsulated in PEO-*b*-PHSA micelles at 11 % caused 100 % haemolysis at 3 µg/ mL (Table 6.1). After 30 min (incubation time of AmB and red blood cells), more AmB was released at 11 % than at higher levels of fatty acid substitution, leading to greater haemolysis. At 50 and 70 %, PEO-*b*-PHSA micelles may also release AmB as unimers (unaggregated state), which are non-toxic for mammalian cells, but cause the leakage of fungal cells (11-13). This point needs further study.

Finally, AmB encapsulated by dialysis was more toxic (100 % haemolysis at 3 µg/ml), owing to rapid release.

The release of AmB from PEO-*b*-PHSA micelles *in vitro* presumably occurs by diffusion in either as unimers or as aggregates (Figure 6.5). *In vivo*, the situation is different in that micelles are subject to sink conditions (below the critical micelle concentration), and the release of drug may be determined by the dissociation of micelles upon dilution. Thus, the kinetic stability of micelles may have an important role in drug release. The stability studies on PEO-*b*-PHSA micelles at 11 % indicate that they rapidly dissociate upon dilution and elution during SEC (Table 6.2, Figure 6.4). We speculate that these PEO-*b*-PHSA micelles would rapidly fall apart after injection in blood. On the other hand, PEO-*b*-PHSA micelles at 50 and 70 % might be able to circulate intact in blood, as indicated by elution as intact micelles during SEC. While it is difficult to

134

extrapolate *in vivo*, Yokoyama *et al.* have shown that micelles composed of PEO-*b*-poly(aspartic acid)-doxorubicin conjugates, that could elute intact as micelles during SEC, could circulate in blood for prolonged periods (14). Thus, PEO-*b*-PHSA micelles at high levels of stearic acid substitution may circulate for prolonged periods in blood and act as nanoscopic depot for AmB.

6.5. Conclusions

PEO-*b*-PHSA micelles can gradually release AmB for prolonged periods. The release of encapsulated AmB from PEO-*b*-PHSA micelles as well as the stability of the micelles can be controlled, by varying the degree of stearic acid substitution. Lastly, the tailoring the structure of PEO-*b*-PHSA might lead to micelles that can improve the efficacy of AmB in the treatment of systemic fungal diseases.

135

Table 6.1. Properties of AmB encapsulated in PEO-*b*-PHSA micelles.

Loading method	Stearic acid substitution level[1] (%)	AmB: PEO-*b*-PHSA (mol: mol)	AmB concentration causing 100 % haemolysis[2] (μg/ml)	Release of AmB in 30 min (%)
Solvent evaporation	11	0.22	3	76.7 ± 0.7
Solvent evaporation	50	0.35	> 23	46.1 ± 5.1
Solvent evaporation	70	0.36	> 22	26.4 ± 1.8
Dialysis	50	0.25	6	61.9 ± 0.8

[1] determined by ^{1}H NMR
[2] from chapter 5

136

Table 6. 2. Size exclusion chromatography results for PEO-*b*-PLAA micelles reconstituted in phosphate buffer 0.1 M, pH 7.4.

Block copolymer	Stearic acid substitution level (%)	SEC elution time ± SD (min)		AUC (%)	
		Unimers	Micelles	Unimers	Micelles
PEO-*b*-PHHA	-	14.5 ± 0.0	-	100 ± 0.00	-
PEO-*b*-PHSA	11	14.1 ± 0.0	11.7 ± 0.0	98.30 ±0.44	1.70 ± 0.43
PEO-*b*-PHSA	20	-	11.5 ± 0.0	-	100 ± 0.00
PEO-*b*-PHSA	40	-	11.1± 0.1	-	100 ± 0.00
PEO-*b*-PHSA	50	-	10.8 ± 0.0	-	100 ± 0.00
PEO-*b*-PHSA	70	-	10.6 ± 0.0	-	100 ± 0.00

137

$CH_3O(CH_2CH_2O)_x(CH_2)_3$ $S(CH_2)$ NH—($COCHNH)_y(COCHNH)_z$ H

CH_2 CH_2

CO CO

NH NH

$(CH_2)_6$ $(CH_2)_6$

O OH

CO

$(CH_2)_{16}$

CH_3

Stearic acid substitution level (%)	x	y	z
0	270	0	24
11	270	3	21
50	270	12	12
70	270	17	7
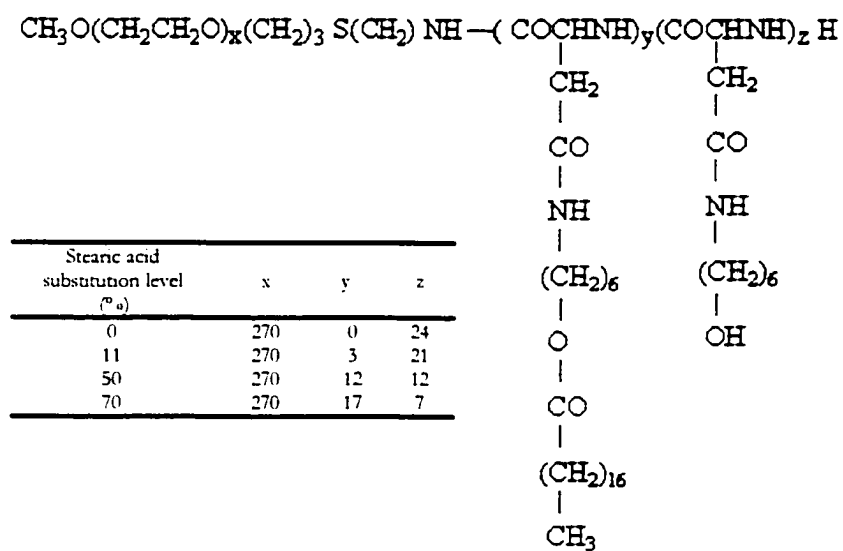
Figure 6.1. Chemical structure of PEO-*b*-PHHA and PEO-*b*-PHSA at three levels of stearic acid substitution.

138
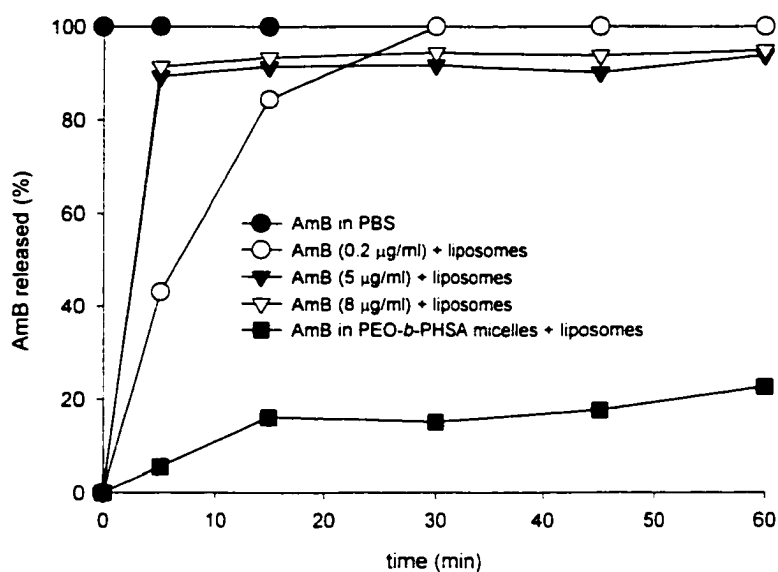
Figure 6.2. The transfer AmB and AmB encapsulated in PEO-b-PHSA micelles into lipid

vesicles (dipalmitoyl phosphatidylcholine, cholesterol and dimyristoyl phosphatidylglycerol

(3:1:0.25)) in PBS, pH=7.4 at 37°C. AmB in PBS, pH=7.4 at 37°C was stable over the duration

of the experiment based on its absorption at 412 nm.

139
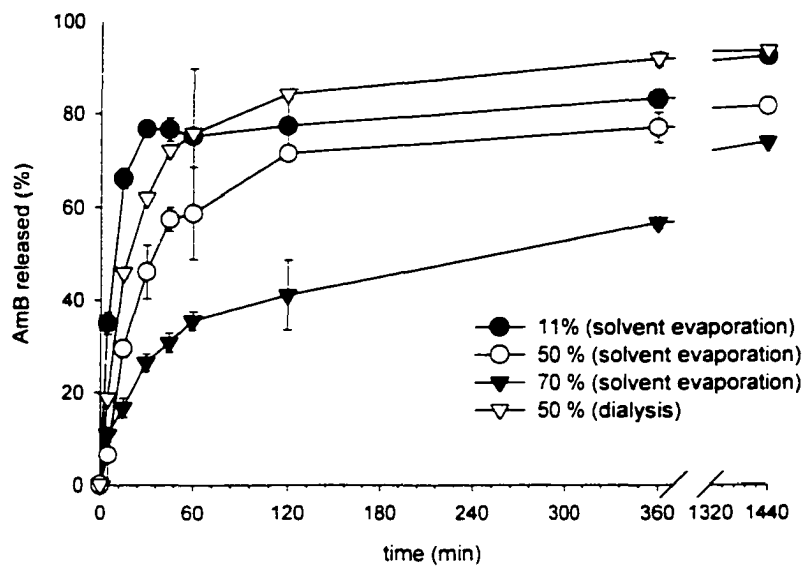
Figure 6.3. The effect of stearic acid substitution and encapsulation method on the *in vitro* release of AmB from PEO-*b*-PHSA micelles (n=3).

140
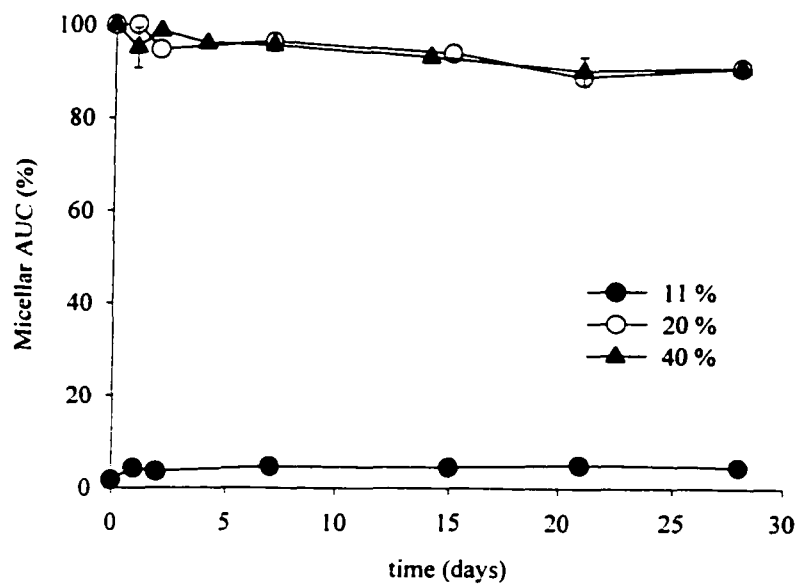
Figure 6.4. Stability of polymeric micelles with varied levels of stearate in the micellar core in phosphate buffer. Samples are prepared by the solvent evaporation method.

141

Figure 6.5. Proposed mechanism for the *in vitro* release of AmB and its membrane activity for PEO-*b*-PHSA micelles at **a)** 50 and 70 % stearic acid substitution and **b)** 11 % stearic acid substitution.

142

6.6. References

1. Lavasanifar, A., Samuel, J. and Kwon, G. S., The effect of alkyl core structure on micellar properties of poly(ethylene oxide)-*block*-poly(L-aspartamide) derivatives, *Colloids & Surfaces B: Biointerfaces* 22:115-126 (2001).

2. Bekersky, I., Fielding, R. M., Buell, D. and Lawrence, I., Lipid-based amphotericin B formulations: from animals to man, *PSTT* 2:230-236 (1999).

3. Slain, D., Lipid based amphotericin B for the treatment of fungal infections, *Pharmacotherapy* 19:306-323 (1999).

4. van Etten, E.M., Snijders, SV, van Vianen, E., and Bakker-Woudenberg, I.M., Superior efficacy of liposomal amphotericin B with prolonged circulation in blood in the treatment of severe candidiasis in leukopenic mice, *Antimicrobial Agents & Chemotherapy* 42:2431-2433 (1998).

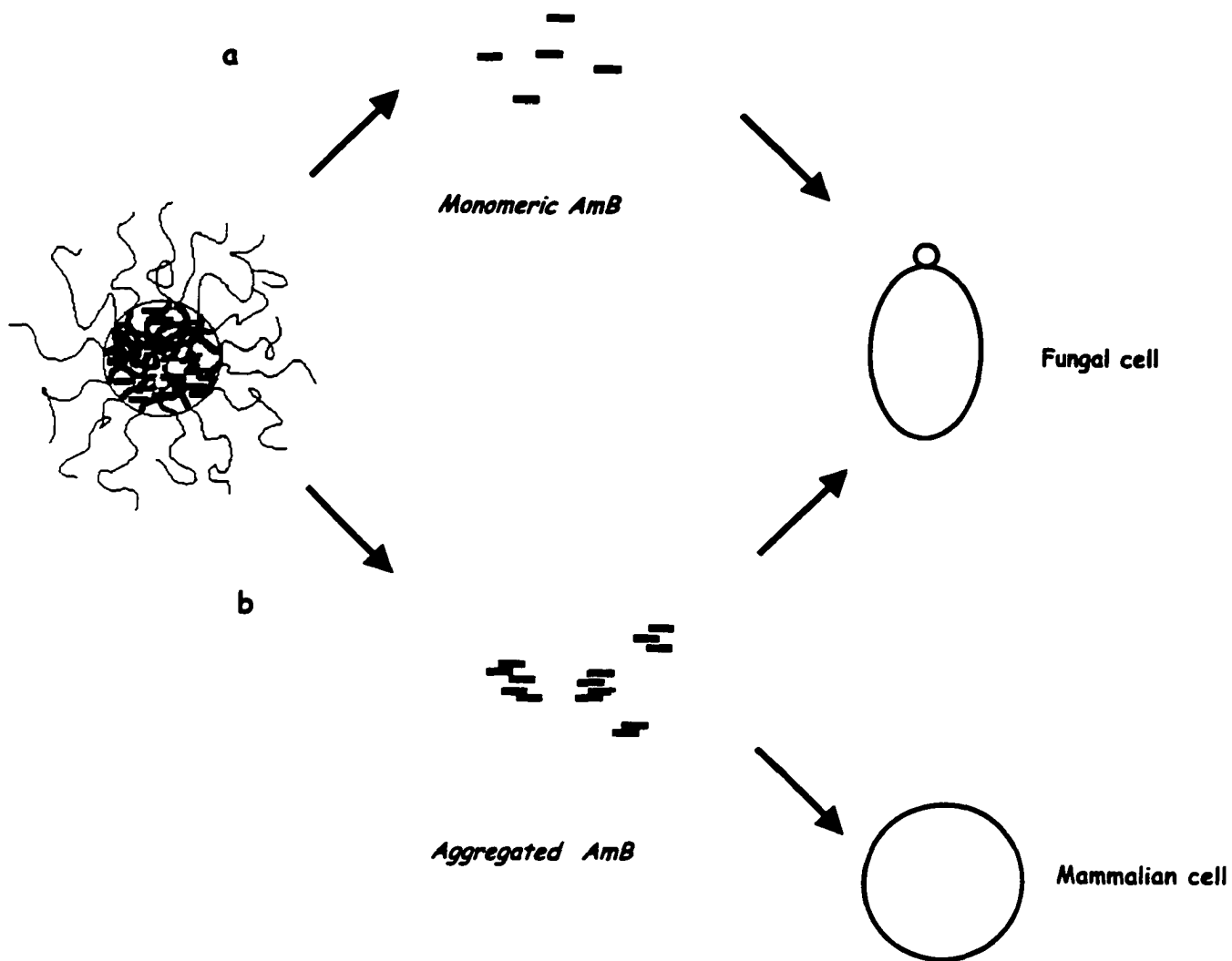5. Lavasanifar, A., Samuel, J. and Kwon, G. S., Micelles of poly(ethylene oxide)-*block*-poly(hydroxy alkyl-L-aspartamide): synthetic analouges of lipoproteins for drug delivery, *Journal of Biomedical Material Research* 52:831-835 (2000).

6. Samuel, J., Budzynski, V., Reddish, M.A., Ding, L., Zimmerman, G., Koganty, R. and Longenecker, B.M., Immnogenicity and Antitumor activity of liposomal MUC1 vaccines, *International Journal of Cancer* 75:295-302 (1998).

7. Bolard, J., Vertut-Croquin, A., Cybulska, B. and Gary-bobo, M., Transfer of the polyene antibiotic amphotericin B between single walled vesicles of dipalmitoylphosphatidylcholine and egg-yolk phosphatidylcholine, *Biochimica et Biophysica Acta* 647:241-248 (1981).

8. Balakrishnan A.R. and Easwaran, K.R., Lipid-amphotericin B complex structure in solution: a possible first step in the aggregation process in cell membranes, *Biochemistry* 32:4139-4144 (1993).

9. Lance, M.R., Washington, C. and Davis, S.S., Evidence for the formation of amphotericin B-phospholipid complexes in Langmuir monolayers, *Pharmaceutical Research* 13:1008-1014 (1996).

10. Kwon, G.S., Naito, M., Yokoyama, M., Okano, T., Sakurai, Y. and Kataoka, K., Block copolymer micelles for drug delivery: Loading and release of doxorubicin, *Journal of Controlled Release* 48:195-201 (1997).

11. Brajtburg, J. and Bolard, J., Carrier effects on biological activity of amphotericin b, *Clinical Microbiology Reviews* 9:512-531 (1996).

12. Bolard, J., Legrand, P., Heitz, F. and Cybulska, B., One-sided action of amphotericin b on cholesterol-containing membranes is determined by its self-association in the medium, *Biochemistry* 30:5707-5715 (1991).

13. Legrand, P., Romero, E. A., Cohen, B. E. and Bolard, J., Effect of aggregation and solvent on the toxicity of amphotericin B to human erythrocytes, *Antimicrobial Agents & Chemotherapy* 36:2518-2522 (1992).

14. Yokoyama, M., Kwon, G.S., Okano, T., Sakurai, Y., Naito, M. and Kataoka, K., Influencing factors on in vitro micelle stability of adriamycin-block copolymer conjugates, *Journal of Controlled Release* 28:59-65 (1994).

144

Chapter 7

General Discussion and Conclusions

7.1 History

Micelles self-assembled from amphiphilic block copolymers are of interest for drug delivery (1-3). Interest is particularly keen in the context of drug solubilization, where many existing drugs and many new ones coming out of drug discovery, lack of water solubility (4-9). Among many block copolymers developed for drug delivery, micelle-forming PEO-*b*-poly(L-amino acid) (PEO-*b*-PLAA)s are unique, owing to the existence of reactive groups in the PLAA block, which provides sites for the attachment of drugs or drug compatible moieties (10-16).

PEO-*b*-poly(L-lysine) attached to cyclophosphamide derivatives and aliphatic side chains on the poly(L-lysine) block was the first example of drug-block copolymer conjugates designed by Ringsdorf *et al.* to form micelles (10). Micelle-forming conjugates or complexes of doxorubicin, methotrexate and cisplatin with PEO-*b*-poly(L-aspartic acid) (PEO-*b*-P(Asp)) have also been prepared and studied for drug delivery (11-13; 17-20). In the category of micellar nanocontainers, tailor-made PEO-*b*-P(Asp) micelles with drug compatible moieties on the core-forming block have been used to improve the delivery of doxorubicin and KRN5500 (21; 22). Limited assessments have been conducted to determine the effect of structural variation on physicochemical and biological properties of polymeric micelles in both cases (20; 23-25). Building structure-property relationships may provide helpful data in designing finely tuned polymeric micelles for effective drug delivery.

146

7.2 General discussion

For the improved encapsulation and selective delivery of amphotericin B (AmB) to fungal cells a micellar, a nanocontainer that can mimic structural and functional aspects of lipoproteins has been proposed (26). Many hydrophobic drugs, including AmB, are solubilized and carried to their destinations by a biological system, namely, serum lipoproteins (27; 28). A synthetic analogue may play the same role with the advantage of safety, stability and pharmaceutical feasibility (29; 30). It may also have a favorable effect on the biodistribution of AmB (28; 31; 32).

AmB is currently available in a low molecular weight surfactant and three lipid based formulations. The surfactant (sodium deoxycholate) formulation is highly water soluble and very effective but severely toxic. The lipid-based formulations are less toxic but less effective and very expensive (33-36).

Lipoproteins have cores rich in triglycerides. We pursued PEO-b-P(Asp) micelles with saturated fatty acid ester substitutes in the core to mimic the structure of the core in lipoproteins. A long PEO chain (molecular weight of 12,000 gmol^{-1}) was chosen as the shell-forming block to stabilize micellar interface and impose long circulating properties. The core-forming block was much shorter than the hydrophilic block (polymerization degree of 15 or 24) to induce water solubility to the polymeric carrier. A nomenclature of 12-15 or 12-24 was used throughout the manuscript to differentiate between the two samples.

The first effort on the synthesis of PEO-b-P(Asp) with fatty acid ester side chains was carried out using 12-15 (Chapter 2). Hydrophobic spacers of different lengths (2 and 6 carbons) with free hydroxyl groups at the end were attached to the P(Asp) block.

147

Stearic acid was then reacted with free hydroxyls, forming PEO-*b*-poly[*N*-(2-ethyl stearate)-L-aspartamide] (PEO-*b*-PESA) and PEO-*b*-poly[*N*-(6-hexyl stearate)-L-aspartamide] (PEO-*b*-PHSA). Polymeric micelles were formed through self-assembly of block copolymers and characterized.

The characterization of polymeric micelles in studies described in Chapters 2 and 3 was accomplished by transmission electron microscopy (TEM) and fluorescent probe techniques. TEM is widely used to determine the shape and size of colloidal dispersions in a dry state (4; 13; 37). The results cannot simply be extrapolated to a biological system, however, as PEO surfaces become hydrated in an aqueous environment.

Changes in the excitation and emission fluorescence spectra of pyrene resulted from its preferential partition to the nonpolar nano-domains of polymeric micelles was used to estimate the onset of micellization and the polarity of the micellar core (6; 38; 39). A decrease in the ratio of light intensities emitted from an excited dipyrene intra-molecular excimer (I_e) to that of isolated pyrene monomer (I_m) was considered as an indication of restricted conformational changes of the di-pyrene probe due to the high viscosity of its environment. Heat and low concentrations of the solubilizate (below saturation solubility in water) were used in this experiment to facilitate the partitioning of pyrene to the micellar core and avoid the formation of inter-molecular excimers, respectively.

Preliminary studies showed the similarity of PEO-*block*-poly[*N*-(alkyl stearate)-L-aspartamide] (PEO-*b*-PASA) micelles to lipoproteins in terms of shape, size (10-30 nm) and high thermodynamic stability (CMC of 20 to 40 µg/ml). It also provided evidence for a reduced polarity and restricted mobility of the polymeric chains in the micellar core.

148

The low CMC and rigidity of the core in polymeric micelles is in sharp contrast to micelles of low molecular weight surfactants. The spherical shape, nanoscopic size, low CMC and high microviscosities of PEO-b-PASA micelles were shared with micelles self assembled from PEO-b-poly(β-benzyl-L-aspartate) (PEO-b-PBLA), which have aromatic cores. The main advantage of PEO-b-PASA over PEO-b-PBLA micelles was its superiority in AmB encapsulation possibly due to a better match between the polarity of the core-forming block and the drug. By using PEO-b-PBLA micelles water solubility of AmB was increased to a limited extent (25 µg/ml) using a dialysis method of drug loading. Under identical loading conditions, the AmB compatible cores of PEO-b-PESA and PEO-b-PHSA micelles enhanced AmB solubility to 133 and 337 µg/ml, respectively. The reason for the difference between the two types of PEO-b-PASA micelles in micellar properties and AmB encapsulation was difficult to assess since two factors, the substitution level of stearic acid esters on the polymeric backbone and the length of the hydrophobic spacers, were different in these samples.

The effect of structural variations on the properties of polymeric micelles composed of fatty acid conjugates of PEO-b-poly(hydroxyalkyl-L-aspartamide) (PEO-b-PHAA) was assessed in a systematic way in Chapter 3. The engineering of block copolymer involved changes in the length of the P(Asp) block, alkyl spacers and fatty acid substitutes as well as variations in the substitution level of the fatty acid side chain. Structure-property relationships were built with regard to micellar properties such as shape, size, CMC, core polarity and viscosity (40).

149

The conjugation of fatty acids even at a short chain length or a low substitution level induced the required amphiphilicity for self-association at a µmolar level of the block copolymer. A reverse relationship between the substitution level of fatty acid on the PHAA block and CMC was revealed. The fatty acid ester core of the polymeric micelles was found to be non-polar and rigid. The core viscosity decreased as the length of the P(Asp) block increased. A high substitution of a 22-carbon chain fatty acid on the polymeric backbone noticeably increased the microviscosity. An increase in the length of the hydrophobic backbone or the side chain and its substitution level caused an increase in micellar size within a range of 15 to 22 nm. Polymeric micelles composed of fatty acid esters of PEO-b-PHHA were spherical, except for micelles self assembled from block copolymers with high degrees of long fatty acid substitution on the core-forming block, which were ellipsoid in shape. This was attributed to the large dimensions of the hydrophobic block and/or an increase in the aggregation number of polymeric micelles.

Stearic acid esters of PEO-b-PHAA (12-24) were chosen for further studies on AmB delivery as micelle-forming block copolymers with optimized micellar properties. The selection was partially based on the superiority of micelles self assembled from 12-24 block copolymers in terms of high core viscosity. Polymeric micelles with rigid cores were expected to resist dissociation and lower the rate of drug diffusion, which may lead to sustained drug release. The core viscosity was even higher in micelles composed of behenic acid (22 carbon) conjugates of PEO-b-PHAA. The micellar solutions were hazy, however. We chose a hexyl spacer since it caused an apparent increase in the substitution level of fatty acid on the polymeric backbone in the synthesis process. Variation in the level of fatty acid substitution on the core-forming block altered micellar size, CMC and

150

core polarity. Owing to a change in core polarity, the level of fatty acid substitution was hypothesized to affect the encapsulation and the release of AmB from polymeric micelles.

AmB was encapsulated in PEO-*b*-PHSA micelles. An optimized polymeric micellar formulation of AmB was developed through changes in the loading procedure and fine-tuning of the block copolymer structure (Chapter 4-6). PEO-*b*-PHSA micelles were evaluated in terms of the level of AmB encapsulation, *in vitro* toxicity and antifungal activity of encapsulated AmB and the rate of AmB release. The goal was to achieve formulations that were water-soluble, non-toxic, but active at clinically relevant concentrations, acting as a depot for AmB delivery and resist dissociation upon dilution. A polymeric micellar carrier with such properties is expected to enhance the efficacy of AmB *in vivo*.

The level of AmB encapsulation in polymeric micelles was measured from its UV/VIS absorption in filtered solutions of polymeric micelles, which were treated with equal volumes of an organic solvent (DMF or methanol) for micelles to be ruptured. Size exclusion chromatography confirmed AmB encapsulation. The haemolytic activity of AmB was used as a measure of AmB toxicity toward mammalian cells. The minimum inhibitory concentration of AmB against the growth of three pathogenic fungi was measured after 24 hs and used to compare the *in vitro* antifungal activity of encapsulated and free AmB.

The assessment of *in vitro* drug release from polymeric micelles is usually carried out by dialysis or size exclusion chromatography (20; 41-44). The quenched fluorescence of encapsulated doxorubicin in polymeric micelles has been used to show

151

sustained drug release (45). These methods were found to be inappropriate in case of AmB due to its poor water solubility and aggregation. We used a lipid recipient phase to separate the released AmB (either in a monomeric or self-associated state) from encapsulated drug and to maintain sink condition during the study (46-48). The rate of AmB release from polymeric micelles was the rate-limiting step in this experiment. Free AmB partitioned to the lipid vesicles rapidly.

AmB was encapsulated in PEO-*b*-PHSA micelles by a dialysis method. The loading procedure was changed and a condition at which water soluble and non-toxic formulations of AmB were achieved was selected. AmB encapsulation in micelles composed of 12-24 block copolymers by the final procedure was generally lower than what we have reported for micelles of 12-15 block copolymer. The higher viscosity of the core in polymeric micelles composed of 12-24 block copolymers might have restricted AmB encapsulation in this case. A final conclusion cannot be drawn at this point, and this needs further evaluation.

Dialysis is the most commonly used method of drug incorporation for polymeric micelles (15; 22; 41; 44; 49-53). High number of variables, limitations in the choice of organic solvent and technical problems make dialysis an unfavourable process for drug loading, particularly in a large scale. We developed a solvent evaporation method for AmB encapsulation in polymeric micelles, which is similar to the method used for drug loading in liposomes (Chapter 4). PEO-*b*-PHSA block copolymers self assembled into smaller micelles by the solvent evaporation in comparison to the dialysis method. The primary advantage of the solvent evaporation over dialysis was the reduced toxicity of encapsulated AmB in PEO-*b*-PHSA micelles (50 % of stearic acid substitution) toward

152

red blood cells. This might be related to a more favourable interaction between AmB and the core-forming block during the solvent evaporation procedure. A similar method has been used to encapsulate AmB in Pluronic micelles (54). The Pluronic formulation, however, failed to protect red blood cells from the lytic effect of AmB.

Non-haemolytic formulations of AmB in PEO-*b*-PHSA micelles (50 % of stearic acid substitution) were obtained at a drug to polymer ratio of 0.4 w/w %. By increasing the initial level of AmB in the loading process, PEO-*b*-PHSA micelles encapsulated more AmB (loading ratio of 0.9 w/w %), reaching an aqueous concentration of 0.9 mg/mL for AmB. The haemolytic activity of encapsulated AmB was partially regained at this level of loading, however (onset of haemolysis was 5 μg/ml).

An increase in the level of fatty acid substitution in PEO-*b*-PHSA micelles improved AmB encapsulation and reduced its toxicity toward red blood cells. AmB encapsulated in PEO-*b*-PHSA micelles inhibited fungal growth at a similar level to AmB alone. The improved encapsulation of AmB in PEO-*b*-PHSA micelles was due to a favourable interaction between AmB and the micellar core at high levels of stearic acid substitution. This was evidenced by UV/VIS spectroscopy. A sustained AmB release from PEO-*b*-PHSA micelles was apparent from a slow transfer of encapsulated AmB to lipid vesicles. The reduced toxicity of encapsulated AmB for mammalian cell membranes was attributed to a sustained drug release from polymeric micelles, again, as a result of an interaction between AmB and the micellar core. An increase in the level of fatty acid esters in the micellar core or replacement of dialysis with solvent evaporation method caused a decrease in the amount of released AmB and an increase for the onset of haemolysis caused by encapsulated AmB. The stability of PEO-*b*-PHSA micelles under

153

the diluting condition of SEC was increased as the level of stearic acid substitution passed 20 %.

Overall, AmB encapsulated in highly substituted PEO-*b*-PHSA micelles (70 % or more) by a solvent evaporation method can be considered as a potential carrier for AmB delivery. The aqueous concentration of AmB encapsulated in optimized condition reached 340 µg/ml. The aqueous solubility of AmB alone is around 0.5 µg/mL and it is administered at a level of 100 µg/mL with sodium deoxycholate. The therapeutic level of AmB is around 1.7 µg/mL when administered as Fungizone® (36) and it causes 100 % haemolysis at a level of 1 µg/mL (55-57). AmB encapsulated in PEO-*b*-PHSA micelles at 70 % stearic acid substitution, on the other hand, was non-haemolytic at 22 µg/ml.

PEO-*b*-PHSA micelles with high levels of stearic acid substitution may circulate intact for long periods in blood and act as a depot for AmB delivery. The distribution of AmB to non-specific organs might be lowered by its encapsulation in long circulating carriers. Instead, AmB concentration in blood may be enhanced. Therefore, it might be possible to reduce the dose of AmB administration, lower the risk of long-term toxicity and cost of therapy by a long circulating carrier.

AmB is released in a sustained manner from PEO-*b*-PHSA micelles, particularly at high levels of stearic acid substitution and a solvent evaporation method of loading. Despite a large surface area, 30 % of encapsulated AmB remained in PEO-*b*-PHSA micelles (70 % of stearic acid substitution) after 24 hs of incubation in the presence of lipid vesicles. PEO-*b*-PHSA micelles may release the drug in a monomeric state. Monomeric AmB acts selectively on fungal membranes at a cellular level. Preferential binding of monomeric AmB with serum albumin and high-density lipoprotein may also

154

lead to a reduced *in vivo* toxicity for AmB. As a result, the therapeutic index of AmB is expected to be improved by the polymeric micellar formulation *in vivo*.

7.3. Conclusions

1. Micelles composed of fatty acid conjugates of PEO-*b*-PHAA have been prepared from PEO-*b*-PBLA by aminolysis, reaction with fatty acids and self-assembly.

2. PEO-*b*-PHSA micelles at a high level of stearic acid substitution have a spherical nanoscopic supramolecular core-shell structure with low CMC, high core viscosity and low core polarity.

3. PEO-*b*-PHSA micelles effectively encapsulate a compatible drug, amphotericin B, through dialysis and solvent evaporation techniques.

4. The degree of substitution of the fatty acid on the core-forming block can be varied to modify the stability of PEO-*b*-PHSA micelles, increase the encapsulation of drug and control the rate of drug release.

5. PEO-*b*-PHSA micelles lower the toxicity of AmB at a membrane level without a loss of its antifungal activity, particularly by a solvent evaporation drug loading method.

7.4. Future perspective

Polymeric micelles have great potential for selective drug delivery (58-66). A small size is the main advantage of polymeric micelles over other colloidal systems used for site-specific drug delivery. This may lead to transfer to extravascular environment and penetration into cells membranes for the micellar carrier. The same factor, however, may restrict the space of encapsulation and limit the ability of polymeric micelles for a sustained drug release, due to a large total surface area. The problem might be overcome

155

if the drug is stably encapsulated in the core of polymeric micelles. We explored this possibility for a model drug, AmB, by tailoring the chemical structure of PEO-*b*-PLAA derivatives through the attachment of AmB compatible moieties in the core. A polymeric micellar formulation was developed for AmB delivery based on PEO-*b*-PHSA that can effectively encapsulate the drug, improve its efficacy and sustain the rate of drug release *in vitro*. The micellar structure was found to be nanoscopic in size and stable upon dilution under *in vitro* conditions.

For PEO-*b*-PHSA micelles, the *in vitro* results showed a reduced toxicity and potent antifungal activity for encapsulated AmB in terms of haemolysis and MIC. In these experiments, the membrane activity of AmB was measured at a cellular level. The basis for the selectivity of AmB towards fungal cells in biological systems is not clear and has been attributed to several mechanisms (33). A fair conclusion on the efficacy of AmB in the polymeric micellar system can only be made by the assessment of toxicity and activity in animal models of systemic fungal disease.

We expect a long circulating behaviour for PEO-*b*-PHSA micelles, owing to its nanoscopic size and PEO shell. The assessment of pharmacokinetics and biodistribution of encapsulated AmB in comparison to AmB is required to validate this hypothesis. AmB has shown an improved efficacy in a murine model of candidiasis when delivered by long circulating liposomes (67).

We built structure-property relationships and studied the effect of alkyl core structure on micellar properties, AmB encapsulation, *in vitro* toxicity, antifungal activity and release. A similar investigation might be conducted to assess the effect of structural

156

variations on the pharmacokinetics and efficacy of AmB encapsulated in PEO-*b*-PHSA micelles in biological system.

From a broader perspective, a better understanding on the role of structural factors on the biodistribution of polymeric micelles may lead to the design of polymeric micelles with preferential accumulation in specific organs for a passive drug targeting. For a third degree of targeting by polymeric micelles, i.e., delivery to subcellular targets, it might be useful to conduct a structure-property study with respect to the uptake of polymeric micelles at the cellular level. Little is known on the effect of micellar structure and the mechanisms involved in the cellular uptake of polymeric micelles (68-71).

PEO-*b*-PHSA micelles may be used to encapsulate many hydrophobic drugs suffering from low water solubility or instability, particularly those that contain aliphatic chains in their chemical structure. Nystatin, another antifungal drug in the category of polyene microlides, is a second candidate for encapsulation in PEO-*b*-PHSA micelles. Despite great potency, nystatin formulations are only available for local administration, possibly due to a poor solubility of the hydrophobic drug and its toxicity (72).

Lastly, PEO-*b*-PHSA micelles have been designed to deliver AmB by intravenous route of administration. We speculate the system might be administered by a pulmonary route and be effective for pulmonary aspergillosis. The pulmonary route is accessible and may lead to local antifungal effects for AmB without toxicity.

157

7.5. References

1. Kwon, G.S. and Okano, T., Soluble self assembled block copolymers for drug delivery, *Pharmaceutical Research* 16:597-600 (1999).

2. Kwon, G.S., Diblock copolymer Nanosparticles for Drug Delivery, *Critical Reviews in Therapeutic Drug Carrier Systems* 15:481-512 (1998).

3. Allen, C., Maysinger, D. and Eisenberg, A., Nano-engineering block copolymer aggregates for drug delivery, *Colloids & Surfaces B: Biointerfaces* 16:3-27 (1999).

4. Hagan, S.A., Coombes, A.G., Garnett, M.C., Davies, M.C., Illum, L. and Davis, S. S., Polylactide-poly(ethylene glycol) copolymers as drug delivery dystems. 1. characterization of water dispersible micelle forming systems, *Langmuir* 12:2153-2161 (1996).

5. Hruka, Z., Riess, G. and Goddard, P. Synthesis and purification of a poly-(ethylene oxide)-poly(γ-benzyl-L-glutamate0, *Polymer* 34:1333-1335 (1993).

6. Kwon, G.S., Naito, M., Yokoyama, M., Okano, T., Sakurai, Y. and Kataoka, K., Micelles based on AB block copolymers of poly(ethylene oxide) and poly(β-benzyl L-aspartate), *Langmuir* 9:945-949 (1993).

7. Zhang X. and Burt, H.M., Diblock copolymers of poly(DL-lactide-*block*-methoxy polyethylene glycol) as mic ellar carriers of taxol, *Pharmaceutical Research* 12:S-265 (1995).

8. Burt, H. M., Zhang, X., Toleikis, P., Embree, L. and Hunter, W. L., Developement of coppolymers of poly(D,L-lactide) and methoxypolyethylene glycol as micellar carriers of paclitaxol, *Colloids & Surfaces B: Biointerfaces* 16: 161-171 (1999).

9. Allen, C., Yu, Y., Maysinger, D. and Eisenberg, A., polycaprolactone-*b*-poly(ethylene oxide) block copolymer micelles as a novel drug delivery vehicle for neurotrophic agents FK506 and L-685,818, *Bioconjugate Chemistry* 9:564-572 (1998).

10. Dorn, K., Hoerpel, G. and Ringsdorf, H., Polymeric antitumor agents on a molecular and cellular level, In C. G. Gebelein and Jr. C. E. Carraher (eds), *Bioactive Polymer Systems:An Overview*, Plenum Press, New York 531-585 (1985).

11. Yokoyama, M., Inoue, S., Kataoka, K., Yui, N. and Sakurai, Y., Preparation of adriamycin-conjugated poly(ethylene glycol)-poly(aspartic acid) block copolymer, *Macromulecular Chemistry Rapid Communications* 8:431-435 (1987).

12. Yokoyama, M., Okano, T., Sakurai, Y., Suwa, S. and Kataoka, K., Introduction of cisplatin into polymeric micelle, *Journal of Controlled Release* 39:351-356 (1996).

13. Li, Y. and Kwon, G. S., Micelle-like structures of poly(ethylene oxide)-*block*-poly(2-hydroxyethyl aspartamide)-methotrexate conjugates, *Colloids & Surfaces B: Biointerfaces* 16:217-226 (1999).

14. Kwon, G. S., Naito, M., Kataoka, K., Yokoyama, M., Sakurai, Y. and Okano, T., Block copolym micelles as vehicles for hydrophobic drugs, *Colloids & Surfaces B: Biointerfaces* 2:429-434 (1994).

15. Kwon, G.S., Naito, M., Yokoyama, M., Okano, T., Sakurai, Y. and Kataoka. K., Physical entrapment of adriamycin in AB block copolymer micelles, *Pharmaceutical Research* 12:192-195 (1995).

16. Harada, A. and Kataoka, K., Formation of stable and monodispersive polyion complex micelles in aqueous medium from poly(L-lysine) and poly(ethulene glycol)-poly(aspartic asid) block copolymer. *Pure and Applied Chemistry* A34: 2119-2133 (1997).

17. Yokoyama, M., Kwon, G.S., Okano, T., Sakurai, Y., Sato, T.and Kataoka. K., Preparation of micelle-forming polymer-drug conjugates, *Bioconjugate chemistry* 3:295-301 (1992).

18. Nishiyama, N., Yokoyama, M., Aoyagi, T., Okano, T., Sakurai, Y., and Kataoka, K. Preparation and characterization of self-assembled polymer-metal complex Micelle from cis-Dichlorodiammineplatinum(II) and Poly(ethylene glycol)-poly(α, β-aspartic acid) block copolymer in an aqueous medium, *Langmuir* 15:377-383 (1999).

19. Nishiyama, N., Kato, Y., Sugiyama, Y. and Kataoka, K., Developement of cisplatin-loaded polymeric micelles with a prolonged circulation in the bloodstream and an enhanced accumulation in the solid tumor, *Proceedings of the Controlled Release Society* 28:5155-5156 (2001).

20. Li, Y. and Kwon, G. S., Methotrexate esters of poly(ethylene oxide)-*block*-poly(2-hydroxyethyl-L-aspartamide). Part I: effects of the level of Methotrexate conjugation on the stability of micelles and on drug release, *Pharmaceutical Research* 17:607-611 (2000).

21. Yokoyama, M., Okano, T., Sakurai, Y., Seto, T. and Kataoka, K., Improved synthesis of adriamycin-conjugated poly(ethylene oxide)-poly(aspartic acid) block copolymer and formation of unimodal micellar structure with controlled amount of physically entrapped adriamycin, *Journal of Controlled Release* 32:269-277 (1994).

159

22. Matsumura, Y., Yokoyama, M., Kataoka, K., Okano, T., Sakurai, Y., Kawaguchi, T. and Kakizoe, T., Reduction of the side effects of an antitumor agent KRN5500, by incorporation of the drug into polymeric micelles, *Japanese Journal of Cancer Research* 90:122-128 (1999).

23. Yokoyama, M., Kwon, G. S., Okano, T., Sakurai, Y., Ekimoto, H., Okamoto, K., Mashiba, H., Seto, T. and Kataoka, K., Composition-dependent *in vivo* antitumor activity of adriamycin-conjugated polymeric micelle against murine colon adenocarcinoma, *Drug Delivery* 1:11-19 (1993).

24. Yokoyama, M., Kwon, G.S., Okano, T., Sakurai, Y., Naito, M. and Kataoka, K., Influencing factors on in vitro micelle stability of adriamycin-block copolymer conjugates, *Journal of Controlled Release* 28:59-65 (1994).

25. Yokoyama, M., Sugiyama, T., Okano, T., Sakurai, Y., Naito, M. and Kataoka, K., Analysis of micelle formation of an adriamycin-conjugated poly(ethylene glycol)-poly(aspartic acid) block copolymer by gel permeation chromatography, *Pharmaceutical Research* 10:895-899 (1993).

26. Lavasanifar, A., Samuel, J. and Kwon, G.S., Micelles of poly(ethylene oxide)-*block*-poly(hydroxy alkyl L-aspartamide): synthetic analouges of lipoproteins for drug delivery, *Journal of Biomedical Material Research* 52:831-835 (2000).

27. Brajtburg, J., Elberg, S., Bolard, J., Kobayashi, G.S., Levy, R. A., Ostlund, R.E., Schlessinger, D. and Medoff, G., Interaction of plasma proteins and lipoproteins with amphotericin B, *The Journal of Infectious Diseases* 149:986-997 (1984).

28. Wasan, K.M., Lopez-Berestein, G., Daemen, M.J., Smits, J.F., Thijssen, H.H., and Struyker-Boudier, H.A., Modification of amphotericin B's therapeutic index by increasing its association with serum high-density lipoproteins, *Annals of the New York Academy of Sciences* 730:93-106 (1994).

29. Bijsterbosch M.K. and Van Berkel, T.C., Native and modified lipoproteins as drug delivery systems, *Advanced Drug Delivery Reviews* 5:231-251 (1990).

30. Shaw, J.M., Shaw, K.V., Yanovich, S., Iwanik, M., Futch, W.S., Rosowsky, A., Schook, LB, and Lundberg, B., Delivery of lipophilic drugs using lipoproteins cytotoxic activity of two new lipophilic steroid nitrogen carbamates incorporated into low-density lipoprotein, *Annals of the New York Academy of Sciences* 507:471-476 (1987).

31. Barwicz, J., Gareau, R., Audet, A., Morisset, A., Villiard, J. and Gruda, I., Inhibition of the interaction between lipoproteins and amphotericin B by some delivery systems, *Biochemical & Biophysical Research Communications* 181:722-728 (1991).

32. Wasan, K.M., Morton, R.E., Rosenblum, M.G. and Lopez-Berestein, G., Decreased toxicity of liposomal amphotericin B due to association of

160

amphotericin B with high-density lipoproteins: role of lipid transfer protein, *Journal of Pharmaceutical Sciences* 83:1006-1010 (1994).

33. Brajtburg, J. and Bolard, J., Carrier Effects on Biological Activity of Amphotericin B, *Clinical Microbiology Reviews* 9:512-531 (1996).

34. Szoka, Jr., F.C.T. and Tang, M., Amphotericin B formulated in liposomes and lipid based systems: A review, *Journal of Liposome Research* 3:363-375 (1993).

35. Bekersky, I., Fielding, R. M., Buell, D. and Lawrence, I., Lipid-based Amphotericin B formulations: from animals to man, *PSTT* 2:230-236 (1999).

36. Slain, D. Lipid based amphotericin B for the treatment of fungal infections, *Pharmacotherapy* 19:306-323 (1999).

37. Mortensen, K. and Yashayahu, T., Cryo-TEM and SANS microstructural study of pluronic polymer solution, *Macromolecules* 28:8829-8834 (1995).

38. Jones, M-C. and Leroux, J. C., Polymeric micelles-a new generation of colloidal drug carriers, *European Journal of Pharmaceutics & Biopharmaceutics* 48:101-111 (1999).

39. Georges, J., Molecular fluorescence in micelles and microemulsions: micellar effects and analytical applications, *Spectochimica Acta reviewes* 13:27-45 (1990).

40. Lavasanifar, A., Samuel, J. and Kwon, G. S., The effect of alkyl core structure on micellar properties of poly(ethylene oxide)-*block*-poly(L-aspartamide) derivatives. *Colloids & Surfaces B: Biointerfaces, 22:115-126. (*2001).

41. La, S. B., Okano, T. and Kataoka, K., Preparation and characterization of the micelle-forming polymeric drug indomethacin-incorporated poly(ethylene oxide)-poly(β-benzyl L-aspartate) block copolymer micelles, *Pharmaceutical Science* 85:85-90 (1996).

42. Kim, S. Y., Shin, I. G., Lee, Y.-M., Cho, C.-S. and Sung, Y.-K., Methoxy poly(ethylene glycol) and ε-caprolctone amphiphilic block copolymeric micelle containing indomethacin: micelle formation and drug release behaviour, *Journal of Controlled Release* 51:13-22 (1998).

43. Jeong, Y.-I, Cheon, J.-B., Kim, S.-H., Nah, J.-W., Lee, Y.-M., Sung, Y.-K., Akaike, T. and Cho, C.-S., Clonazepam release from core-shell type nanoparticles in vitro, *Journal of Controlled Release* 51:169-178 (1998).

44. Allen, C., Han, J., Yu, Y., Maysinger, D. and Eisenberg, A., Polycaprolactone-*b*-poly(ethylene oxide) copolymer micelles as a delivery vehicle for dihydrotestostrone, *Journal of Controlled Release* 63:275-286 (2000).

45. Kwon, G.S., Naito, M., Yokoyama, M., Okano, T., Sakurai, Y. and Kataoka, K., Block copolymer micelles for drug delivery: loading and release of doxorubicin, *Journal of Controlled Release*, 48:195-201 (1997).

46. Bolard, J., Vertut-Croquin, A., Cybulska, B. and Gary-bobo, M., Transfer of the polyene antibiotic amphotericin B between single walled vesicles of dipalmitoylphosphatidylcholine and egg-yolk phosphatidylcholine, *Biochimica et Biophysica Acta* 647:241-248 (1981).

47. Fujii, G., Chang, J.E., Coley, T. and Steere, B., The formation of amphotericin B ion channels in lipid bilayers, *Biochemistry* 36:4959-4968 (1997).

48. Lance, M.R., Washington, C. and Davis, S.S., Evidence for the formation of amphotericin B-phospholipid complexes in Langmuir monolayers, *Pharmaceutical Research*, 13:1008-1014 (1996).

49. Kwon, G.S. and Okano, T., Polymeric micelles as new drug carriers, *Advanced Drug Delivery Reviews* 21:107-116 (1996).

50. Shin, I.G., Kim, S.Y., Lee, Y.M., Cho, C.S. and Sung, Y.K., Methoxy poly(ethylene glycol)/ε-caprolactone amphiphilic block copolymeric micelle containing indomethacin. I. preparation and characterization, *Journal of Controlled Release* 51:1-11 (1998).

51. Inoue, T., Chen, G., Nakamae, K. and Hoffman, A.S., An AB block copolymer of oligo(methyl methacrylate) and poly(acrylic acid) for micellar delivery of hydrophobic drags, *Journal of Controlled Release* 51:221-229 (1998).

52. Nah, J.-W., Jeong, Y.-I and ChoC.-S., Norfloxacin release from polymeric micelle of poly(γ-benzyl L-glutamate)/poly(ethylene oxide)/poly(γ-benzyl L-glutamate)block copolymer, *Bulletin of Korean Chemical Society* 19 :962-967 (1998).

53. Yu, B.G., Okano, T., Kataoka, K. and Kwon, G.S., Polymeric micelles for drug delivery: solubilization and hemolytic activity of amphotericine B, *Journal of Controlled Release* 33:131-136 (1998).

54. Forster, D., Washington, C. and Davis, S. S., Toxicity of solubilized and colloidal Amphotericin B formulations to human erythrocytes, *Journal of Pharmacy & Pharmacology* 40:325-328 (1988).

55. Brezis, M., Heyman, S.N. and Sugar.A.M., Reduced amphotericin toxicity in an albumin vehicle, *Journal of Drug Targeting* 1:185-189 (1993).

56. Aramwit, P., Yu, B. G., Lavasanifar, A., Samuel, J. and Kwon, G. S., The effect of serum albumin on the aggregation state and toxicity of amphotericin B, *Journal of Pharmaceutical Sciences* 89:1589-1593 (2000).

162

57. Yu, B. G., Sardari, S. and Kwon, G. S., Dissociated toxicity, but enhanced antifungal efficacy of amphotericin B loaded poly(ethylene oxide)-*block*-poly(β-benzyl L aspartate) micelles, *Pharmaceutical Research* 14:S284 (1997).

58. Kwon, G.S. and Kataoka, K., Block copolymer micelles as long circulating drug vehicles, *Advanced Drug Delivery Reviews* 16:295-309 (1995).

59. Kabanov, A., Batrakova, E.V., Melik-Nubarov, N.S., Fedoseev, N.A., Dorodnich, T.Y., Alakhov, V., Chekhonin, V.P., Nazarova, I.R. and Kabanov, V.A., A new dlass of drug carriers: micelles of poly(oxyethylene)-poly(oxypropylene) block copolymers as microcontainerrs for drug targetting from blood in brain, *Journal of Controlled Release* 22:141-158 (1992).

60. Scholz, C., Iijima, M., Nagasaki, Y. and Kataoka, K. A novel reactive polymeric micelles with aldehyde groups on its surfaces, *Macromolecules* 28:7295-7297 (1995).

61. Yamamoto, K., Nagasaki, Y., Kato, M. and Kataoka, K. Surface charge modulation of poly(ethylene glycol)-poly(D,L-lactide)block copolymer micelles: conjugation of charged peptides, *Colloids & Surfaces B: Biointerfaces* 16:135-146 (1999).

62. Vinogradov, S. V., Baratkova, EV., Li, S. and Kabanov, A.V., Polyion complex micelles with protein-modified corona for receptor-mediated delivery of oligonucleotides into cells. *Bioconjugate Chemistry* 10:851-860 (1999).

63. Jeong, B., Bae, Y.H., Lee, D.S. and Kim, S.W., Biodegradable block copolymers as injectable drug-delivery systems, *Nature* 388:860-862 (1997).

64. Taillefer, J., Jones, M.-C., Brasseur, N., Van lieer, J. e. and Leroux, J. C., Preparation and characterization of pH-responsive polymeric micelles for the delivery of photosensitizing anticancer drugs, *Journal of Pharmaceutical Sciences* 89:52-62 (2000).

65. Kataoka, K., Harada, A. and Nagasaki, Y., Block copolymer micelles for drug delivery: design, characterizatio and biological significance, *Advanced Drug Delivery Reviews* 47:113-131 (2001).

66. Kabanov, A.V. and Kabanov, V.A., Interpolyelectrolyte and block Ionomer complexes for gene delivery: physico-chemical aspects, *Advanced Drug Delivery Reviews* 30:49-60 (1998).

67. Van Etten, E.M., Snijders, SV., Van Vianen, W. and Bakker-Woudenberg, I.M., Superior efficacy of liposomal amphotericin B with prolonged circulation in blood in the treatment of severe candidiasis in leukopenic mice, *Antimicrobial Agents & Chemotherapy* 42:2431-2433 (1998).

68. Pratten, M. K., Lioyd, J. B. , Horpel, G. and Ringsdorf, H., Micelle-forming block copolymers: pinocytosis by macrophages and interaction with model membranes, *Makromolecule Chemistry* 186:725-733 (1985).

69. Batrakova, E.V., Han, H.Y. , Miller, D.W. and Kabanov, A.V., Effects of pluronic p85 unimers and micelles on drug permeability in polarized BBMEC and caco-2 cells, *Pharmaceutical Research* 15:1525-1532 (1998).

70. Batrakova, E.V., Han, H.Y. , Alakhov, V.Y., Miller, D.W. and Kabanov, A.V., Effects of pluronic block copolymers on drug absorption in caco-2 cell monolayers, *Pharmaceutical Research* 15:850-855 (1998).

71. Miller, D.W., Batrakova, E.V., Waltner, T.O., Alakhov, V.Y. and Kabanov, A.V., Interactions of pluronic block copolymers with brain microvessel endothelial cells: evidence of two potential pathways for drug absorption, *Bioconjugate Chemistry* 8:649-657 (1997).

72. Arikan, S. and Rex, JH., Lipid-based antifungal agents: current status, *Current Pharmaceutical Design* 7:393-415 (2001).